CalVal Saral/ Altika

Saral/ Altika validation and cross calibration activities (Annual report 2013)

Contract No 104685/00 - lot 1.2A

Reference : CLS.DOS/NT/13-228

Nomenclature : SALP-RP-MA-EA-22271-CLS

Issue : 1rev 1

Date : April 15, 2014

CLS - 8-10 Rue Hermès - Parc Technologique du Canal - 31520 Ramonville St-Agne - FRANCE
Telephone 33 5 61 39 47 00 / Fax 33 5 61 75 10 14

Chronology Issues:		
Issue:	Date:	Reason for change:
1rev0	Jan 10, 2014	Creation
1rev1	Apr 15, 2014	Revision after comments from N. Picot

People involved in this issue :				
	AUTHORS	**COMPANY**	**DATE**	**INITIALS**
Written by:	S. Philipps P. Prandi V. Pignot	CLS CLS CLS		
Checked by:		CLS		
Approved by:		CLS CLS		
Application authorised by:				

Index Sheet :	
Context:	
Keywords:	
Hyperlink:	

Distribution:		
Company	Means of distribution	Names
CLS/DOS	electronic copy	G.DIBARBOURE
CNES	electronic copy	thierry.guinle@cnes.fr emilie.bronner@cnes.fr nicolas.picot@cnes.fr amandine.guillot@cnes.fr jean-damien.desjonqueres@cnes.fr aqgp_rs@cnes.fr dominique.chermain@cnes.fr delphine.vergnoux@cnes.fr

List of tables and figures

List of Tables

List of Figures

List of items to be defined or to be confirmed

Applicable documents / reference documents

Contents

1. Introduction

This document presents the synthesis report concerning validation activities of Saral/AltiKa GDRs in 2013 under SALP contract (N° 104685/00 Lot 1.2A) supported by CNES at the CLS Space Oceanography Division. It covers several points: CAL/VAL Saral/AltiKa activities, Saral/AltiKa / Jason-2 cross-calibration, and particular studies and investigations. **The focus is on GDR (Patch1) products, but results using IGDR or OGDR products are also shown. For information about Patch2 data see chapter 7.3. or 11.2., or the report [17] concerning the reprocessed Patch2 data (early 2014)**.
The ISRO/CNES mission Saral/AltiKa was successfully launched on February, 25th 2013. Since March, 13th, Saral/AltiKa is on its operational orbit. During the first few months, it was not exactly on the same ground track as Envisat (roughly 2 km difference at pass extremities). After inclination maneuvers, Saral reached the same ground track as Envisat on October, 7th 2013. Since the beginning of the mission, Saral/AltiKa data have been analyzed and monitored in order to assess the quality of Saral/AltiKa products. Cycle per cycle reports are available on AVISO web page (http://www.aviso.altimetry.fr/en/data/calval/systematic-calval/validation-reports.html).
This present report assesses the Saral/AltiKa data quality. Missing and edited measurements are monitored. Furthermore relevant parameters derived from instrumental measurements and geophysical corrections are analyzed. Saral/AltiKa is the first altimeter using the Ka-band frequency. The advantage of this higher frequency is a reduced footprint that leads to a better spatial resolution. Nevertheless it is also more sensitive to rainy and cloudy conditions. A higher level of missing data than for Ku-band altimeters were expected for these conditions.

Hereafter, analyzes focus on Saral/AltiKa / Jason-2 cross-calibration. Though both satellites are on different ground tracks, comparison is possible. Even if only low order statistics are mainly presented here, other analyzes including histograms, plots and maps are continuously produced and used in the quality assessment process.
Indeed, it is now well recognized that the usefulness of any altimeter data only makes sense in a multi-mission context, given the growing importance of scientific needs and applications, in particular for operational oceanography. One major objective of the Saral/AltiKa mission is to ensure in association with Jason-2 the continuity of ocean observations through high precision altimetry. This kind of comparisons between different altimeter missions flying together provides a large number of estimations and consequently efficient long term monitoring of instrument measurements.

2. Processing status

2.1. Processing

Only about 4 months after launch of the Saral/AltiKa mission, Ogdr and Igdr data were available to all users beginning of July 2013. They were first released with some flaws (unit problem for liquid cloud water,...) or some corrections voluntary disabled (atmospheric attenuation at default value) or with disclaimers (ice_flag, altimeter wind not to use, ...). Some of these issues where addressed by the Patch1 (see table 1 concerning when this patch was used for the several products and 11.1. for its content). Beginning of September 2013 the GDR products were released (using from the beginning the Patch1). A description of the different Saral/AltiKa products and their disclaimers is available in the Saral/AltiKa Products handbook ([4]). Patch2, containing further improvements for Saral/AltiKa data, is scheduled to be used from mid-February 2014 onwards (for information of content of Patch2, see also chapter 7.3..

Data version	Ogdr	Igdr	Gdr
Version T without Patch	till cycle 4 segment 0609	till cycle 4 pass 394	-
Version T with Patch1 (chapter 11.1.) (L1 library=V3.1p1p2, L2 library=V4.2p1p6p9 Processing Pilot=V3-4-1p2p5p6p7p8p9)	from cycle 4 segment 0611 onwards (2013-07-18 13h44m04)	from cycle 4 pass 0395 onwards (2013-07-10 23h56m18)	from cycle 1 pass 0001 onwards
Version T with Patch2 (chapter 11.2.) (L1 library=V4.2p1, L2 library=V5.2p1, Processing Pilot=V4.1)	from cycle 10 segment 0407 onwards (2014-02-06 10h46m58)	from cycle 10 pass 566 onwards (2014-02-11 23h17m37)	from cycle 8 onwards (cycles 1 to 7 will be re-processed)

Table 1: *Product versions*

2.2. CAL/VAL status

2.2.1. List of events

The following table shows the major events during the beginning of Saral/AltiKa mission.

cycle number	pass number	start time	stop time	event
1	0001-1002	14/03/2013 06:00	17/04/2013	cycle 1 (starting altimeter mode : DIODE acquisition / median tracking)
1	0001-0200	14/03/2013	20/03/2013	altimeter mode : DIODE acquisition / median tracking
1	0172-0175	20/03/2013 05:10:03	20/03/2013 08:30	CAL1 for expertise
1	0201-0400	21/03/2013 05h19mn20	27/03/2013	altimeter mode : DIODE acquisition / EDP tracking
1	0266	23/03/2013 12h13mn54		semi major axis maneuver
1	0372, 0374	27/03/2013 27/03/2013		CAL2 long calibrations at 04:51 (28min missing data) and 06:40 (11min missing data)
1	0401-0600	28/03/2013 04h59mn20	03/04/2013	altimeter mode : DIODE acquisition / median tracking
1	0601-0800	04/04/2013 10/04/2013		altimeter mode : DIODE / MNT tracking (with the updated value of the DIODE_MNT_TPG_ALTI parameter)
1	0801-1002	11/04/2013 17/04/2013		altimeter mode : DIODE acquisition / EDP tracking
1	0801	11/04/2013		AltiKa CNG calibration I2+Q2 (over land)
1	0868	13/04/2013 12:53:53.508	13/04/2013 12:53:53.508	station keeping maneuver
1	0898	14/04/2013		AltiKa CNG calibration I&Q (over land)
1	0984	17/04/2013		AltiKa CNG calibration I2+Q2 (over land)
2	0001-1002	18/04/2013 22/05/2013		altimeter mode : DIODE acquisition / median tracking
2	0034, 0035	19/04/2013 9h37	19/04/2013 10h25	cross calibration test over S-band station Biak (Indonesia)
2	0057	20/04/2013		AltiKa CNG calibration I&Q (over land)
				.../...

cycle number	pass number	start time	stop time	event
2	0127	22/04/2013 15h26	22/04/2013 15h54	cross calibration maneuver
2	0206	25/04/2013 9:53:07		pitch maneuver (0.045°) to correct the PF/RF alignment (alignment between the platform and the radiofrequency axis)
2	0355	30/04/2013 14:35	30/04/2013 15:03	cross calibration maneuver
2	0782	15/05/2013 12:47:48.975	15/05/2013 12:47:50.975	station keeping maneuver
3	0001-0200	23/05/2013	29/05/2013	altimeter mode : DIODE acquisition / median tracking
3	0201-0400	30/05/2013	05/06/2013	altimeter mode : DIODE acquisition / median tracking
3	0401-0600	06/06/2013	12/06/2013	altimeter mode : DIODE acquisition / EDP tracking
3	0438	07/06/2013 12:24:36.449	07/06/2013 12:24:37.449	station keeping maneuver
3	0601-0800	13/06/2013	19/06/2013	altimeter mode : DIODE acquisition / EDP tracking
3	0800-1002	20/06/2013 04:18:07	26/06/2013	altimeter mode : DIODE acquisition / median tracking
3		20/06/2013	23/06/2013	Due to processing issues at X-band station and link disturbances between Inuvik and Kiruna, some data gaps can be observed in the OGDR products
	0814-0816			20th June : from 15:17:56 to 16:57:42
	0831-0842			21th June : from 06:11:23 to 14:46:35
	0859-0872			22th June : from 05:39:06 to 15:54:53
	0887-0890			23th June : from 05:06:56 to 06:56:57
3	0887-0890	23/06/2013 05:14:07	23/06/2013 06:54:43	no O/I/GDR product due to PLTM lost
				.../...

cycle number	pass number	start time	stop time	event
3	0926	24/06/2013 13:30:36.630	24/06/2013 13:30:37.172	station keeping maneuver. Impact on SSHA in SRL_OPN_2PTS003_0925_20130624_125902_20130624_145220. SRL_OPN_2PTS003_0928_20130624_145219_20130624_163200.
3	0992-0005	26/06/2013 20:27:50	27/06/13 09:48:22	data gap in the OGDR products
4	0001-1002	27/06/2013	31/07/2013	altimeter mode : DIODE acquisition / median tracking
		27/06/2013		dissemination of O/IGDR-T products on AVISO ftp server
4	0498	14/07/2013 14:42:09.432	14/07/2013 14:42:11.432	station keeping maneuver. Impact on SRL_OPN_2PTS004_0497_20130714_140949_20130714_160311.
4	0556	16/07/2013		AltiKa CNG calibration I&Q (over land)
4	0586	17/07/2013		AltiKa CNG calibration I2+Q2 (over land)
4	0911	29/07/2013 00:53:51	29/07/2013 00:57:50	inclination maneuver (1 burn on Y and Z axis). Impact on SRL_OPN_2PTS004_0909_20130728_233829_20130729_011612.
4	0929-0944	29/07/2013 15:36	30/07/2013 04:15	some data gaps in the O/IGDR
4	0984	31/07/2013 14:07:30	31/07/2013 14:07:37	station keeping maneuver. Impact on SRL_OPN_2PTS004_0983_20130731_133528_20130731_152859.
5	0001-1002	01/08/2013 04/09/2013		altimeter mode : DIODE acquisition / median tracking
5	0182	07/08/2013 13:47:32.601	07/08/2013 13:47:35	station keeping maneuver. Impact on SRL_OPN_2PTS005_0181_20130807_131525_20130807_150845.
5		18/08/2013 14:10	19/08/2013 07:05	communication cable failure. No OGDR file between SRL_OPN_2PTS005_0495_20130818_123039_20130818_141004. and SRL_OPN_2PTS005_0518_20130819_070515_20130819_084
5	0726	26/08/2013 13:50:27.735	26/08/2013 13:50:29.735	station keeping maneuver. Impact on SRL_OPN_2PTS005_0725_20130826_131837_20130826_151158.
5	0958	03/09/2013 16:02:15	03/09/2013 16:19:56	AltiKa CNG calibration I&Q (over land)
				.../...

cycle number	pass number	start time	stop time	event
5		31/08/2013 17:34	01/09/2013 06:56	Link issue between Kiruna and Eumetsat. No OGDR file between SRL_OPN_2PTS005_0872_20130831_155446_20130831_173425. and SRL_OPN_2PTS005_0890_20130901_065649_20130901_083
5		01/09/2013 13:29	01/09/2013 15:23	Link issue between Kiruna and Eumetsat. No OGDR file between SRL_OPN_2PTS005_0895_20130901_115106_20130901_132958. and SRL_OPN_2PTS005_0900_20130901_152320_20130901_170
6	0001-1002	05/09/2013	09/10/2013	altimeter mode : DIODE acquisition / median tracking
6	0038	06/09/2013 12:44 :00	06/09/2013 13:01:45	AltiKa CNG calibration I2+Q2 (over land)
6	0812	03/10/2013 13:55:39.254	03/10/2013 13:57:17.254	1st inclination maneuver to reach the Envisat ground track (1 burn on Z axis) impact on SRL_OPN_2PTS_006_0811_20131003_132432_20131003_151754
6	0926	07/10/2013 13:29:45.048	07/10/2013 13:31:25.048	2nd inclination maneuver to reach the Envisat ground track impact on SRL_OPN_2PTS006_0925_20131007_125904_20131007_145220.
6	0984	09/10/2013 14:07:52.135	09/10/2013 14:07:57.205	station keeping maneuver
7	0001-1002	10/10/2013	13/11/2013	altimeter mode : DIODE acquisition / median tracking
7	0089	13/10/2013 7:58:25	13/10/2013 08:01:34	gap in the IGDR products
7	0352	22/10/2013 12:13:12	22/10/2013 12:15:27	Gap in the radiometer measurements due to the modification of the onboard radiometer database values. Step of around 5mm on the wet tropospheric correction.
7	0526	28/10/2013 14:10:49.754	28/10/2013 14:10:50.162	station keeping maneuver. Impact on SRL_OPR_2PTS007_0525_20131028_133846_20131028_153210.
7		31/10/2013 05:21:29	31/10/2013 07:11:03	No OGDR file between SRL_OPN_2PTS007_0599_20131031_034039_20131031_052129. and SRL_OPN_2PTS007_0604_20131031_071103_20131031_084 still under investigation
				.../...

cycle number	pass number	start time	stop time	event
7		04/11/2013 06:37	04/11/2013 08:03	Data gaps in SRL_OPN_2PTS007_0718_20131104_065555_2013
7	0812	07/11/2013 13:56:26.782	07/11/2013 13:56:27.790	station keeping maneuver. Impact on SRL_OPN_2PTS007_0811_20131107_132430_20131107_151751.
7		22/10/2013 12:15:27	13/11/2013 12:17:18	Incorrect value of the MNT_TPG_ALTI parameter (do to the AltiKa init performed to modify the radiometer database)
8	0001-1002	14/11/2013	18/12/2013	altimeter mode : DIODE acquisition / median tracking
8		19/11/2013		ECMWF model upgrade
8	0326	25/11/2013 14:30:55	25/11/2013 14:30:56	station keeping maneuver
8	0812	12/12/2013 13:56:23	12/12/2013 13:56:25	station keeping maneuver
9		19/12/2013	22/01/2014	altimeter mode : DIODE acquisition / median tracking
9	0240	27/12/2013 14:25:06	27/12/2013 14:25:08	station keeping maneuver

Table 2: *E*vents

2.2.2. Missing measurements

This section presents a summary of major satellite or ground segment events that occurred from cycle 1 to 7. Table 3 gives a status about the number of missing passes (or partly missing) for GDRs, as well as the associated events for each cycle.
Up to now, Saral/AltiKa has little missing measurements. In the first couple of days (before the 2013-03-17), they were mainly caused by station acquisition problems. Furthermore the routine calibrations (generally 3 per day) were scheduled at fixed hours (instead over desert regions, as it is done now), leading also to missing science data over ocean for short durations (90 seconds). Now, missing data are mostly due to scheduled events (like altimeter expert calibrations).

Saral/Alti Cycles/Pass	Dates	Events
001/0007	2013-03-14 10:59:58 to 11:01:34	routine calibration
001/0016	2013-03-14 18:59:59 to 19:01:34	routine calibration
001/0026	2013-03-15 02:59:59 to 03:01:34	routine calibration
001/0032	2013-03-15 08:02:51 to 08:14:59	acquisition problems for X-band stations
001/0032-0033	2013-03-15 08:23:14 to 09:06:41	acquisition problems for X-band stations
001/0036	2013-03-15 10:59:59 to 11:01:34	routine calibration
001/0038	2013-03-15 13:08:12 to 13:19:09	acquisition problems for X-band stations
001/0038-0039	2013-03-15 13:28:08 to 13:41:00	acquisition problems for X-band stations
001/0039	2013-03-15 13:48:43 to 14:06:33	acquisition problems for X-band stations
001/0039-0040	2013-03-15 14:09:32 to 14:23:17	acquisition problems for X-band stations
001/0044	2013-03-15 18:10:11 to 18:21:11	acquisition problems for X-band stations
001/0044-0045	2013-03-15 18:30:11 to 18:40:49	acquisition problems for X-band stations
001/0045	2013-03-15 18:59:59 to 19:01:34	routine calibration
001/0045-0046	2013-03-15 19:12:01 to 19:26:57	acquisition problems for X-band stations
001/0046	2013-03-15 19:33:54 to 19:37:18	acquisition problems for X-band stations
001/0047	2013-03-15 20:35:25 to 20:57:31	acquisition problems for X-band stations
		.../...

Saral/Alti Cycles/Pass	Dates	Events
001/0047-0048	2013-03-15 20:57:43 to 21:08:58	acquisition problems for X-band stations
001/0048	2013-03-15 21:17:45 to 21:32:56	acquisition problems for X-band stations
001/0048	2013-03-15 21:38:34 to 21:49:45	acquisition problems for X-band stations
001/0051	2013-03-15 23:40:13 to 23:54:57	acquisition problems for X-band stations
001/0051	2013-03-16 00:01:12 to 00:16:57	acquisition problems for X-band stations
001/0051-0052	2013-03-16 00:22:49 to 00:37:41	acquisition problems for X-band stations
001/0052	2013-03-16 00:43:31 to 00:58:15	acquisition problems for X-band stations
001/0055	2013-03-16 02:59:59 to 03:01:34	routine calibration
001/0062-0063	2013-03-16 09:02:22 to 09:57:57	acquisition problems for X-band stations
001/0063	2013-03-16 09:58:29 to 10:09:01	acquisition problems for X-band stations
001/0063	2013-03-16 10:10:16 to 10:12:42	acquisition problems for X-band stations
001/0063	2013-03-16 10:19:18 to 10:23:46	acquisition problems for X-band stations
001/0064	2013-03-16 10:30:42 to 10:33:07	acquisition problems for X-band stations
001/0064	2013-03-16 10:53:38 to 10:56:45	acquisition problems for X-band stations
001/0064	2013-03-16 10:59:59 to 11:01:34	routine calibration
001/0064-0065	2013-03-16 11:03:40 to 11:20:13	acquisition problems for X-band stations
		.../...

Saral/Alti Cycles/Pass	Dates	Events
001/0066	2013-03-16 12:25:28 to 12:36:38	acquisition problems for X-band stations
001/0066-0067	2013-03-16 12:45:31 to 13:01:03	acquisition problems for X-band stations
001/0067-0068	2013-03-16 13:06:18 to 13:52:01	acquisition problems for X-band stations
001/0074	2013-03-16 19:00:00 to 19:01:34	routine calibration
001/0083	2013-03-17 02:59:59 to 03:01:34	routine calibration
001/0102	2013-03-17 18:59:59 to 19:01:34	routine calibration
001/0172-0175	2013-03-20 05:10 to 08:30	expertise calibrations → small data gaps every 10 minutes
001/0372	2013-03-27 04:50:59 to 05:18:19	CAL2 long calibration
001/0374	2013-03-27 06:39:59 to 06:51:29	CAL2 long calibration
001/0801	2013-04-11 04:41:59 to 04:59:46	altimeter gain calibration I2+Q2 (mostly over land)
001/0898	2013-04-14 13:41:59 to 13:59:46	altimeter gain calibration I&Q (mostly over land)
001/0984	2013-04-17 13:46:59 to 14:04:46	altimeter gain calibration I2+Q2 (mostly over land)
002/0057	2013-04-20 04:52:59 to 05:10:45	altimeter gain calibration I&Q (over land)
003/0887-0890	2013-06-23 05:06:56 to 06:56:58	PLTM loss
004/0556	2013-07-16 15:01:00 to 15:19:01	altimeter gain calibration I&Q (mostly over land)
004/0586	2013-07-17 16:13:00 to 16:30:46	altimeter gain calibration I2+Q2 (mostly over land)
		.../...

Saral/Alti Cycles/Pass	Dates	Events
004/0929	2013-07-29 15:45:56 to 15:55:23	downlink acquisition problem
004/0929	2013-07-29 16:05:23 to 16:25:34	downlink acquisition problem
004/0931	2013-07-29 17:33:54 to 17:44:14	downlink acquisition problem
004/0931	2013-07-29 17:54:13 to 18:06:33	downlink acquisition problem
004/0932	2013-07-29 18:06:52 to 18:11:01	downlink acquisition problem
004/0933	2013-07-29 19:08:07 to 19:15:03	downlink acquisition problem
004/0933	2013-07-29 19:17:09 to 19:27:49	downlink acquisition problem
004/0933	2013-07-29 19:28:29 to 19:36:07	downlink acquisition problem
004/0933	2013-07-29 19:38:00 to 19:43:44	downlink acquisition problem
004/0938	2013-07-29 23:20:23 to 23:26:59	downlink acquisition problem
004/0939	2013-07-30 00:16:30 to 00:30:48	downlink acquisition problem
004/0940	2013-07-30 01:11:00 to 01:13:59	downlink acquisition problem
004/0940	2013-07-30 01:31:06 to 01:32:49	downlink acquisition problem
004/0941	2013-07-30 01:42:43 to 01:47:35	downlink acquisition problem
004/0941	2013-07-30 02:12:17 to 02:18:29	downlink acquisition problem
004/0942	2013-07-30 02:34:08 to 02:40:27	downlink acquisition problem
		.../...

Saral/Alti Cycles/Pass	Dates	Events
004/0942	2013-07-30 02:49:30 to 03:09:18	downlink acquisition problem
004/0942-0943	2013-07-30 03:10:08 to 03:21:43	downlink acquisition problem
004/0943-0944	2013-07-30 03:30:41 to 04:13:16	downlink acquisition problem
005/0958	2013-09-03 16:02:00 to 16:20:01	altimeter gain calibration I&Q (mostly over land)
006/0038	2013-09-06 12:44:01 to 13:01:45	altimeter gain calibration I2+Q2 (over land)
006/0940	2013-10-08 01:17:00 to 01:23:48	station tracking issue
006/0941	2013-10-08 01:46:59 to 01:57:43	station tracking issue
006/0941	2013-10-08 02:06:46 to 02:18:50	station tracking issue
007/0089	2013-10-13 07:58:24 to 08:01:35	missing TM (which had not been filled by PLTM GAP files)
007/0352	2013-10-22 12:13:04 to 12:15:45	modification of onboard radiometer database values
007/0586	2013-10-30 16:11:00 to 16:28:45	altimeter gain calibration I2+Q2 (mostly over land)

Table 3: *M*issing pass status

2.2.3. Edited measurements

Table 4 indicates particular high editing periods (see section 3.2.1.). Most of the occurrences correspond to maneuvers.

Saral/AltiKa Cycles/Passes	Date	Comments
001/0266	2013-03-23	Partly edited by several parameters out of threshold (semi major axis maneuver)
001/0868	2013-04-13	Partly edited by several parameters out of threshold (maneuver)
002/0728	2013-05-15	Partly edited by several parameters out of threshold (station keeping maneuver)
003/0438	2013-06-07	Partly edited by several parameters out of threshold (station keeping maneuver)
003/0926	2013-06-24	Partly edited by several parameters out of threshold (station keeping maneuver)
004/0498	2013-07-14	Partly edited by several parameters out of threshold (station keeping maneuver)
004/0911	2013-07-29	Partly edited by several parameters out of threshold (inclination maneuver)
004/0941	2013-07-30	about 3 minutes of this pass have two 1-Hz data per second, instead of one
004/0984	2013-07-31	Partly edited by several parameters out of threshold (inclination maneuver)
005/0182	2013-08-07	Partly edited by several parameters out of threshold (station keeping maneuver)
005/0726	2013-08-26	Partly edited by several parameters out of threshold (station keeping maneuver)
006/0812	2013-10-03	Partly edited by several parameters out of threshold (inclination maneuver)
006/0926	2013-10-07	Partly edited by several parameters out of threshold (inclination maneuver)
006/0984	2013-08-26	Partly edited by several parameters out of threshold (station keeping maneuver)
007/0526	2013-10-28	Partly edited by several parameters out of threshold (station keeping maneuver)
007/0812	2013-11-07	Partly edited by several parameters out of threshold (station keeping maneuver)

Table 4: *E*dited measurement status

2.3. Models and Standards History

During 2013 only GDR products in version T were available for cycles 1 to 7. These products were homogeneous and used all the Patch1 (see content of Patch 1 in chapter 11.1.). The standards used in the GDR products are listed in table 5. Beginning 2014, some improvements for Saral/AltiKa data will be available with the Patch 2 (see chapter 11.2.) or [17].

Model	Product version "T" Patch1
Orbit	Based on Doris onboard navigator solution for OGDRS. DORIS tracking data for IGDRs DORIS+SLR tracking data for GDRs. Using POE-D
Altimeter Retracking	"Ocean MLE4" retracking: MLE4 fit from 2nd order Brown analytical model: MLE4 simultaneously retrieves the 4 parameters that can be inverted from the altimeter waveforms: • Epoch (tracker range offset) → altimeter range • Composite Sigma → SWH • Amplitude → Sigma0 • Square of mispointing angle "Ice 1" retracking: Geometrical analysis of the altimeter waveforms, which retrieves the following parameters: • Epoch (tracker range offset) → altimeter range • Amplitude → Sigma0

.../...

Model	Product version "T" Patch1
	"Ice 2" retracking: The aim of the ice2 retracking algorithm is to make the measured waveform coincide with a return power model, according to Least Square estimators. Retrieval of the following parameters: • Epoch → altimeter range • Width of the leading edge • Amplitude → Sigma0 • Slope of the logarithm of the waveform at the trailing edge → Mispointing angle • the thermal noise level (to be removed from the waveform samples) "Sea Ice" retracking: In this algorithm, waveform parameterization based on peak threshold retracking is applied to the Ka-band waveform. From this parameterization, a tracking offset and backscatter estimate are determined. Tests are made on the extent of the tracking offset, and extreme values are flagged as retracking failures. The sea-ice waveform amplitude is determined by finding the maximum value of the waveform samples and the tracking offset is determined by finding the point on the waveform (by interpolation) where the waveform amplitude exceeds a threshold determined from the above sea-ice amplitude. A tracking offset is determined. The Centre Of Gravity offset correction must be included in the range measurement as the correction is not available separately in the L2 product. • Amplitude → Sigma0 • Tracking offset → altimeter range • Centre Of Gravity offset correction → correction to altimeter range measurement N.B.: Please note that ice1, sea ice and ice2 retrackings have been lightly validated and that these algorithms should be tuned to Ka-band.
Altimeter Instrument Corrections	consistent with MLE4 retracking
Saral/AltiKa Radiometer Parameters	Using on-board calibration
	.../...

Model	Product version "T" Patch1
Dry Troposphere Range Correction	From ECMWF atmospheric pressures and model for S1 and S2 atmospheric tides
Wet Troposphere Range Correction from Model	From ECMWF model
Ionosphere correction	Based on Global Ionosphere TEC Maps from JPL
Sea State Bias Model	3.5% of SWH values
Mean Sea Surface	MSS_CNES-CLS11
Mean Dynamic Topography	MDT_CNES-CLS09
Geoid	EGM96
Bathymetry Model	DTM2000.1
Inverse Barometer Correction	Computed from ECMWF atmospheric pressures after removing S1 and S2 atmospheric tides
Non-tidal High-frequency De-aliasing Correction	Mog2D high resolution ocean model on (I)GDRs. None for OGDRs. Ocean model forced by ECMWF atmospheric pressures after removing S1 and S2 atmospheric tides.
Tide Solution 1	GOT4.8
Tide Solution 2	FES2004 + S1 and M4 ocean tides. S1 and M4 load tides ignored
Equilibrium long-period ocean tide model.	From Cartwright and Taylor tidal potential.
Non-equilibrium long-period ocean tide model.	Mm, Mf, Mtm, and Msqm from FES2004
Solid Earth Tide Model	From Cartwright and Taylor tidal potential.
Pole Tide Model	Equilibrium model
Wind Speed from Model	ECMWF model
Altimeter Wind Speed	Derived from Jason-1 data - not to be used with Patch1 products
Trailing edge variation Flag	Derived from Matching Pursuit algorithm (from J. Tournadre, IFREMER) - not to be used with Patch1 products
	.../...

Model	Product version "T" Patch1
Ice flag	Derived from comparison of the model wet tropospheric correction to a dual-frequency wet tropospheric correction retrieved from radiometer brightness temperatures, with a default value issued from a climatology table

Table 5: Models and standards adopted for the Saral/AltiKa version "T" products (using Patch 1). Adapted from [4]

3. Data coverage and edited measurements

As Saral/AltiKa is the first altimeter using a Ka-band frequency and as this frequency is more sensitive to rain and cloud which can lead to signal attenuation, it was expected that there are more missing or rejected data than for altimeters using Ku-band frequency.

3.1. Missing measurements

3.1.1. Over land and ocean

Determination of missing measurements relative to the theoretically expected orbit ground pattern is an essential tool to detect missing telemetry or satellite events for instance. Applying the same procedure for Saral/AltiKa and Jason-2, the comparison of the percentage of missing measurements has been performed.

AltiKa can use several on board tracking modes: Median, EDP (Earliest Detectable Part) and Diode/DEM. Median mode is similar to the one used by Envisat and for most cycles of Jason-2. EDP tracker should improve the tracker behavior above continental ice surfaces and hydrological zones. Finally, Diode/DEM mode is a technique using information coming from Diode and a digital elevation model available on board. It was already tested on Jason-2. For more information about the different on board tracker algorithms see [9]. The information about the acquisition / tracking mode used is available in the GDR (fields alt_state_flag_acq_mode_40hz and alt_state_flag_tracking_mode_40hz).

Considering all surface types, Saral/AltiKa has more data available than Jason-2 (which uses most of the time (and after its first year always) the median tracker), independently from the tracker mode used for Saral. Figure 1 shows the percentage of available measurements for Saral/AltiKa and Jason-2 (all surfaces) computed with respect to a theoretical possible number of measurements. As long as a record exists for a given date, the measurement is accounted as present (though it may be that there is no useful science data). Differences appear on land surfaces as shown in figure 2. The missing data are highly correlated with the mountains location. Note that the routine calibrations for Saral/AltiKa are done over desert regions, such as Sahara, over Australia, in the south of Africa and over Asia (Mongolia). Therefore the percentage of available data is low in these regions. Otherwise Saral has more available data over land surface than Jason-2. This is probably due to the reduced footprint of Saral compared to Jason-2.

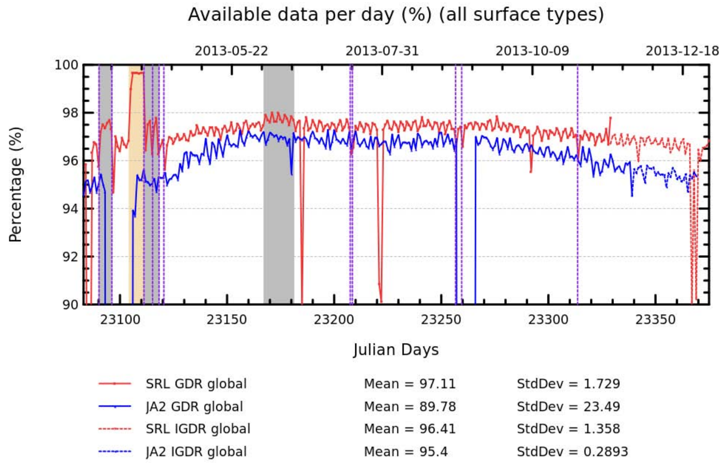

Figure 1: *Percentage of available measurements over all types of surfaces for SRL and JA2. Gray bands indicate when Saral/AltiKa uses EDP tracking, wheat color band indicates when Saral/AltiKa used Diode/DEM tracking. Vertical dotted lines in lilac indicate days with special calibrations.*

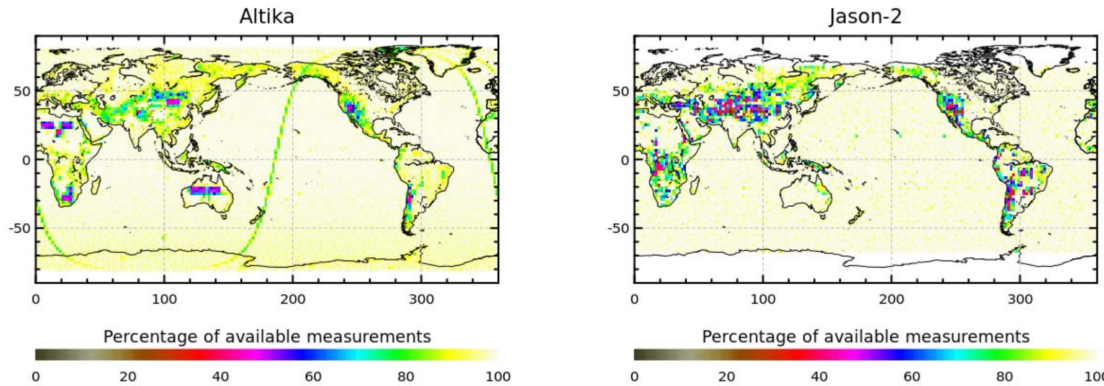

Figure 2: *Map of percentage of available measurements over land for Saral/AltiKa on cycle 3 and for Jason-2 on cycle 183 (right).*

3.1.2. Over ocean

When considering ocean surface, the same analysis method leads generally to slightly less available data for Saral/AltiKa compared to Jason-2 data coverage, as plotted on the left of figure 3. It represents the percentage of available measurements relative to the theory, when limited to ocean surfaces. Over the shown period, the mean value is about 93.2% for Jason-2, and 99.6% for Saral/AltiKa. Note that Jason-2 has two periods when it was in safe-hold mode, which explains the globally lower value for Jason-2. Saral/AltiKa had also some periods with reduced data availability. All these events are described on table 3.
On the right of figure 3, the percentage of available measurements is plotted without taking into account the days where instrumental events or other big anomalies occurred. The mean value of

available measurements increased to 99.97% for Jason-2 and 99.88% for Saral/AltiKa. These 0.1% of fewer data over ocean for Saral/AltiKa compared to Jason-2 are likely due to the impact of rain due to the Ka-band frequency. This exceeds largely the specifications for Saral/AltiKa, which were (see [24]) 95% of all possible over-ocean data during a 3-year period with no systematic gaps plus the specific Ka-band limitation (5% of measurements may be not achieved due to rain rate > 1.5 mm/h according to geographic areas).
Combining the location of the missing ocean data and information of the global precipitation for the month of May 2013 (figure 4), shows indeed for Saral/AltiKa (on the left) a strong correlation between missing data and regions with precipitation. This is not the case for Jason-2 (right side), note also that during May 2013, Jason-2 had some issues with the TM receiver, which explains most of the missing Jason-2 data on the figure.

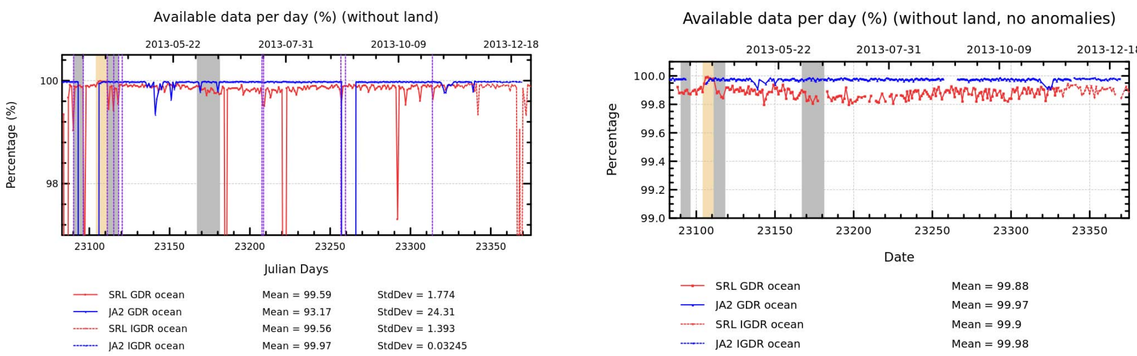

Figure 3: *Cycle per cycle percentage of available measurements over ocean (left) and without anomalies (right). Lilac vertical lines, indicate days with special calibrations, which can be over ocean.*

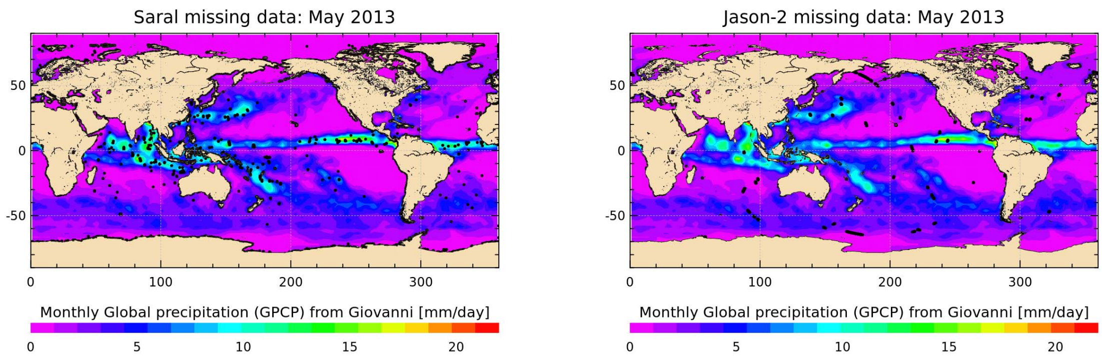

Figure 4: *Map of missing data for Saral/AltiKa (left) and Jason-2 (right) for May 2013 superposed on global precipitation for the same period. The global precipitation analyses were produced with the Giovanni on-line data system, developed and maintained by the NASA GES DISC.*

3.2. Edited measurements

3.2.1. Editing criteria definition

Editing criteria are used to select valid measurements over ocean. The editing process is divided into 4 parts. First, only measurements over ocean and lakes are kept (see section 3.2.2.). Second, some flags are used as described in section 3.2.3.. Note that currently no rain flag is available in the GDR products. But most measurements corrupted by rain are well detected by other altimeter parameter criteria. Then, threshold criteria are applied on altimeter, radiometer and geophysical parameters and are described in the table 6. Moreover, a spline criterion is applied to remove the remaining spurious data. For each criterion, the day per day percentage of edited measurements has been monitored. This allows detection of anomalies in the number of removed data, which could come from instrumental, geophysical or algorithmic changes. Cycle per cycle statistics of edited data are also routinely monitored, but not shown here, as only a few cycles are available. Note, that the altimeter wind speed (present in the GDR-T Patch1 data) is not usable.

Parameter	Min thresholds	Max thresholds	mean edited
Sea surface height	$-130\,m$	$100\,m$	0.46%
Sea level anomaly	$-10\,m$	$10.0\,m$	0.68%
Number measurements of range	20	*Not applicable*	1.11%
Standard deviation of range	0	$0.2\,m$	1.49%
Squared off-nadir angle	$-0.2\,deg^2$	$0.15\,deg^2$	0.31%
Dry troposphere correction	$-2.5\,m$	$-1.9\,m$	0.00%
Inverted barometer correction	$-2.0\,m$	$2.0\,m$	0.00%
Radiometer wet troposphere correction	$-0.5m$	$-0.001\,m$	0.12%
Significant wave height	$0.0\,m$	$11.0\,m$	0.38%
Sea State Bias	$-0.5\,m$	$0.0\,m$	0.32%
Number measurements of Ka-band Sigma0	20	*Not applicable*	1.04%
Standard deviation of Ka-band Sigma0	0	$1.0\,dB$	0.94%
Ka-band Sigma0	$3.0\,dB$	$30.0\,dB$	0.38%
Ocean tide	$-5.0\,m$	$5.0\,m$	0.01%
Equilibrium tide	$-0.5\,m$	$0.5\,m$	0.00%
Earth tide	$-1.0\,m$	$1.0\,m$	0.00%
			.../...

Parameter	Min thresholds	Max thresholds	mean edited
Pole tide	$-0.15\,m$	$0.15\,m$	0.00%
All together	-	-	2.6%

Table 6: *E*diting criteria, statistics obtained for cycles 1 to 7.

3.2.2. Selection of measurements over ocean and lakes

In order to remove data over land, a land-water mask is used (surface_type in the GDR products). Only measurements over ocean or lakes are kept. This allows to keep data near the coasts and so to detect potential anomalies in these areas. Furthermore, there is no impact on global performance estimations since the most significant results are derived from analyzes in deep ocean areas. Figure 5 shows the day per day percentage of measurements eliminated by this selection. The curve is quite stable. But it reveals the impact of the different altimeter tracking modes: when the DIODE/DEM (digital elevation model) tracking mode is used (wheat colored stripe), slightly more data are edited by land flag.

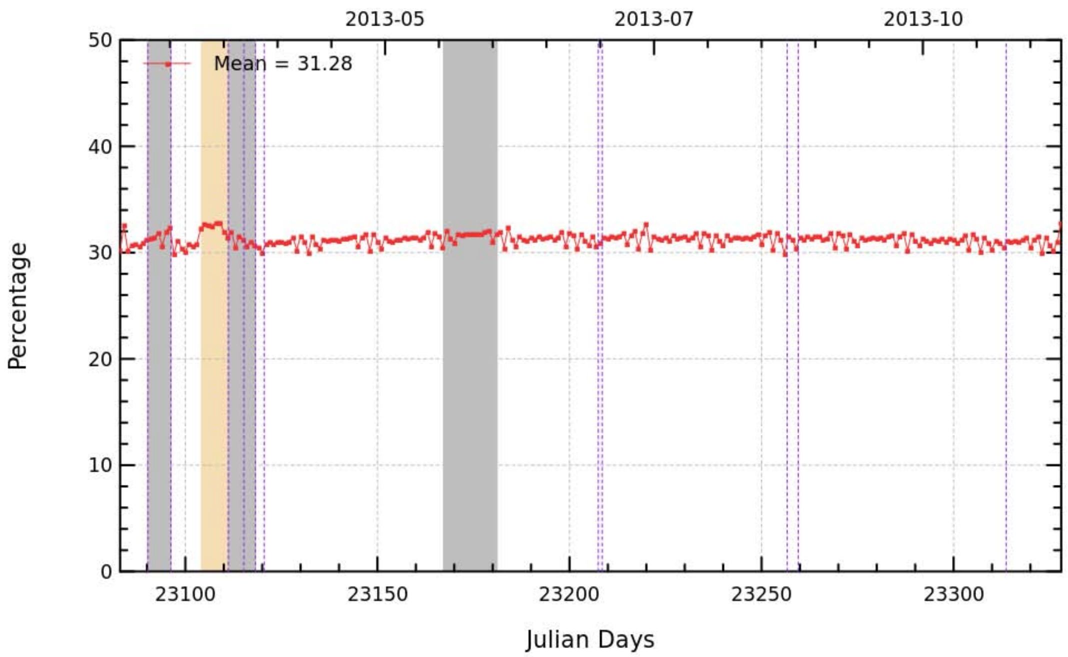

Figure 5: *Day per day percentage of eliminated measurements during selection of ocean/lake measurements. Gray bands indicate when Saral/AltiKa uses EDP tracking, wheat color band indicates when Saral/AltiKa used Diode/DEM tracking, elsewhere Median tracking is used. Vertical dotted lines in lilac indicate days with special calibrations.*

3.2.3. Flagging quality criteria: Ice flag

The ice flag (ice_flag in the GDR products) is used to remove the sea ice data. Figure 6 shows the day per day percentage of measurements edited by this criterion. Over the shown period, no anomalous trend is detected (figure 6 left) but the nominal seasonal cycle is visible. Considering the black curve, which indicates the percentage of edited Saral/AltiKa data without geographical selections, the minima (∼16% of edited data) appear during the beginning of the mission (here March) and in September. These are also the periods, where the antarctic respectively the arctic sea ice extension is minimum. The maxima (∼20% of edited data) of the curve are around May/June and October/November. These are the periods, where both arctic and antarctic sea ice extension have approximately mid-values. When limited to |latitude| <66°, Saral/AltiKa and Jason-2 percentage of data edited by sea ice have a similar annual cycle, which is correlated to the antarctic sea ice extension. Indeed, the maximum number of points over ice is reached during the southern winter (ie. August - October). When limiting measurements between 66° north and south, thawing of sea ice, which takes place especially in northern hemisphere over 66°N, can not be detected. The percentage of measurements edited by ice flag is plotted in the right of figure 6 for a period of 8 months.

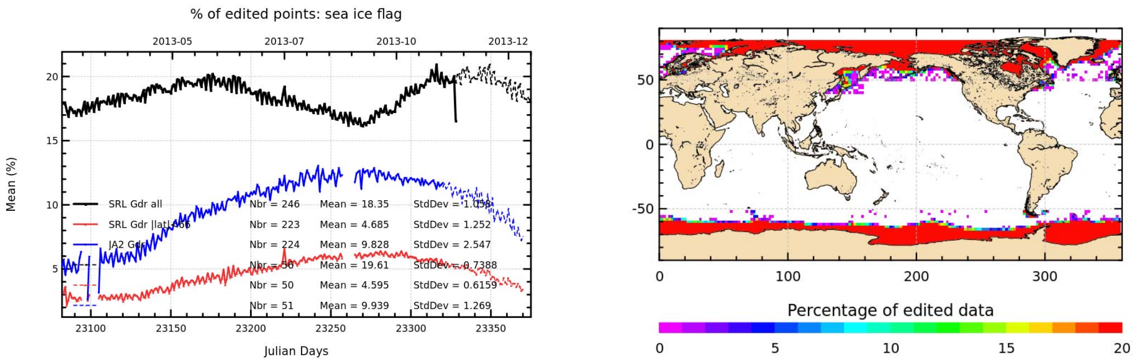

Figure 6: *Percentage of edited measurements by ice flag criterion. Left: Daily statistics (plain lines: GDR, dotted lines: IGDR) for Saral/AltiKa (all latitudes: black, limited to 66° latitude: red) and Jason-2 (blue). Right: Map over a 8 months period (cycles 1 to 7).*

Though the sea ice flag of Saral/AltiKa (top left of figure 7) shows similar sea ice extent for Antarctic as the one distributed by the NSIDC (National Snow and Ice Data Center) (top right of figure 7), it is not yet tuned. The surface type flag is set to ocean over ice shelfs. But the ice flag does not flag all the ice shelfs as ice (see figure 7). Using the thresholds criteria listed in table 6 (or also in the user handbook [[4]]), allows to edited the ice over the ice shelfs, as well as some ice at the limit between sea ice and open ocean. Nevertheless, it is possible that not all measurements impacted by the presence of ice are edited.

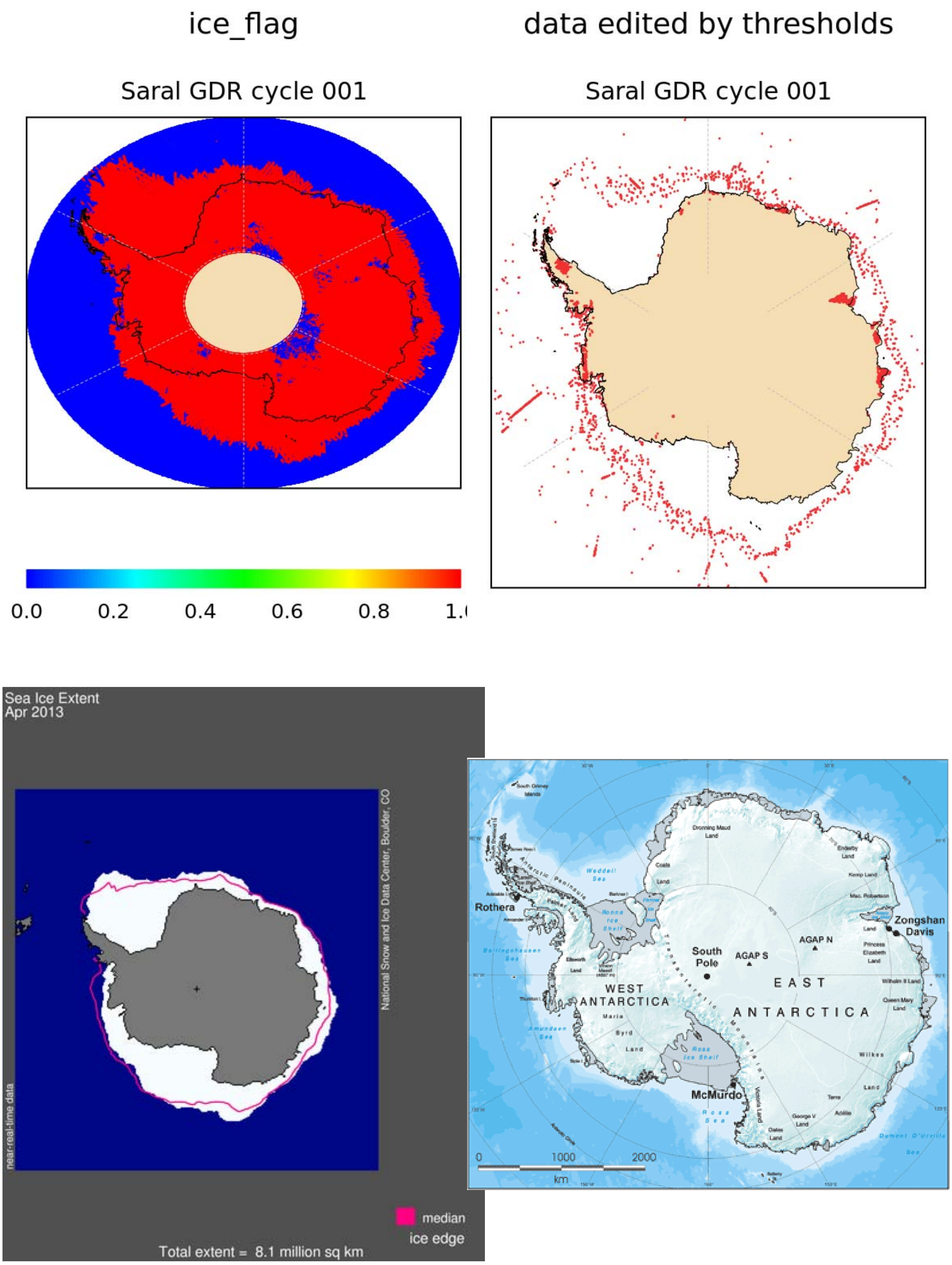

Figure 7: *Data edited over Antarctic by ice flag for Saral/AltiKa cycle 001 (top left), data edited by thresholds criteria (after removing land and ice) on top right, sea ice extension in April 2013 (downloaded from ftp://sidads.colorado.edu/DATASETS/NOAA/G02135/Apr/) on bottom left, map of Antarctic downloaded from http://planetearth.nerc.ac.uk/news/story.aspx?id=423 on bottom right.*

3.2.4. Threshold criteria: Global

Instrumental parameters have also been analyzed concerning their quality from comparison with thresholds, after having selected only ocean/lakes measurements and removing sea ice with the ice flag. Note that no measurement is edited by the following corrections : dry troposphere correction, inverted barometer correction (including DAC), equilibrium tide, earth and pole tide. Indeed these parameters are only verified in order to detect data at default values, which might happen during a processing anomaly.

The percentage of measurements edited using each criterion is monitored on a day per day basis (figure 8). The mean percentage of edited measurements is about 2.6% (2.4% when |latitude| is limited to 66°). This is about 1% below the Jason-2 figure. Some weak variation is visible.

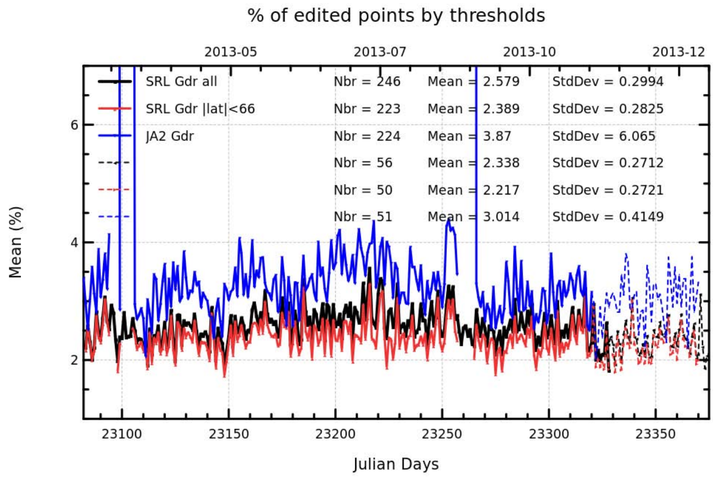

Figure 8: *Daily statistics of percentage of edited measurements by threshold criteria (plain lines: GDR, dotted lines: IGDR) for Saral/AltiKa (all latitudes: black, limited to 66° latitude: red) and Jason-2 (blue).*

3.2.5. Threshold criteria: 40-Hz measurements number

The percentage of edited measurements because of a too low number of 40-Hz measurements is represented on the left side of figure 9. No trend neither any anomaly has been detected. The statistics, when limiting the latitude to less than 66° are slightly reduced. The percentage of edited data is similar for Saral/AltiKa and Jason-2

The map of measurements edited by 40-Hz measurements number criterion is plotted on right side of figure 9 and shows correlation with heavy rain and wet areas (in general regions with disturbed sea state), as well as regions close to sea ice. Indeed waveforms are distorted by rain cells, which makes them often meaningless for SSH calculation. As a consequence, edited measurements due to several altimetric criteria are often correlated with wet areas.

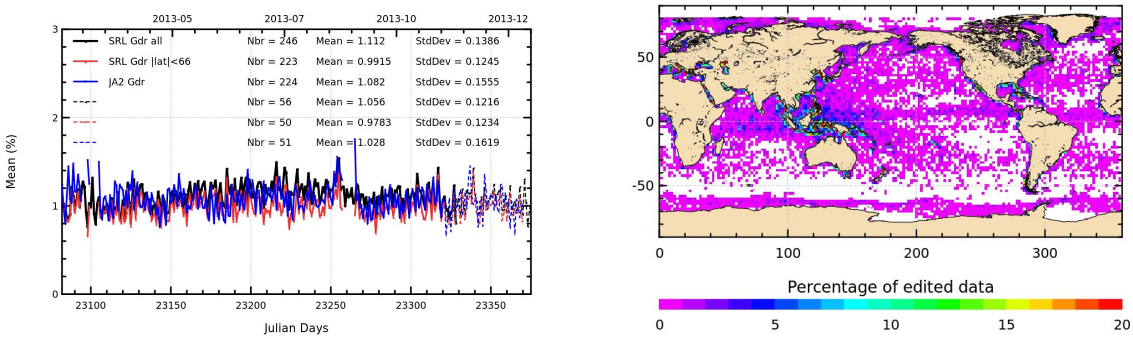

Figure 9: *Percentage of edited measurements by 40-Hz measurements number criterion (20-Hz for Jason-2). Left: Daily statistics for Saral/AltiKa (all latitudes: black, limited to 66° latitude: red) and Jason-2 (blue). Right: Map over a 8 months period (cycles 1 to 7).*

3.2.6. Threshold criteria: 40-Hz measurements standard deviation

The percentage of edited measurements due to 40-Hz measurements standard deviation criterion (~1.5%) is shown in figure 10 (left). For some days, more data are edited by this criterion. This is mostly due to maneuver burns (see also table 2), indicated by lilac vertical lines. In this case, the data a few minutes before and after the maneuver are edited. The right side of figure 10 shows a map of measurements edited by the 40-Hz measurements standard deviation criterion. As in section 3.2.5., edited measurements are correlated with wet areas.

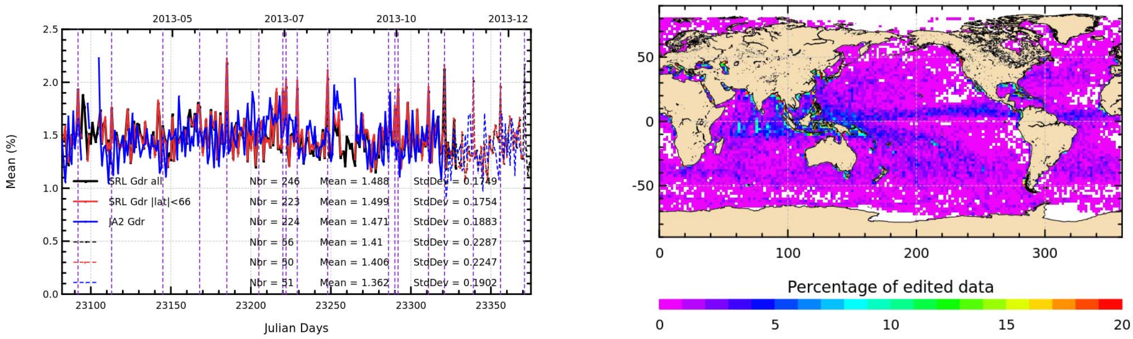

Figure 10: *Percentage of edited measurements by 40-Hz measurements standard deviation criterion (20-Hz for Jason-2). Left: Daily statistics for Saral/AltiKa (all latitudes: black, limited to 66° latitude: red) and Jason-2 (blue). Lilac vertical lines indicate days with maneuvers on Saral/AltiKa. Right: Map over a 8 months period (cycles 1 to 7).*

3.2.7. Threshold criteria: Significant wave height

The percentage of edited measurements due to significant wave height criterion is represented in figure 11. It is about 0.38%. As for standard deviation of 40-Hz data, more data are edited by this criterion for some days. This is mostly due to maneuver burns (see also table 2), indicated by lilac vertical lines. In this case, the data a few minutes before and after the maneuver are edited. Note that for Jason-2, roughly 0.66% of data are edited by SWH out of thresholds. This is mainly due to Jason-2 having almost twice as much SWH data at default values than Saral/AltiKa. Figure 11 (right part) shows that measurements edited by SWH criterion are especially found in wet regions.

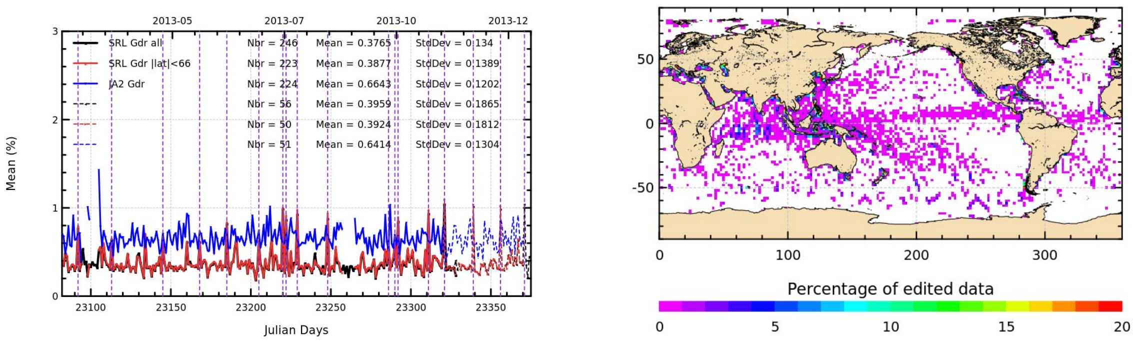

Figure 11: *Percentage of edited measurements by SWH criterion. Left: Daily statistics (plain lines: GDR, dotted lines: IGDR) for Saral/AltiKa and Jason-2 (blue). Lilac vertical lines indicate days with maneuvers on Saral/AltiKa. Right: Map over a 8 months period (cycles 1 to 7).*

3.2.8. Backscatter coefficient

The percentage of edited measurements due to backscatter coefficient criterion is represented in figure 12. It is about 0.38% (whether considering all latitudes or limiting to 66°), compared to 0.61% for Jason-2. It is also impacted by most of the maneuvers (see vertical lilac lines). As for SWH, Jason-2 has almost twice as much backscattering values at default values than Saral/AltiKa. The right part of figure 12 shows that measurements edited by backscatter coefficient criterion are especially found in wet regions.

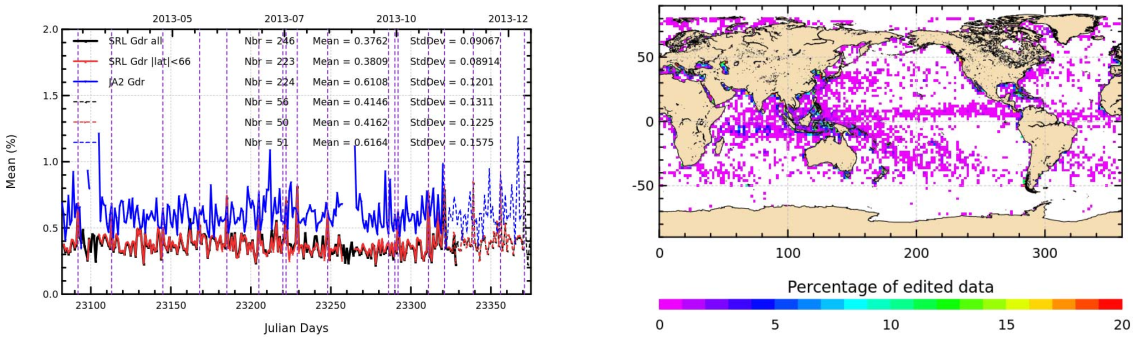

Figure 12: *Percentage of edited measurements by Sigma0 criterion. Left: Daily statistics for Saral/AltiKa (all latitudes: black, limited to 66° latitude: red) and Jason-2 (blue). Lilac vertical lines indicate days with maneuvers on Saral/AltiKa. Right: Map over a 8 months period (cycles 1 to 7).*

3.2.9. Backscatter coefficient: 40 Hz standard deviation

The percentage of edited measurements due to 40 Hz backscatter coefficient standard deviation criterion is represented in figure 13. It is about 0.93%, compared to 2.02% for Jason-2. The right part of figure 12 shows that measurements edited by 40 Hz backscatter coefficient standard deviation criterion are especially found in wet regions, but also elsewhere.

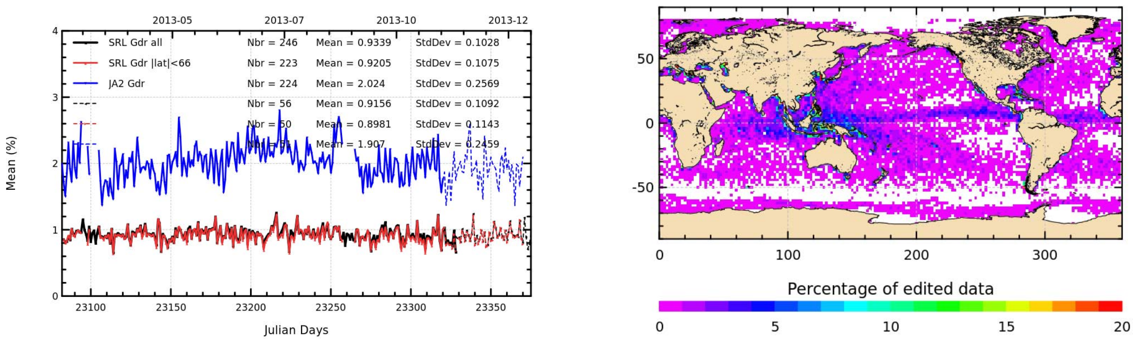

Figure 13: *Percentage of edited measurements by 40 Hz Sigma0 standard deviation criterion. Left: Daily statistics for Saral/AltiKa (all latitudes: black, limited to 66° latitude: red) and Jason-2 (blue). Right: Map over a 8 months period (cycles 1 to 7).*

3.2.10. Radiometer wet troposphere correction

The percentage of edited measurements due to radiometer wet troposphere correction criterion is represented in figure 14. It is about 0.12%. Jason-2 edits generally slightly less data (except after safe-hold modes, when the radiometer is switched on some time after the altimeter). The edited data for Saral/AltiKa are generally due to wet troposphere wetter than the −0.5 m threshold.

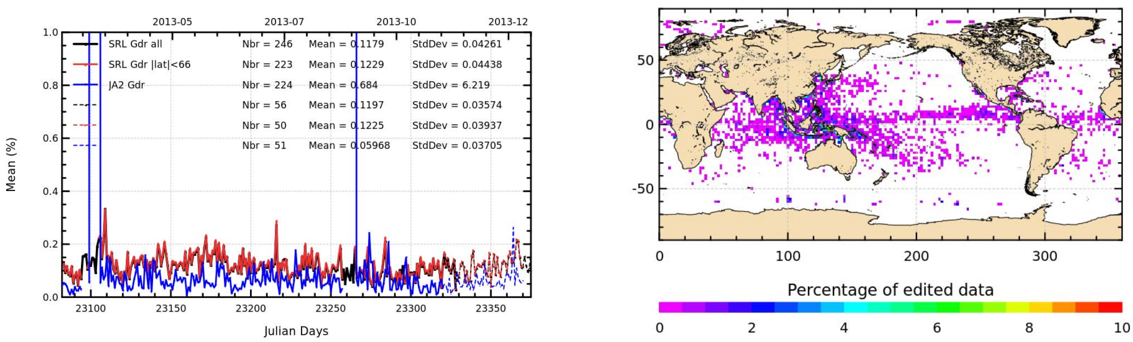

Figure 14: *Percentage of edited measurements by radiometer wet troposphere criterion. Left: Daily statistics for Saral/AltiKa (all latitudes: black, limited to 66° latitude: red) and Jason-2 (blue). Right: Map over a 8 months period (cycles 1 to 7).*

3.2.11. Square off-nadir angle

The percentage of edited measurements due to square off-nadir angle criterion is represented in figure 15. It is about 0.31% (when considering all latitudes, and 0.32% when considering only data with latitudes up to 66°). As for other parameters, maneuvers have an impact on the number of edited data. The map 15 shows that edited measurements are mostly found in wet regions or places, where the maneuvers take place (Indian Ocean).

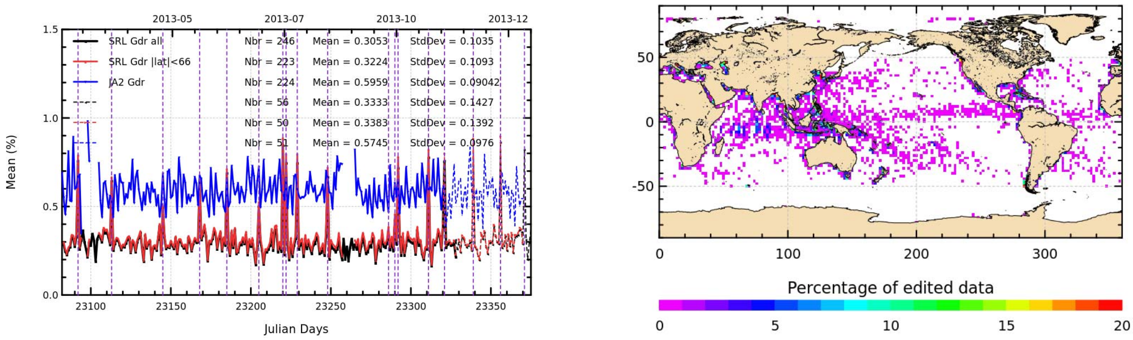

Figure 15: *Percentage of edited measurements by square off-nadir angle criterion. Left: Daily statistics for Saral/AltiKa (all latitudes: black, limited to 66° latitude: red) and Jason-2 (blue). Lilac vertical lines indicate days with maneuvers on Saral/AltiKa. Right: Map over a 8 months period (cycles 1 to 7).*

3.2.12. Sea state bias correction

The percentage of edited measurements due to sea state bias correction criterion is represented in figure 16. The percentage of edited measurements is about 0.32% and increases when maneuver take place. The percentage of edited Jason-2 by sea state bias criteria is around twice as high, mainly due to more data at default value.
The map 16 shows that edited measurements are mostly found in wet regions.

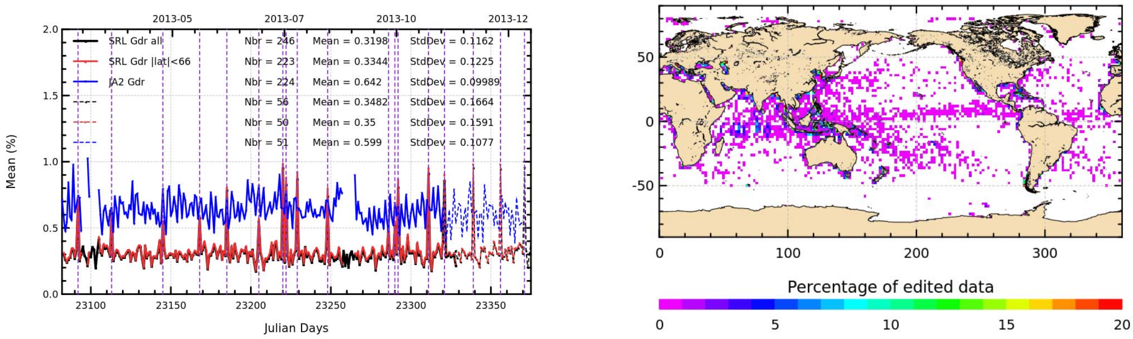

Figure 16: *Percentage of edited measurements by sea state bias criterion. Left: Daily statistics for Saral/AltiKa (all latitudes: black, limited to 66° latitude: red) and Jason-2 (blue). Lilac vertical lines indicate days with maneuvers on Saral/AltiKa. Right: Map over a 8 months period (cycles 1 to 7).*

3.2.13. Ocean tide correction

The percentage of edited measurements due to ocean tide correction criterion is represented in figure 17. It is less than 0.01%. The ocean tide correction is a model output, there should therefore be no edited measurements. Indeed there are no measurements edited in open ocean areas, but only very few near coasts (Alaska, Labrador). These measurements are mostly at default values.

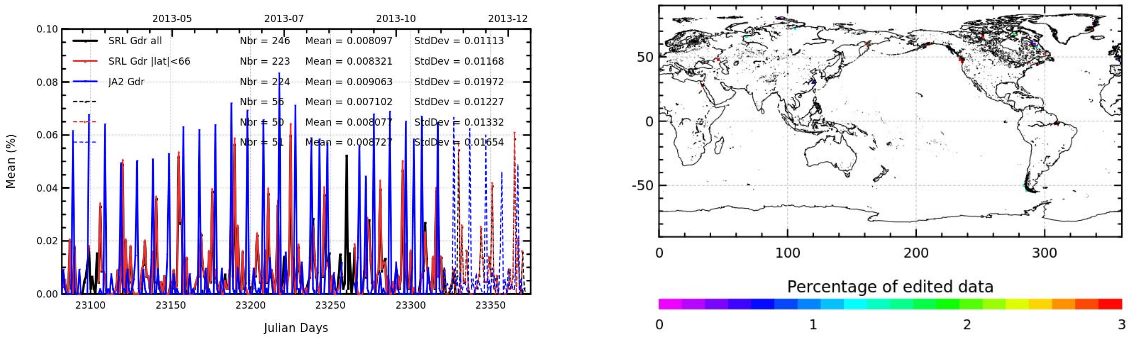

Figure 17: *Percentage of edited measurements by ocean tide criterion. Left: Daily statistics for Saral/AltiKa (all latitudes: black, limited to 66° latitude: red) and Jason-2 (blue). Right: Map over a 8 months period (cycles 1 to 7).*

3.2.14. Sea surface height

The percentage of edited measurements due to sea surface height (orbit - Ka-band range) criterion is represented in figure 18. It is about 0.46% (considering all latitudes and 0.49% considering only data with latitudes up to 66°). The measurements edited by sea surface height criterion are mostly found near coasts in equatorial and mid-latitude regions, as well as for regions with low significant wave heights (see map 18). The majority of the edited measurements has defaulted range values.

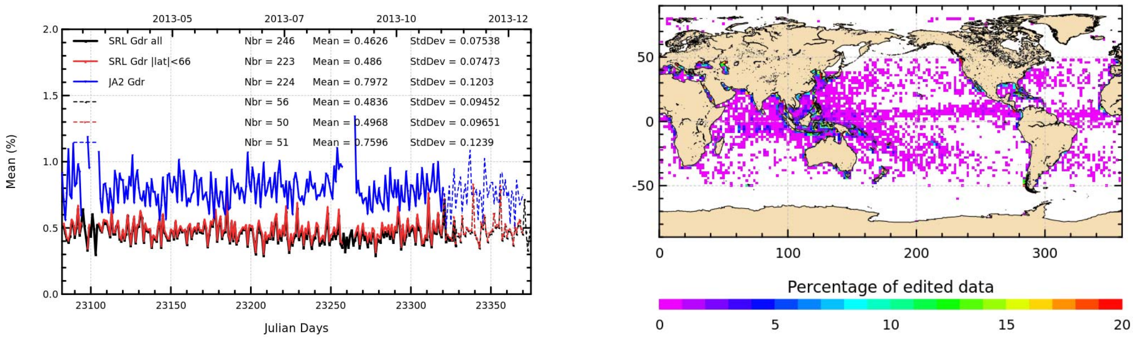

Figure 18: *Percentage of edited measurements by sea surface height criterion. Left: Daily statistics for Saral/AltiKa (all latitudes: black, limited to 66° latitude: red) and Jason-2 (blue). Right: Map over a 8 months period (cycles 1 to 7).*

3.2.15. Sea level anomaly

The percentage of edited measurements due to sea level anomaly criterion is represented in figure 19. It is about 0.68% (considering all latitudes and 0.61% considering only data with latitudes up to 66°). During maneuvers, the percentage of edited data is generally slightly increased.
Whereas the map in figure 19 allows us to plot the measurements edited due to sea level anomaly out of thresholds (after applying all other threshold criteria). There are only very few measurements, principally located in Caspian Sea, but also near Antarctic, when data were neither edited by surface type flag nor by ice flag.

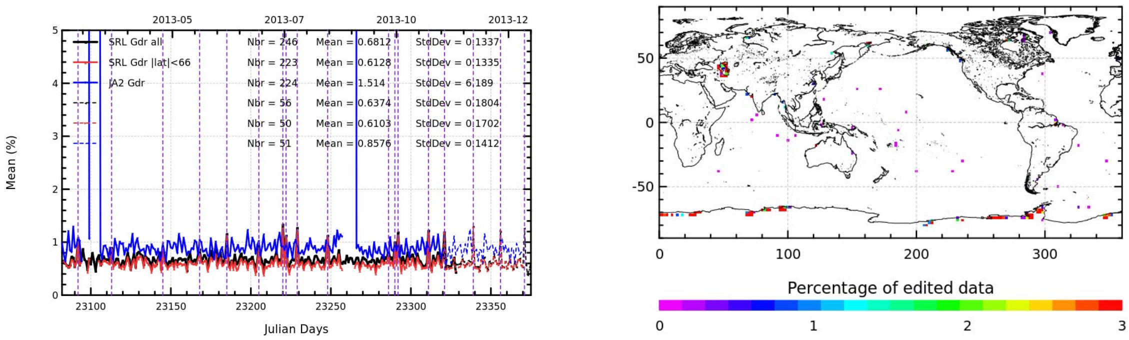

Figure 19: *Percentage of edited measurements by sea level anomaly criterion. Left: Daily statistics for Saral/AltiKa (all latitudes: black, limited to 66° latitude: red) and Jason-2 (blue). Right: Map over a 8 months period (cycles 1 to 7).*

3.3. Level of edited data and pertinence of chosen editing: Comparison with other altimeter missions

In the previous sub-chapters the individual editing criteria were shown in detail. Comparing the maps of edited data for Saral/AltiKa and Jason-2 for the same month (May 2013) on figure 20, shows that besides data edited by sea ice, both missions have data edited mostly in wet regions. At first glance the Saral/AltiKa map seems to have more edited data, which is mainly due to the fact that Saral/AltiKa covers regions up to 81° latitude, and therefore edits more sea ice. But for ocean regions please note, that the ground track separation at the equator is quite small (75 km) and a month period does not cover an entire repeat cycle of Saral/AltiKa, whereas Jason-2 covers during this period 3 repeat cycles. In some regions the edited Jason-2 data are therefore superposed for several cycles. Also the ground track separation at the equator is around 315 km for Jason-2, contributing to the impression that the Jason-2 map shows less edited data over ocean than Saral.

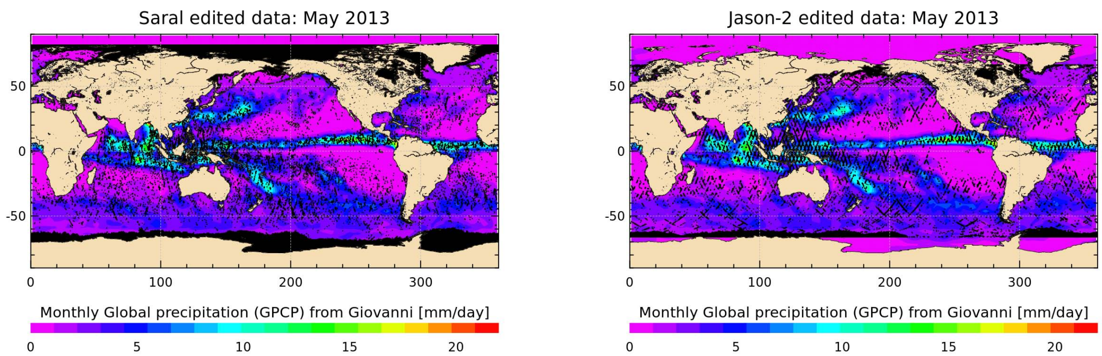

Figure 20: *Map of edited data for Saral/AltiKa (left) and Jason-2 (right) for May 2013 superposed on global precipitation for the same period. The global precipitation analyses were produced with the Giovanni on-line data system, developed and maintained by the NASA GES DISC.*

This is confirmed when computing the map of percentage of valid data over the first 3 cycles of Saral/AltiKa (figure 21). Indeed, Jason-2 has slightly less valid data in wet regions (especially around Indonesia). Showing the percentage of edited data in function of latitude bands (figure 22) yields that Jason-2 edits more data in northern hemisphere and tropical regions than Saral/AltiKa, whereas in southern hemisphere the percentage of edited data is equivalent for both missions. For comparison a curve for Envisat is also shown, the data are from the same season, but from 3 years earlier. Envisat edits even less data than Saral/AltiKa.

Figure 23 shows the difference maps between valid data from Saral/AltiKa and Jason-2 (left) and Saral/AltiKa and Envisat (right). Saral/AltiKa has more valid data than Jason-2 in the region around Indonesia, which is generally quite wet. The reason for this loss in valid data for Jason-2 might be due to the fact that Jason-2 is in a higher orbit (∼ 1336 km) than Saral or Envisat (∼ 800 km), therefore its footprint is larger and therefore more impacted by perturbations (for example by rain). In this region some Jason-2 1 Hz parameters are at default value and therefore edited. When comparing Saral/AltiKa and Envisat, it is Envisat which has more valid data than Saral/AltiKa, both satellites are at the same altitude, but Saral/AltiKa has nevertheless a smaller footprint (as it has a higher vertical resolution). But as Saral/AltiKa uses Ka-band instead of the Ku-band used for the other altimeters, it is more sensitive to rain. The loss of valid Saral/AltiKa data

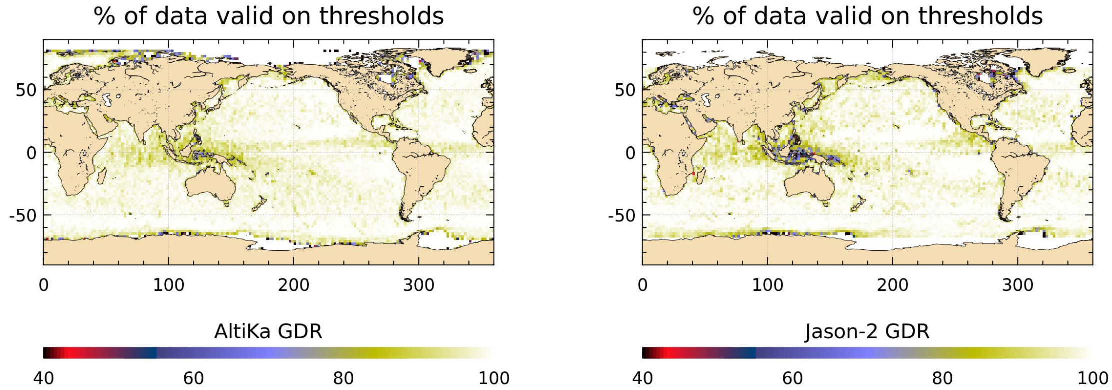

Figure 21: *Percentage of valid data for Saral (left) and Jason-2 (right). Saral cycles 1 to 3, Jason-2 over the same period.*

compared to Envisat data seems therefore due to this Ka-band sensitivity to rain. The number of valid Saral/AltiKa data which remain in wet region exceeds the pre-launch expectations. This very good behavior in wet regions (concerning available and valid data) is due to margins applied in the link budget (see [23]), therefore the in-flight signal-to-noise ratio is better than expected. Nevertheless keep in mind, that the Envisat data are from a different period (3 years earlier) than Saral/AltiKa, it is therefore likely, that the rain condition are not the same, though the same season was chosen.

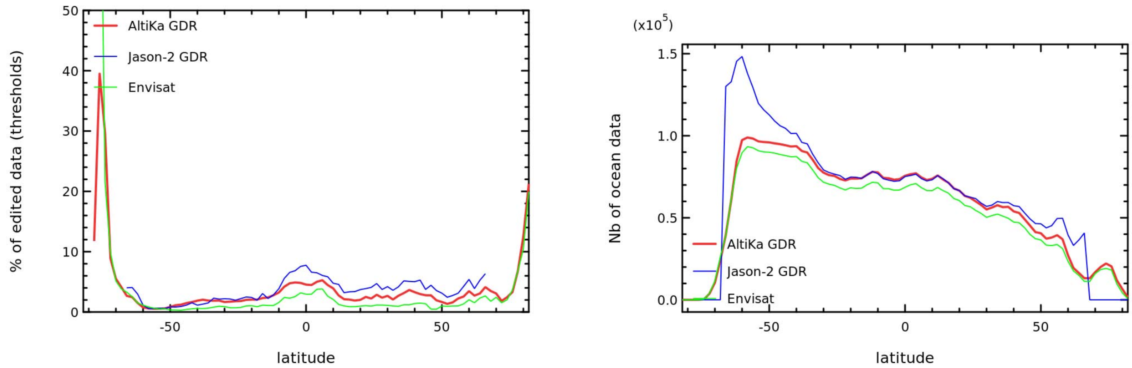

Figure 22: *Percentage of edited data in function of latitude bands (left). Number of ocean data in function of latitude bands (right). Latitude bands have a width of 2°. Saral cycles 1 to 3, Jason-2 over the same period. Envisat for the same period, but 3 years earlier.*

Finally, in order to assess if the editing criteria are well chosen (though they are not perfect), variance of SLA is shown for Saral/AltiKa, Jason-2 and Envisat (3 years earlier) in function of 2° latitude bands (left of figure 24). Only valid data are chosen with bathymetry less than -1000 m and ocean variability less than 0.2 m (which removes the strongest currents, such as Gulf Stream). Saral/AltiKa and Jason-2 show very similar results. Envisat results have roughly the same features (as Saral/AltiKa and Jason-2), such as higher variance around 35°N (likely not all of the Gulf Stream and Kuroshio Current were removed by the selection of ocean variability less than 0.2 m),

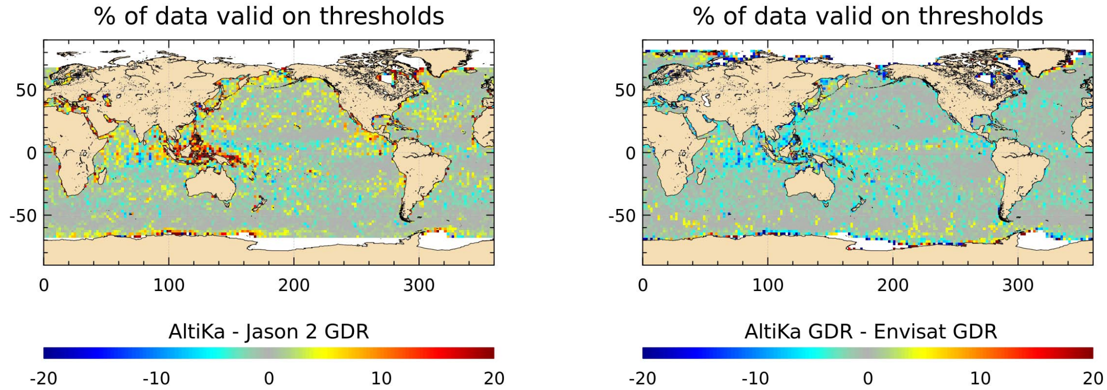

Figure 23: *Percentage of difference of valid data for Saral (left) and Jason-2 (right). Saral cycles 1 to 3, Jason-2 over the same period. Envisat for the same period, but 3 years earlier.*

but in detail the Envisat SLA variance shows differences from the other mission (as Envisat are from an earlier period). Another quality criteria is the standard deviation of the ascending/descending SSH differences at mono-mission crossover points. It should ideally be low. On the right side of figure 24 this value is shown for the 3 missions in function of 4° latitude bands. In addition to valid points, only data fulfilling the following selections were chosen: |latitude| <50°, bathymetry less than -1000 m and ocean variability less than 0.2 m. The performance of the three missions is similar, showing that editing criteria chosen for Saral/AltiKa allows the mission to obtain similar results as Jason-2 and Envisat. Note also that some algorithms for Saral/AltiKa are not yet tuned (for example sea state bias, radiometer wet troposphere correction, altimeter wind speed). Results using the future Patch2 version of Saral/AltiKa GDR-T (see also chapter 7.3.) will show even better results.

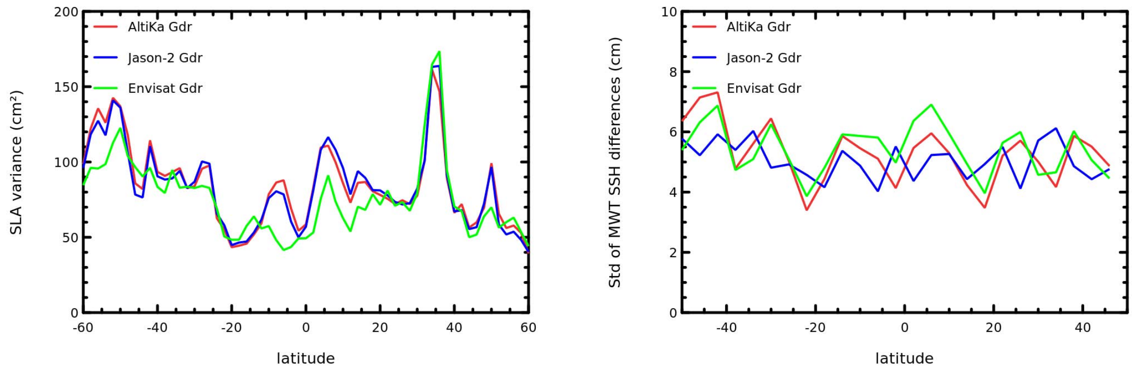

Figure 24: *Standard deviation of SLA (left, using radiometer wet troposphere correction) and SSH differences at crossovers (right, using model wet troposphere correction) in function of latitude bands. Saral cycles 1 to 3, Jason-2 over the same period. Envisat for the same period, but 3 years earlier. Only valid data with bathymetry < -1000m and ocean variability less than 0.2m are chosen.*

4. Monitoring of altimeter and radiometer parameters

4.1. Methodology

Both mean and standard deviation of the main parameters of **valid** Saral/AltiKa (GDR-T Patch1) data have been monitored since the beginning of the mission. Therefore ordinary daily statistics have been computed, but also box statistics with weighting of latitude. Indeed, as the measurement distribution is not homogeneous with latitude (see also right side of figure 22), this can skew the statistics to values of the data in data-rich latitudes. Moreover, a comparison with Jason-2 parameters has also been performed. As both satellites are on different ground tracks no point-to-point comparisons (as it was possible during flight formation phase between Jason-1 and Jason-2) are feasible. Comparisons are done by superposing monitoring of daily or cycle per cycle statistics or histograms. Furthermore, parameters are averaged on a grid-structure for both satellites, which are then subtracted one from the other. Another mean of comparison are dispersion diagrams between Saral/AltiKa and Jason-2 data at 3h-crossover points.

Note that for daily monitoring of Jason-2 there are some gaps end of March/ early April, as well as in September 2013. This is due to safe-hold mode of the Jason-2 satellite.
Some monitoring show first GDR data (plain lines) and are continued with IGDR data (dotted lines).

4.2. 40 Hz Measurements

The monitoring of the number and standard deviation of 40 Hz elementary range measurements used to derive 1 Hz data is presented here. These two parameters are computed during the altimeter ground processing. For both Saral/AltiKa and Jason-2, before performing a regression to derive the 1 Hz range from 40 Hz or 20 Hz data, a MQE (mean quadratic error) criterion is used to select valid 40/20 Hz measurements. This first step of selection consists in verifying that the 40/20 Hz waveforms can be approximated by a Brown echo model (Brown, 1977 [3]) (Thibaut et al. 2002 [25]). Then, through an iterative regression process, elementary ranges too far from the regression line are discarded until convergence is reached. Thus, monitoring the number of 40/20 Hz range measurements and the standard deviation computed among them is likely to reveal changes at instrumental level.

4.2.1. 40 Hz measurements number

Number of elementary 40 Hz range measurements is close to 38.5 (black curve on figure 25). Before the correction of the PF/RF alignment (alignment between the platform and the radiofrequency axis) on 25th of April 2013 this value was slightly higher (around 38.6). Jason-2 has an average close to 19.6 as number of elementary 20 Hz range measurements (which is when multiplied by 2, higher than the value of Saral/AltiKa). It also shows smaller temporal variability. Note that before Patch1 version, the MQE threshold was not applied during the 40 Hz to 1 Hz compression (IGDR data till cycle 4, pass 394), the daily mean of the number of the elementary 40 Hz range measurements was 39.0. So in average 0.5 40 Hz elementary range measurements are removed during the 40 Hz to 1 Hz compression by the MQE criteria. These removed data might be due to perturbations in the footprint (rain, sigma bloom). For both missions, the number of elementary range measurements is correlated with the significant wave height. Figure 26 shows less elementary range measurements around Indonesia, the Mediterranean Sea and close to coasts, which are all regions of low significant wave heights (see also map of SWH 36) and therefore regions where sigma bloom may occur.

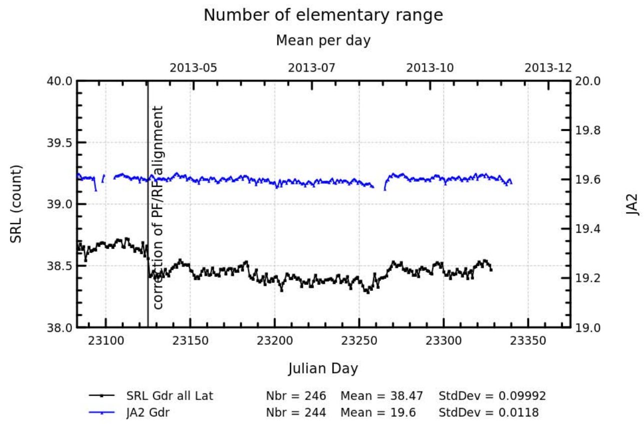

Figure 25: *Daily monitoring of mean of number of elementary Saral/AltiKa 40 Hz (left ordinate) and Jason-2 20 Hz (right ordinate) range measurements.*

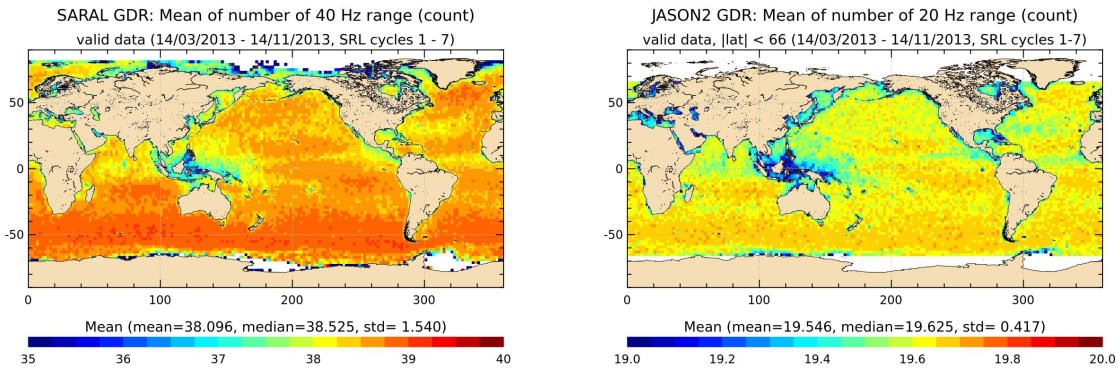

Figure 26: *Average map of number of Saral/AltiKa elementary 40 Hz range measurements (left) and Jason-2 elementary 20 Hz range measurement (right) over cycles 1 to 7.*

4.2.2. 40 Hz measurements standard deviation

Saral/AltiKa standard deviation of the 40 Hz measurements is 5.8 cm, whereas it is 8.0 cm for Jason-2 (right side of figure 27). Using latitude weighted box statistics (left side of figure 27), these values decrease to respectively 5.6 and 7.7 cm. These values are very close to the ones found when computing the power spectrum (see chapter 7.2.). The value of Saral/AltiKa is lower than the one of Jason-2 due to the altimeter band-width, which is 480 MHz for Saral/AltiKa instead of 320 MHz for Jason-2 (see [23]). As for the number of elementary range measurements, the standard deviation of the elementary range measurements are correlated to the significant wave height (see maps on figures 28 and 36).

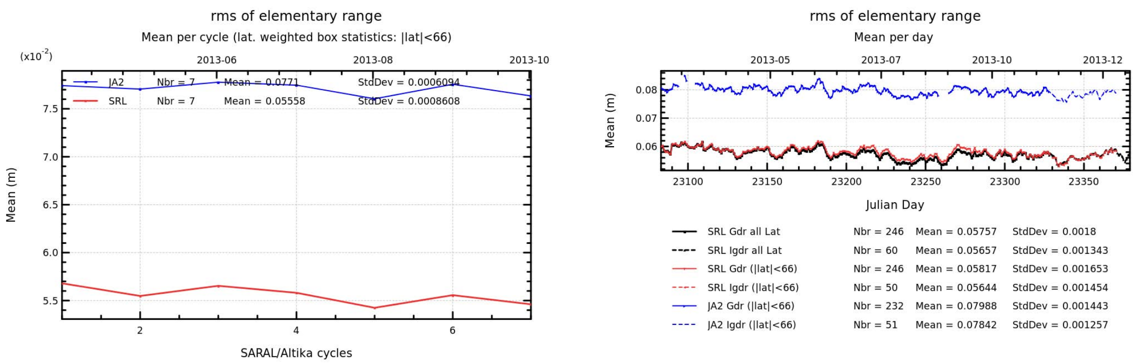

Figure 27: *Cyclic monitoring of rms of elementary 40/20 Hz range measurements for Saral/AltiKa and Jason-2 (left), computing latitude weighted box statistics. Daily mean of rms of elementary Saral/AltiKa 40 Hz and Jason-2 20 Hz range measurements (right). GDR data are plotted with plain lines, IGDR with dotted lines.*

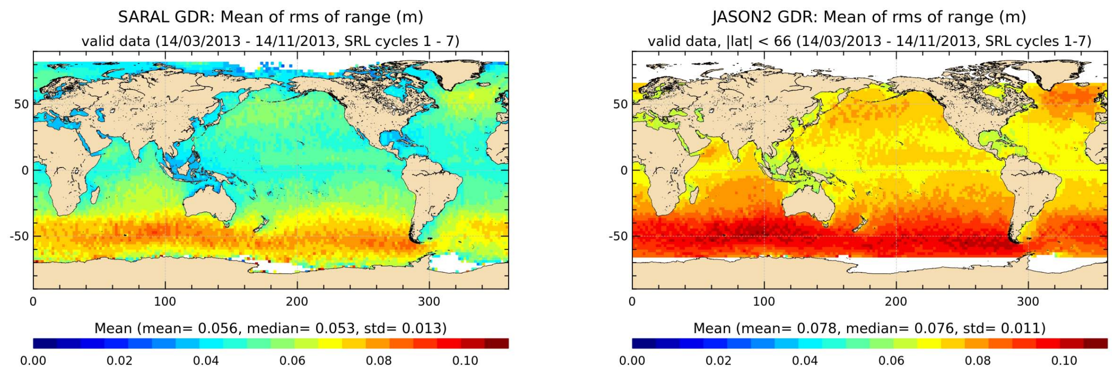

Figure 28: *Average map of rms of Saral/AltiKa elementary 40 Hz range measurements (left) and Jason-2 elementary 20 Hz range measurement (right) over cycles 1 to 7.*

4.3. Off-Nadir Angle from waveforms

The off-nadir angle is estimated from the waveform shape during the altimeter processing. The off-nadir angle, averaged on a daily basis, has been plotted for Saral/AltiKa and Jason-2 on the left side of figure 29, whereas the right side shows the daily standard deviation of the off-nadir angle from waveforms. In the beginning of the Saral/AltiKa mission the off-nadir angle from waveforms was slightly positive (around 0.003 degrees2), a X-cross calibration maneuver with $+0.3^{\circ}/-0.3^{\circ}$ in pitch and than $+0.3^{\circ}/-0.3^{\circ}$ in roll was done on 22th of April (see N. Stenou [23]). This allowed to determine that a correction of -0.045 degree in pitch direction was necessary. It was performed on 25th of April. A last X-cross calibration on 30th of April 2013 shows that the correction was successful. Off-nadir angle from waveforms is from this day onwards extremely close to zero and very stable spatially and temporally. Though Jason-2 off-nadir angle from waveforms is also close to zero (though mostly slightly negative), it shows more variations. Standard deviation of the off-nadir angle from waveforms is also higher for Jason-2 than for Saral/AltiKa (right of figure 29). This is also visible on the histograms (figure 31). The shape of Saral/AltiKa off-nadir angle from waveforms histogram is much narrower than for Jason-2.

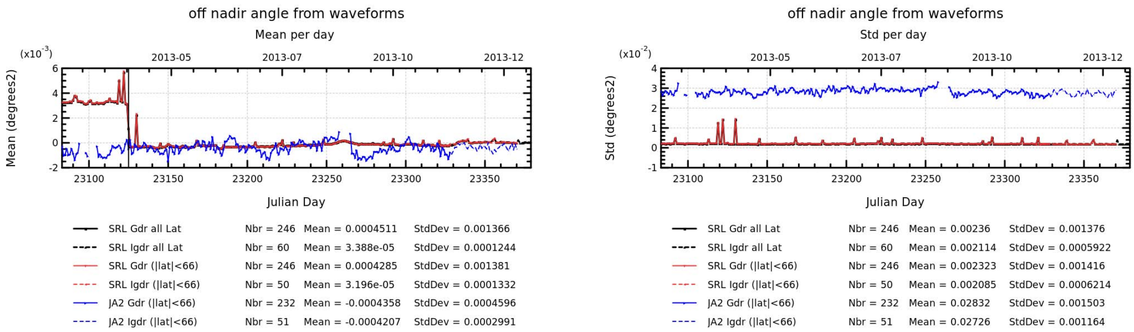

Figure 29: *Daily monitoring of mean (left) and standard deviation (right) of Saral/AltiKa and Jason-2 off-nadir angle from waveforms. GDR data are in plain lines, IGDR data in dotted lines. The vertical black line indicates the day where the PF/RF alignment (alignment between the platform and the radio-frequency axis) was corrected.*

Both missions are extremely stable concerning the platform pointing and have no mispointing. The reason that Jason-2 shows more variation for the off-nadir angle from waveforms is originated in the different values of antenna aperture. Jason-2 has an antenna beamwidth of 1.29°, whereas Saral/AltiKa has only 0.6°. In addition Jason-2 is in a higher orbit. The Jason-2 footprint is therefore larger (radius of 9.6 km) than the Saral/AltiKa footprint (5.7 km). Therefore the probability of perturbations within the footprint - which modify the backscattering properties of the surface - is higher for Jason-2 than for Saral/AltiKa. The off-nadir angle from waveforms represents either real mispointing (which is not the case for Saral/AltiKa and Jason-2, except for some special cases such as X-cross calibrations or maneuvers) or is due to backscattering properties of the surface, which can modify the slope of the trailing edge of the waveforms.
Therefore the map of Saral/AltiKa off-nadir angle from waveforms (left of figure 30) is very homogeneous, except for maneuvers (in Indian ocean) and close to sea ice. It is very slightly positive around Indonesia and close to coasts. On the other hand, the region around 50°S has slightly negative values. The map of Jason-2 (right of figure 30) is generally slightly negative, except for regions

around Indonesia, and close to coasts (especially) in the northern hemisphere, the amplitudes of the off-nadir angle from waveforms are greater for Jason-2 than for Saral/AltiKa. Nevertheless both maps are correlated to the maps of backscattering coefficient (figure 33).

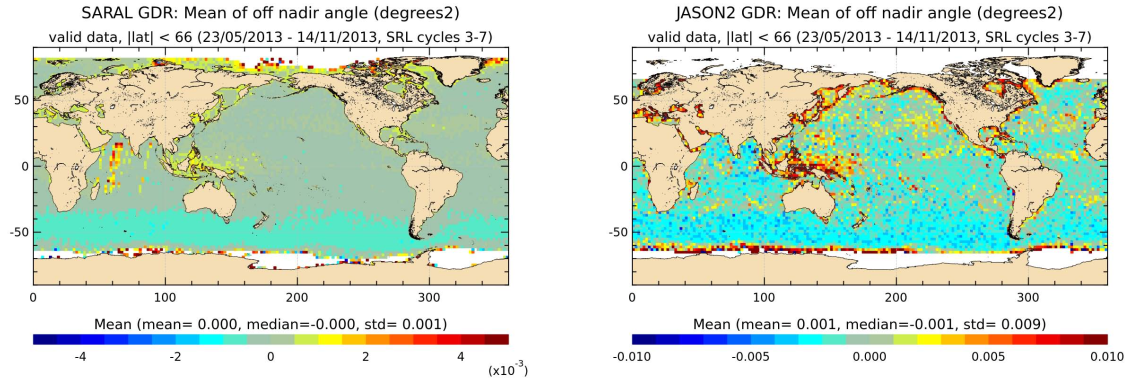

Figure 30: *Average map of off-nadir angle from waveforms for Saral/AltiKa (left) and Jason-2 (right) after the correction of the PF/RF alignment over cycles 3 to 7.*

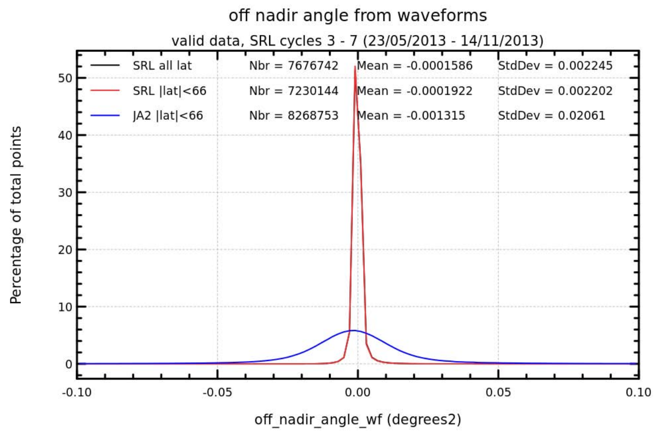

Figure 31: *Histogram (of along-track data) of off-nadir angle from waveforms for Saral/AltiKa and Jason-2 (computed for Saral/AltiKa cycles 3 to 7).*

4.4. Backscatter coefficient

Saral/AltiKa is the first altimeter mission using the Ka-band frequency. It has therefore a different behavior than altimeters using Ku-band frequency. Several studies were done to prepare the Saral/AltiKa mission. They found that the Ka-band backscattering coefficient will be about 3.5 dB smaller than the Ku-band backscattering coefficient (see [23]). Concerning the real Saral/AltiKa data, the difference to Ku-band backscattering coefficient is smaller: 2.7 dB in average (see bottom of figure 32). The difference of Saral/AltiKa minus Jason-2 latitude weighted cycle per cycle mean shows a small drift between approximately cycle 4 and 6. This is related to the saturation of the hot calibration counts (more details in chapter 7.1.) for Saral/AltiKa 37 GHz channel, which impacts the values of the atmospheric attenuation and therefore the backscattering coefficient (as it includes the atmospheric attenuation). The daily evolution of Saral/AltiKa backscattering coefficient shows the same signals as the one of Jason-2 (top left of figure 32) and the dispersion diagram of backscattering coefficients at 3h crossover points shows also a good correlation.

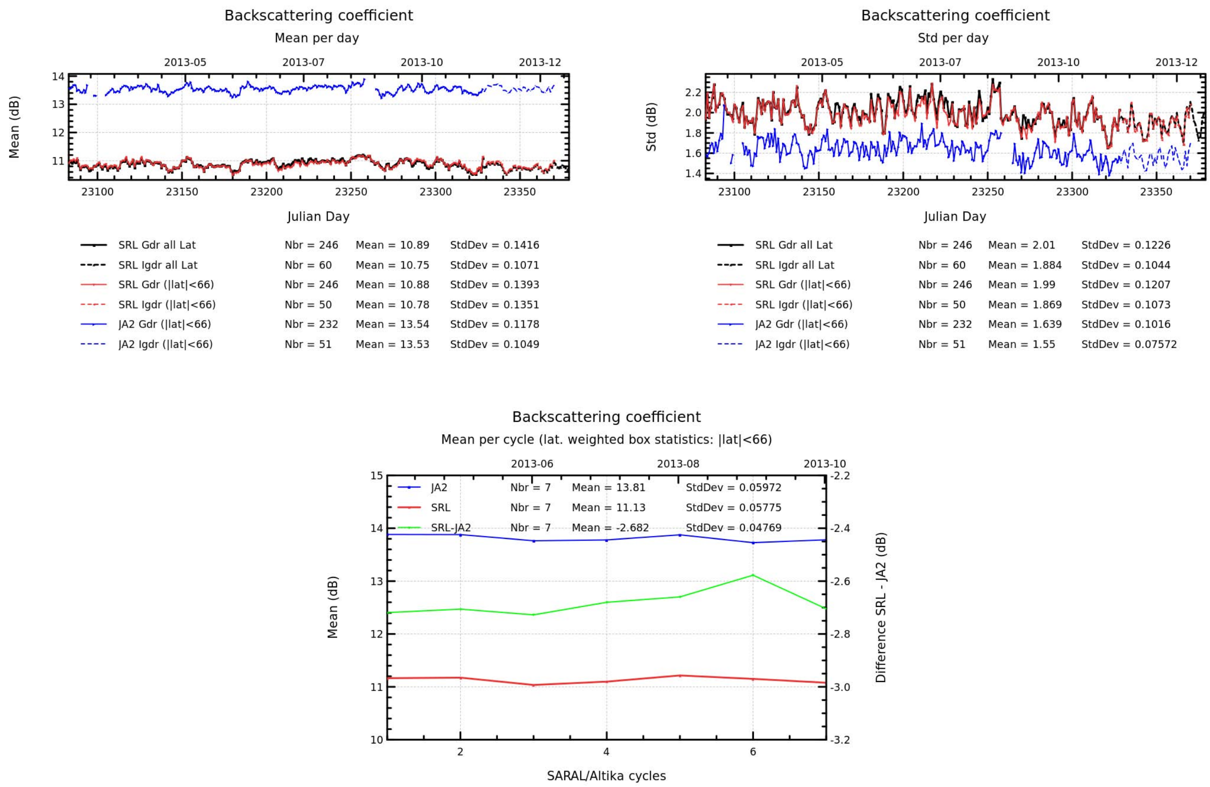

Figure 32: *Daily monitoring of mean and standard deviation of Saral/AltiKa and Jason-2 backscattering coefficient (top) and cycle per cycle monitoring of latitude weighted box mean for both missions, as well as the difference of the two (SRL-JA2) on the bottom.*

Nevertheless there is quite a dispersion, and indeed the daily standard deviation of backscattering coefficient is higher for Saral/AltiKa than for Jason-2 (top right of figure 32). Though the maps (centered around the mean value for better comparison between Saral and Jason-2) of backscattering coefficient show the same structures for both missions (see top of figure 33), the amplitudes of these structures are stronger for Saral/AltiKa than for Jason-2. Also the difference between

Ka- and Ku-band backscattering coefficient is not a simple bias, as shown on the difference map (bottom of figure 33).

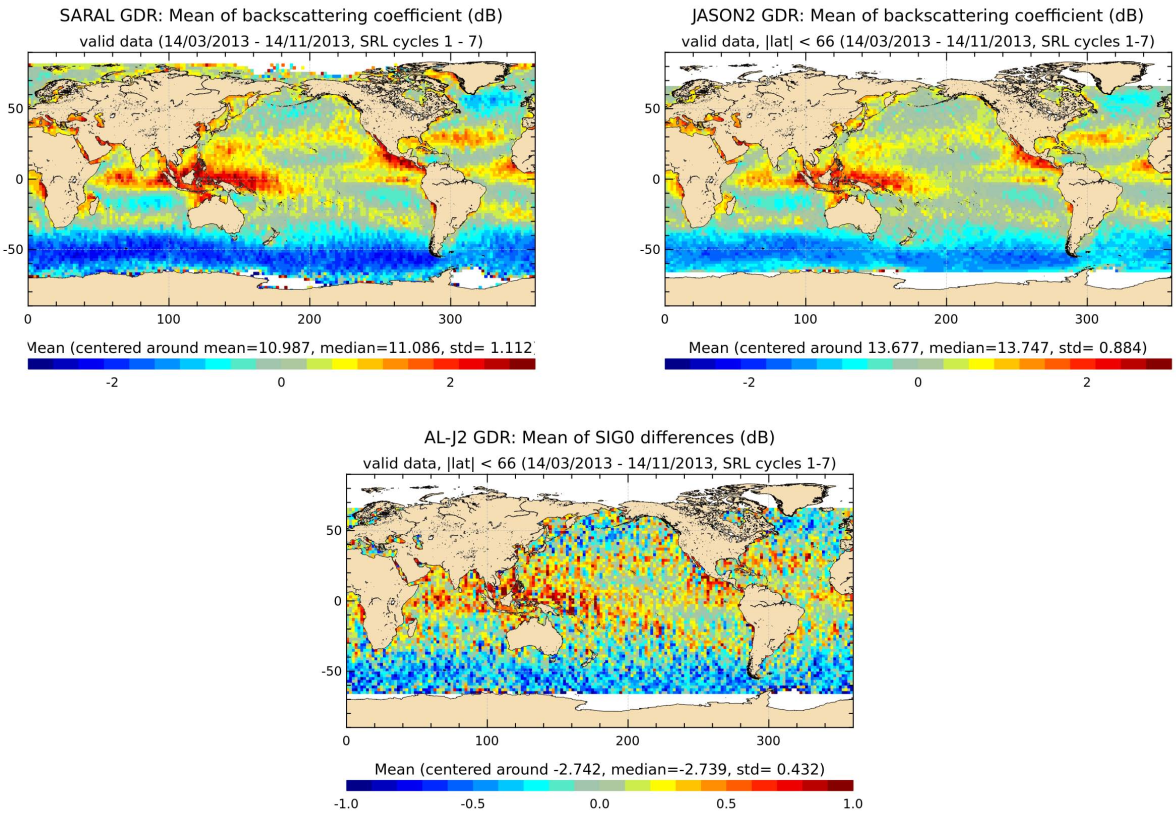

Figure 33: *Average map of backscattering coefficient for Saral/AltiKa (left) and Jason-2 (right) cycles 1 to 7. Difference map of gridded Saral and Jason-2 backscattering coefficient for cycles 1 to 7.*

Furthermore the shape of the histograms is quite different for the Ka- and Ku-band frequencies. The backscattering coefficient is one of the parameters which is quite different for the two frequencies. From the difference of the Ka- and Ku-band backscattering coefficients follows also that algorithms based on backscattering coefficient need carefully tuning in order to be applied to Ka-band data. The altimeter wind speed of available in Patch1 products is therefore not usable.
Note that Patch2 GDR-T will contain altimeter wind speed computed with an algorithm tuned to Ka-band data (see also chapter 7.3.1.).

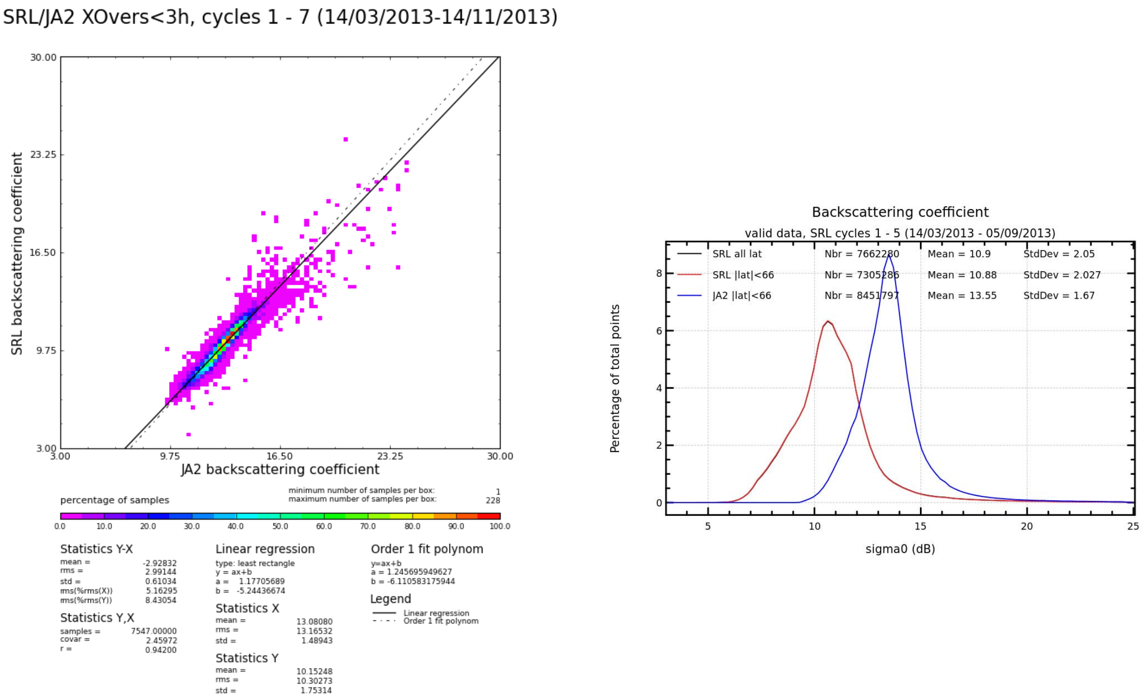

Figure 34: *Dispersion diagram of backscattering coefficient between Saral/AltiKa and Jason-2 at 3h crossover points (computed for cycles 1 to 7) on the left and histogram (of along-track data) on the right.*

4.5. Significant wave height

The significant wave height (SWH) is one of the parameters derived from the waveforms. Daily monitoring of mean and standard deviation of SWH vary temporally, but are very similar for Saral/AltiKa and Jason-2 (see top of figure 35). The mean is very close for both missions when limited to 66° latitude. When taking into account all latitudes, SWH is slightly reduced for Saral/AltiKa as small SWH occur in very high northern latitudes when the sea ice recedes (see also left map of figure 36). The maps of SWH show the same structures: low SWH around Indonesia, in the Mediterranean Sea and the Gulf of Mexico and high SWH around 50°S (as well as in North Atlantic). The difference map between the two satellites (bottom of figure 36) is centered around a difference of 3 to 4 cm, with slightly higher values for Saral/AltiKa. Stronger differences occur in high latitudes (in regions, where SWH is higher than 2-3 m). These differences are probably due to time differences in the sampling. When considering dispersion diagram of Saral/AltiKa and Jason-2 SWH at 3h crossovers (left of figure 37), a strong correlation coefficient of over 0.98 is obtained.

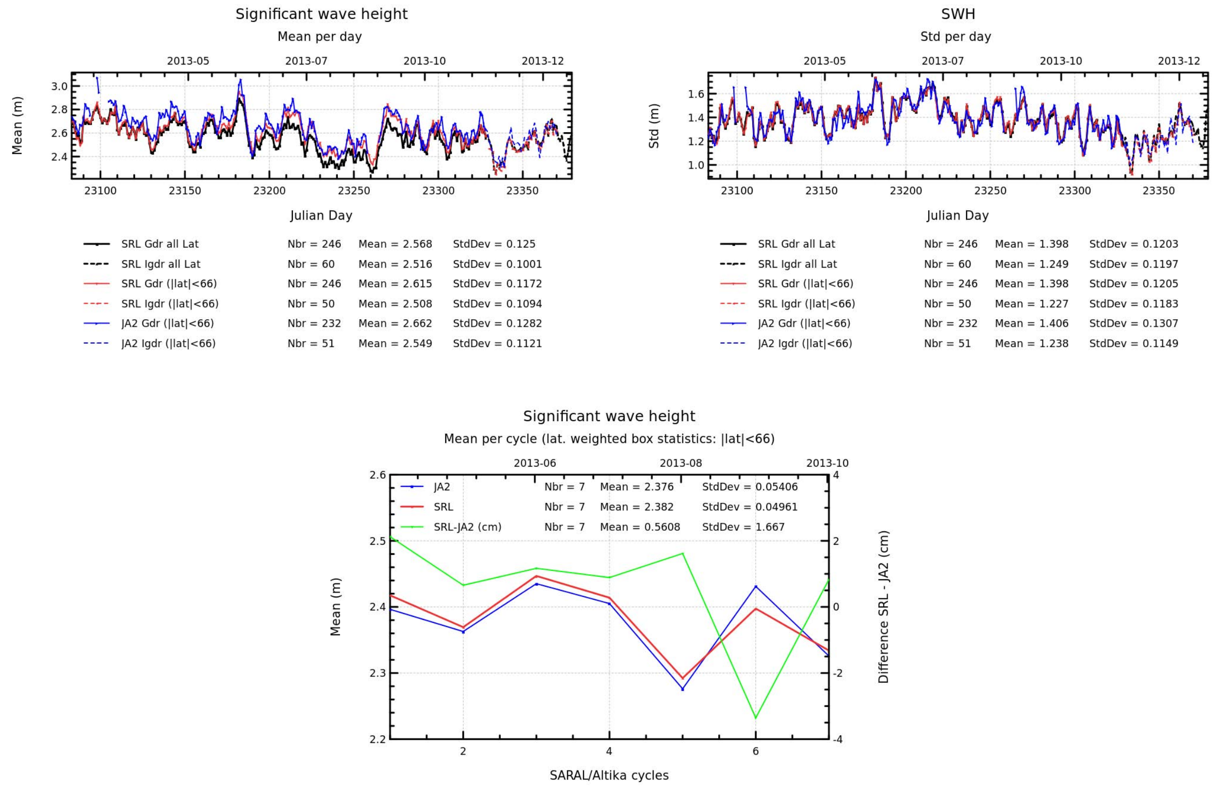

Figure 35: *Daily monitoring of mean and standard deviation significant wave height for Saral/AltiKa and Jason-2 (top) and cycle per cycle monitoring of latitude weighted box mean for both missions, as well as the difference of the two (SRL-JA2) on the bottom.*

The dispersion diagram shows a mean value for Jason-2 SWH at 3h SRL/JA2 crossover points of 3.14 m and 3.20 m for Saral/AltiKa. This is considerably higher than the mean values of daily along-track SWH (around 2.60 m). This is related to the geographical positions of the 3h crossover points: there are more crossover points in latitudes around 50°, than in low latitudes. And around

50°S the SWH has high values (see also top of figure 36), which skews the mean of SWH computed at 3h crossovers to higher values. Nevertheless, this diagnostic shows that for the same positions (SRL/JA2 3h crossovers) with a time difference less than 3h, Saral/AltiKa SWH is slightly higher than Jason-2. This is also the case when computing latitude weighted box statistics (in order to homogenize the unequally over latitudes distributed data), as shown on bottom of figure 35, where Jason-2 SWH is generally slightly lower than Saral/AltiKa SWH. When taking only into account along-track statistics (top of figure 35), this order is inverted (Jason-2 SWH higher than Saral/AltiKa SWH), as Jason-2 has more data in high latitudes, especially in southern hemisphere, where is less land (see also distribution of number of ocean data in function of latitude bands: right side of figure 22). In these regions the SWH is high, which therefore skews the along-track mean to higher values.

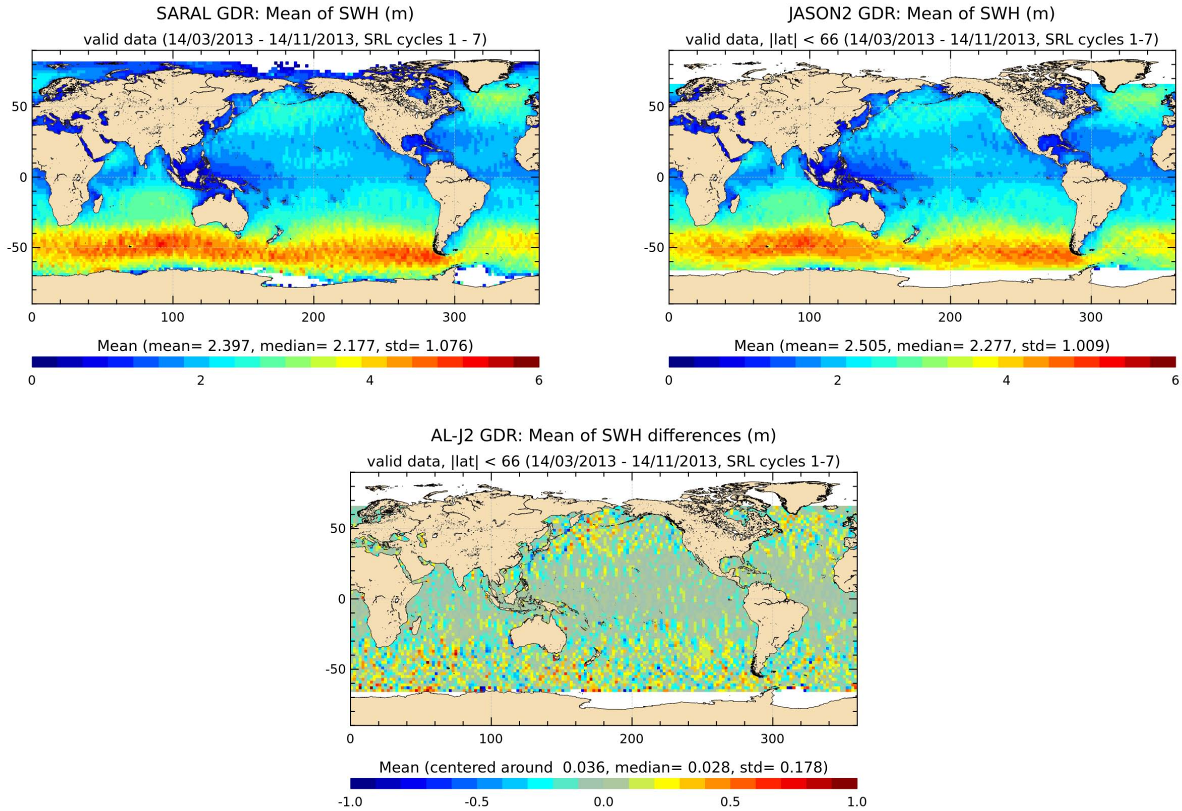

Figure 36: *Average map of significant wave height for Saral/AltiKa (left) and Jason-2 (right) cycles 1 to 7. Difference map of gridded Saral and Jason-2 significant wave height for cycles 1 to 7.*

The shapes of the histograms are very similar (see right side of figure 37) for Jason-2 and Saral/AltiKa, except for small SWH. Since application of Patch1 the minimum value of Saral/AltiKa SWH is 12.6 cm (related to the look-up table), it is 0 for Jason-2. Nevertheless, small SWH of current Jason-2 or Jason-1 data are not precise (errors of about 15 cm), as the look-up table correction for small SWH is not correct, whereas the Saral/AltiKa look-up tables were updated for Patch1. Furthermore, the histogram for Saral/AltiKa shows a small bump for SWH around 50cm. Note that in the wave forecasting systems of Meteo-France, altimeter significant wave height from Jason-2 and Saral/AltiKa are only assimilated for values higher than 50 cm. According to L. Aouf, the Saral/AltiKa SWH data have a positive impact on the wave analysis and forecast of the Meteo-France wave analysis model ([2]).

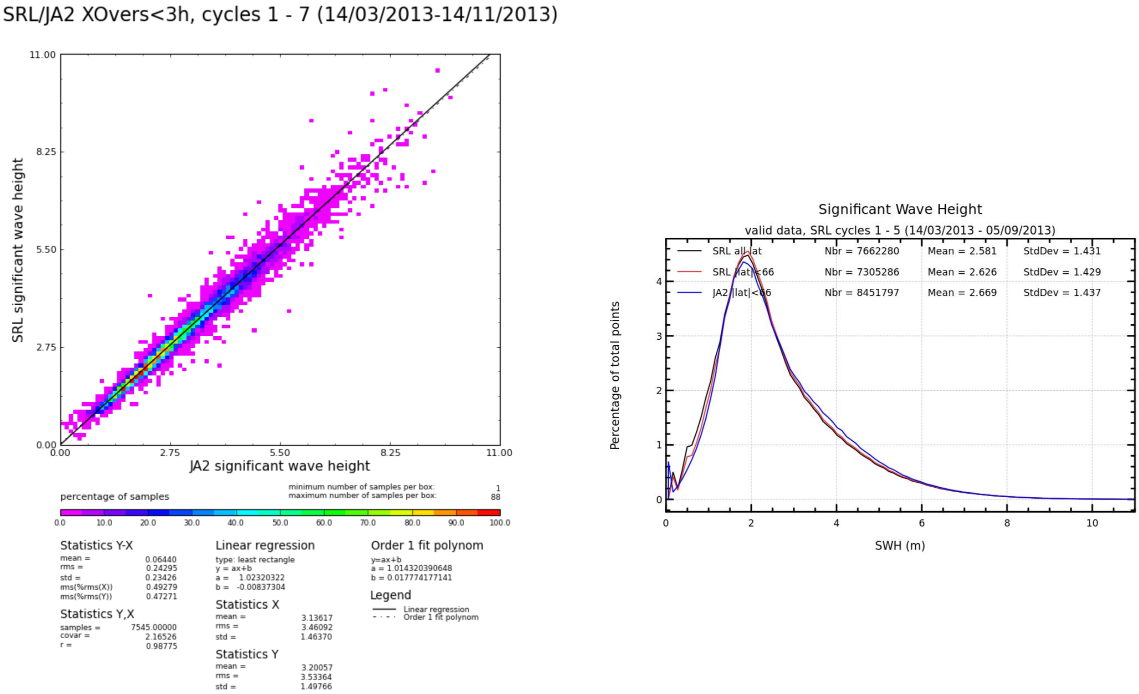

Figure 37: *Dispersion diagram of significant wave height between Saral/AltiKa and Jason-2 at 3h crossover points (computed for cycles 1 to 7) on the left and histogram (of along-track data) on the right.*

4.6. Ionosphere correction

As the Saral/AltiKa altimeter uses a frequency of 35.75 GHz (Ka-band), the ionospheric effects are very small (divided by roughly seven compared to Ku-band frequency). Therefore a mono-frequency altimeter was chosen for the Saral/AltiKa mission, so it is not possible to compute a dual-frequency ionospheric correction such as for Jason-2. Instead, the Saral/AltiKa GDR products contain only the GIM ionosphere correction.
The large differences between Ka-band and Ku-band ionosphere corrections are shown on the latitude weighted box statistics (bottom of figure 38), where Saral/AltiKa GIM ionosphere correction has small values (around 6 mm) and it varies little in time, whereas Jason-2 filtered dual-frequency ionosphere correction has values of around 5 cm, which vary temporally. Also the standard deviation of along-track data is much higher for Jason-2 than for Saral/AltiKa (right of figure 38).

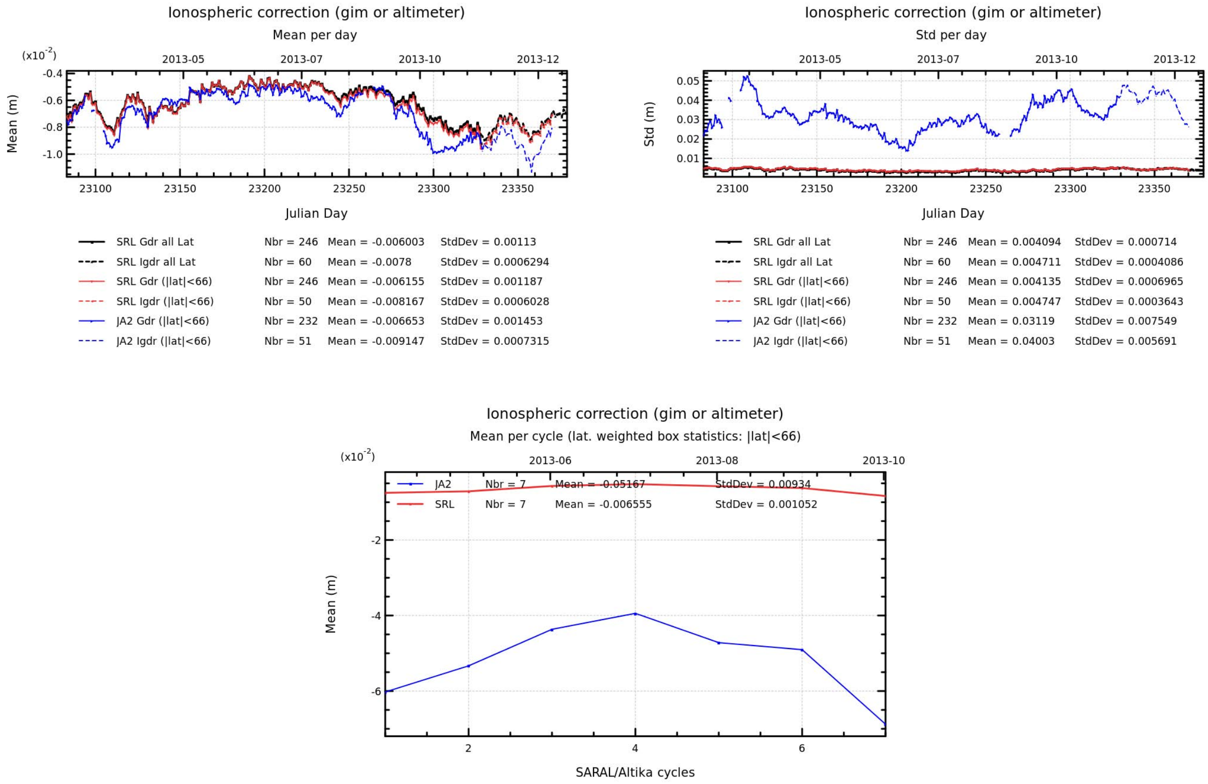

Figure 38: *Daily monitoring of mean and standard deviation ionosphere correction for Saral/AltiKa (GIM) and Jason-2 (filtered dual-frequency ionosphere correction with scale factor 0.14418 for mean computation) on top and cycle per cycle monitoring of latitude weighted box mean for both missions (without the scale factor for Jason-2) on the bottom.*

Top left of figure 38 shows the daily mean of ionosphere correction for Saral/AltiKa (GIM ionosphere using all latitudes (black line) or limiting to 66° latitude) and for Jason-2 (filtered dual-frequency ionosphere correction), where a scale factor of 0.14418 is applied in order to set it on the same level as Ka-band frequency ($13.575^2/35.75^2$). Generally the two curves show a similar evolution, but locally differences of around 2 mm may occur (with generally Jason-2 having stronger values). This may be due to the fact that Saral/AltiKa uses a model ionosphere correction, whereas Jason-2 has a dual-frequency ionosphere correction. It may also be due to the fact that Saral/AltiKa is a sun-synchronous satellite with 6:00 local time for ascending node and 18:00 local time for descending node. As ionosphere correction varies with local time, it is very small for ascending (morning) passes and has absolute values up to 2 cm in the equatorial region for descending (evening) passes. Jason-2 on the other hand is not sun-synchronous and revisits only every 12 cycles the same local hours.

Increased ionosphere correction (absolute values) can be found in the same regions (equatorial region) for Saral/AltiKa and Jason-2 (see maps of figure 39), but the amplitude is of course very different (due to the different frequencies). This can also be seen on the histogram (right of figure 40), where the shape of Saral/AltiKa histogram is very narrow with a strong mode close to zero and a quite small secondary peak around 1.5 cm (corresponding to the data in the equatorial region for descending passes). The shape of Jason-2 histogram is much more spread out and flatter.

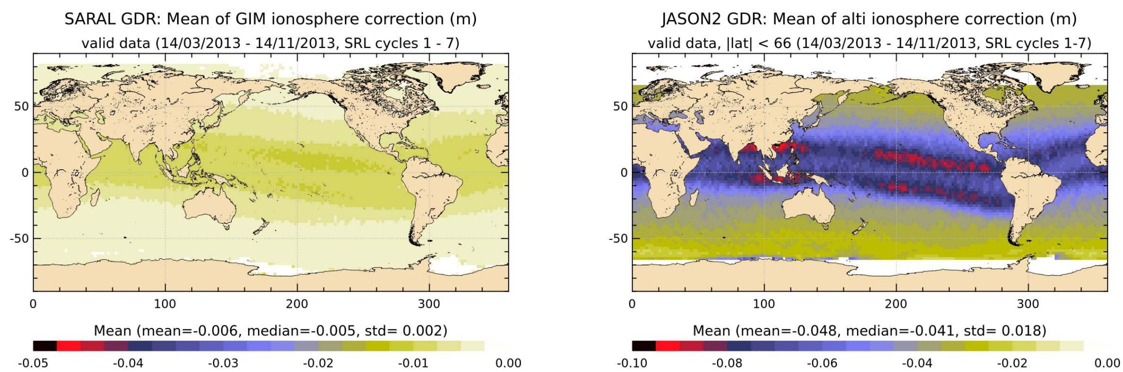

Figure 39: *Average map of ionosphere correction for Saral/AltiKa (GIM, left) and Jason-2 (filtered dual-frequency ionosphere correction, right) cycles 1 to 7. Note that color scales are different for Saral and Jason-2*

The dispersion diagram of ionosphere corrections (the Jason-2 one is rescaled to Ka-band frequency) at 3h multi-mission crossovers shows correlation, but not very good (with a correlation coefficient of only 0.76).

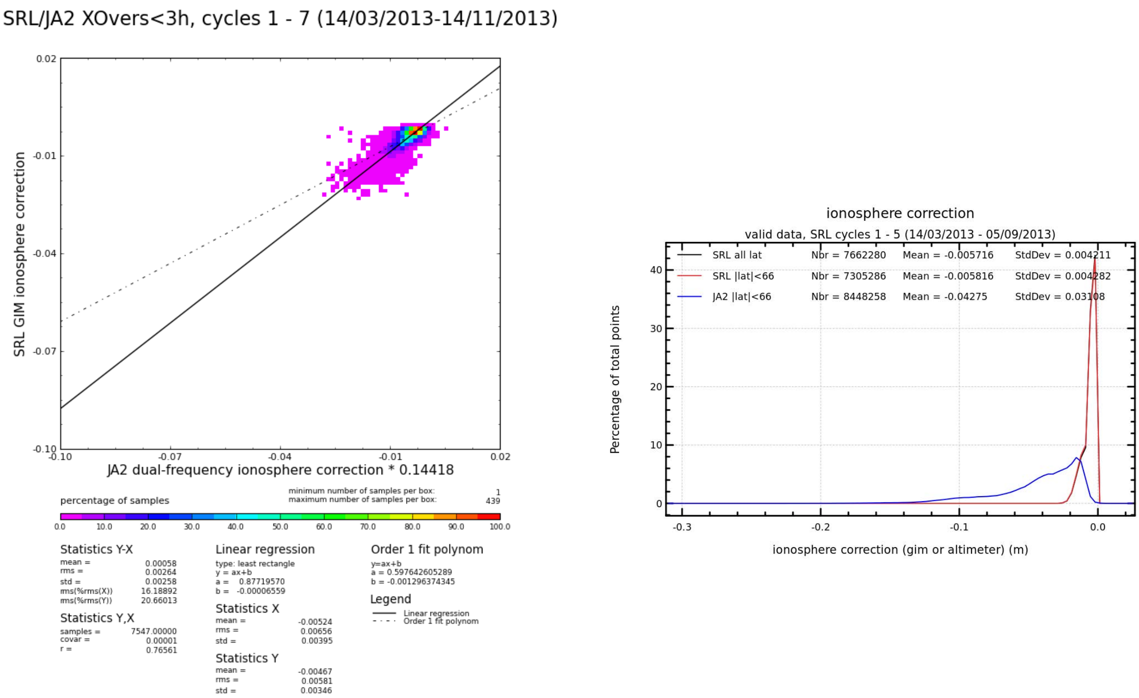

Figure 40: *Dispersion diagram of ionosphere correction between Saral/AltiKa (GIM) and Jason-2 (filtered dual-frequency with scale factor of 0.14418 for Jason-2) at 3h crossover points (computed for cycles 1 to 7) on the left and histogram of along-track data (without scale factor for Jason-2) on the right.*

4.7. Radiometer wet troposphere correction

4.7.1. Overview

In order to have access to radiometer wet troposphere correction, liquid water content, water vapor content and atmospheric attenuation, Saral/AltiKa uses a dual-frequency radiometer (23.8 GHz +/- 200 MHz & 37 GHz +/- 500 MHz), whereas Jason-2 has a three-frequency radiometer (18.7, 23.8 and 34.0 GHz). Figure 41 shows the daily mean and standard deviation of radiometer wet troposphere correction for Saral/AltiKa and Jason-2. The standard deviation is smaller for Jason-2 than for Saral/AltiKa. For a couple of months, Saral/AltiKa standard deviation was diminished and quite close to the one of Jason-2. Concerning the mean of radiometer wet troposphere correction, Jason-2 has dryer values than Saral/AltiKa. This is on the one hand related to different radiometer wet troposphere correction retrieval algorithms, but on the other hand, this can also be related to different local times of the satellites (sun-synchronous 6h/18h for Saral/AltiKa). During several months the radiometer wet troposphere correction of Saral/AltiKa went dryer, this is related to the saturation of the hot calibration counts (see chapter 7.1.), which was corrected on 22 October 2013 (explaining the jump of around 5 mm amplitude visible on the monitoring).
Note that improvement of the radiometer wet troposphere correction retrieval algorithms are still on-going. **Patch2 will have an updated version of the retrieval algorithms (see chapter 7.3.3.). A particular challenge of the tuning of the retrieval algorithms is the backscattering coefficient used in the algorithms, as it is in Ka-band (instead of Ku-band like for the other altimeters)**.

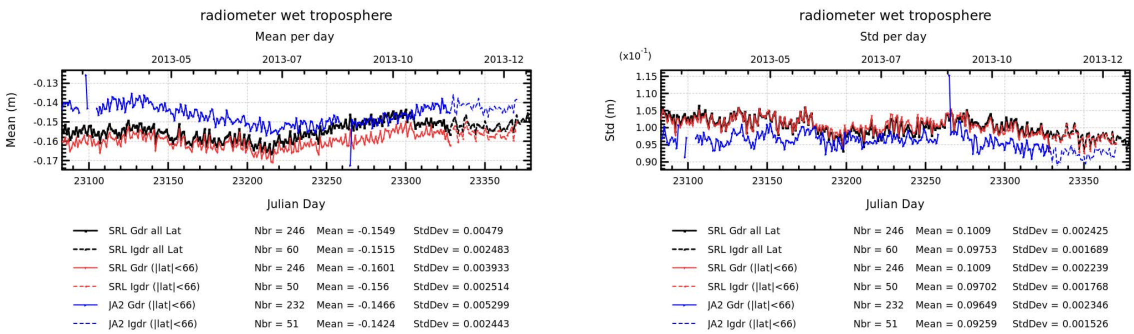

Figure 41: *Daily monitoring of mean and standard deviation of radiometer wet troposphere correction for Jason-2 (blue) and Saral/AltiKa (black all latitudes, red latitudes limited to ± 66°).*

4.7.2. Comparison with the ECMWF model

The ECWMF wet troposphere correction has been used to check the Saral/AltiKa and Jason-2 radiometer corrections. Daily differences are calculated and plotted in figure 42. The drift in the radiometer wet troposphere correction of Saral/AltiKa due to the saturation of the hot calibration count (see chapter 7.1.) is clearly visible on the left part of figure 42. Outside of this drift the difference between radiometer and ECMWF wet troposphere correction for Saral/AltiKa and Jason-2 is around 5 mm. The two ECMWF model updates (June and November 2013) occurred during the observed period, which might have an impact on the model wet troposphere correction, do not show any impact on the data.
The standard deviation of radiometer minus model wet troposphere correction is higher for Saral/AltiKa (around 1.8 cm) compared to Jason-2 (around 1.2 cm), shown on left of figure 42 and also on the histogram on figure 44. **For the data using Patch2, the standard deviation for Saral/AltiKa will decrease to 1.6 cm (see chapter 7.3.3.)**.

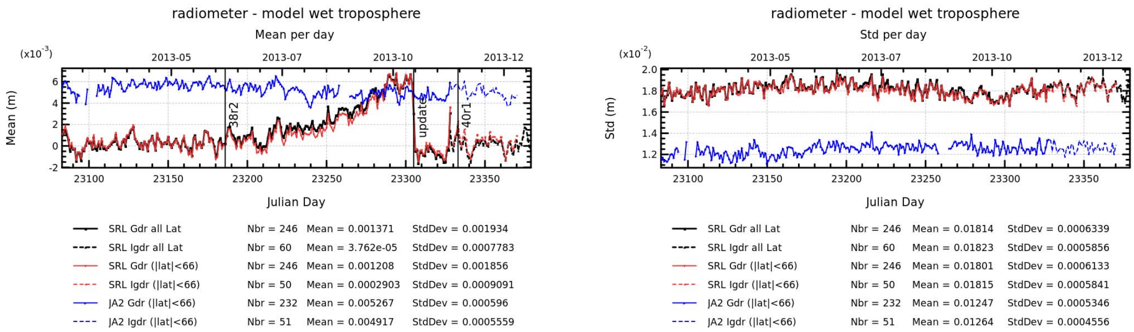

Figure 42: *Daily monitoring of mean and standard deviation of radiometer minus model wet troposphere correction for Saral/AltiKa and Jason-2.*

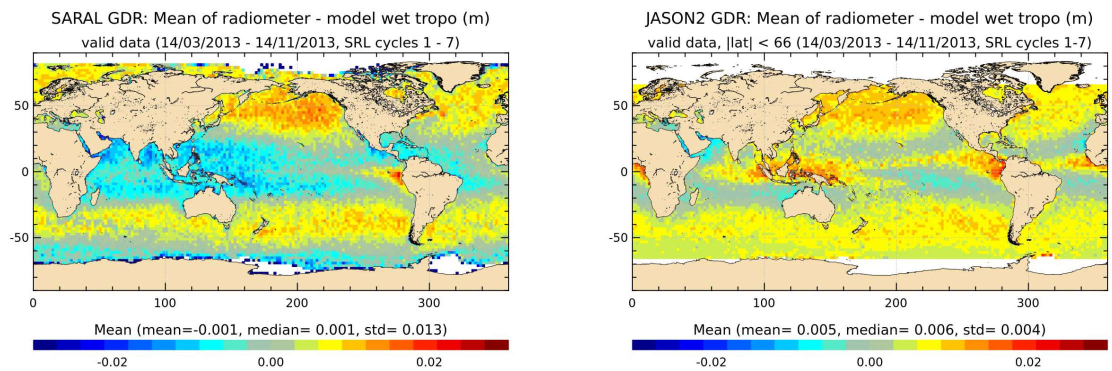

Figure 43: *Average map of radiometer minus ECMWF model wet troposphere correction for Saral/AltiKa (left) and Jason-2 (right) cycles 1 to 7.*

The maps of radiometer minus ECMWF model wet troposphere correction (figure 43) are centered around the mean value (5 mm for Jason-2, −1 mm for Saral/AltiKa). The mean of the Saral/AltiKa map is impacted on the one side by the saturation of the hot calibration counts (which tends to overestimate the difference) and on the other side by some boxes near the frontier between sea-ice and free water (which tends to underestimate the mean). These boxes with strong negative values are an indication that probably not all sea ice cases are edited. Geographical structures of the radiometer minus model wet troposphere corrections are similar for the two satellites in high latitudes (around $\pm$ 50°), but quite different for low latitudes.

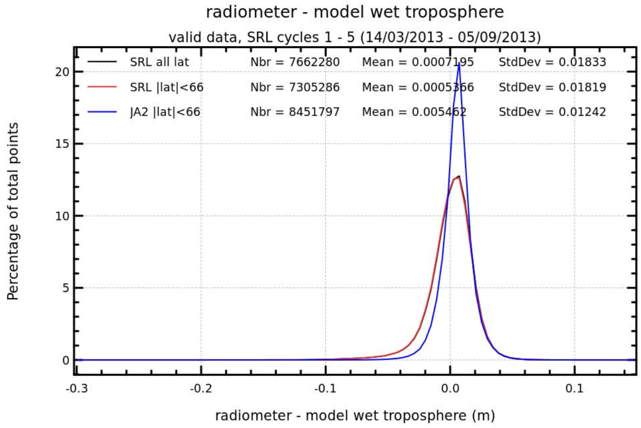

Figure 44: *Histogram (of along-track data) of radiometer minus ECMWF model wet troposphere correction between Saral/AltiKa and Jason-2.*

4.8. Altimeter wind speed

The altimeter wind speed present in the Patch1 GDR-T version is not usable, since the look-up table from Jason-1 is used, but the Ka-band backscattering coefficient is very different from the Ku-band one. Therefore hereafter, no analysis of the Saral/AltiKa altimeter wind speed is shown. **Nevertheless from Patch2 onwards, the altimeter wind speed will be usable, see also chapter 7.3.1. for more details**.

4.9. Sea state bias

As before Saral/AltiKa launch there did not exist a sea state bias (SSB) model (generally dependent on SWH (significant wave height) and altimeter wind speed or backscattering coefficient) for Ka-band frequency, the sea state bias of the GDR-T Patch1 data is computed as 3.5% * SWH. Of course, this is just a first approximation of the Saral/AltiKa SSB and less precise than a dedicated model (such as used for Jason-2). Nevertheless the daily monitoring of the along-track sea state bias for Saral/AltiKa and Jason-2 show similar temporal evolution, but Saral/AltiKa SSB has higher absolute values (around 1 cm higher) than Jason-2 (see left side of figure 45). This is also the case when considering latitude weighted box statistics (bottom of figure 45). But this is not a homogeneous bias, it varies geographically, as shown on bottom of figure 46. Furthermore the daily standard deviation is also slightly increased for Saral/AltiKa compared to Jason-2 (see right side of figure 45).

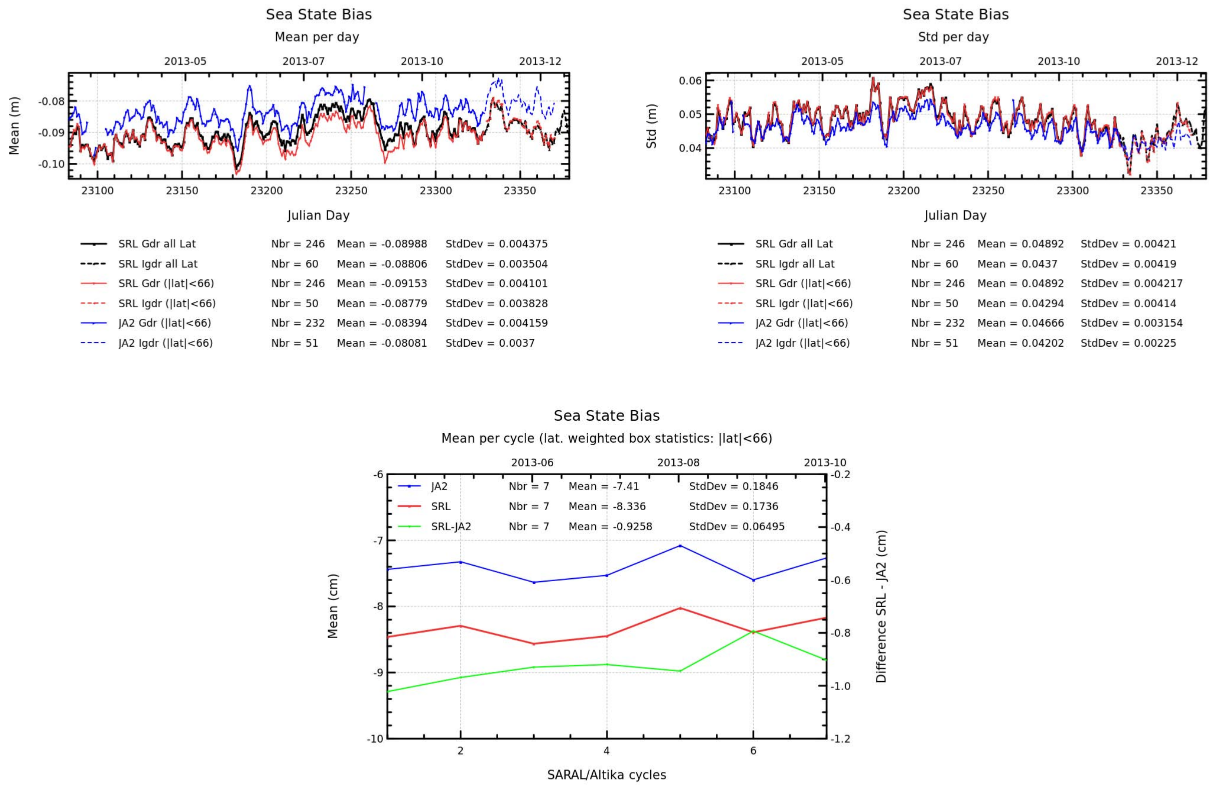

Figure 45: *Daily monitoring of mean and standard deviation of (along-track) sea state bias of Saral/AltiKa and Jason-2 on the top and cycle per cycle monitoring of latitude weighted box mean for both missions on the bottom.*

Indeed the map of Saral/AltiKa sea state bias shows higher values in the region of 50˚S (where SWH is strong) than the map of Jason-2 (top of figure 46). The dispersion diagram of Saral/AltiKa and Jason-2 sea state bias at 3h multi-mission crossovers confirms that the Saral/AltiKa SSB is overestimated for high SSB (equals high SWH). The different nature of the SSB models used for Saral/AltiKa (linear relation) and Jason-2 (dedicated model) is also visible on the right side of figure 47, showing very different shapes of histograms.

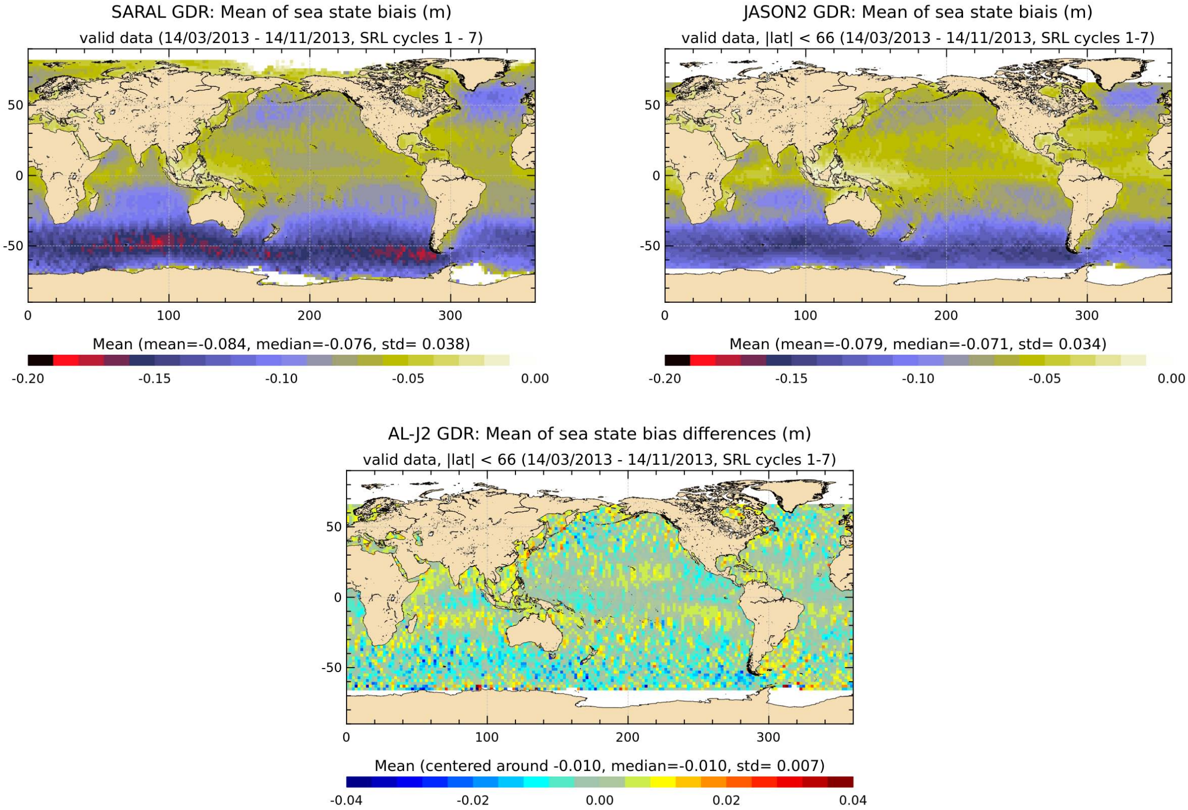

Figure 46: *Average map of sea state bias for Saral/AltiKa (left) and Jason-2 (right) cycles 1 to 7. Difference map of gridded Saral and Jason-2 sea state bias for cycles 1 to 7.*

This difference in sea state bias between the two missions has also an impact on the geographically correlated biases between the two missions, as shown in chapter 5.3., concerning maps of sea surface height differences at multi-mission crossover points.
Note that for Patch2 a preliminary (computed using 5 cycles of Saral/AltiKa GDR data) sea state model was developed and will greatly improve the Saral/AltiKa performance (see chapter 7.3.2. for further details).

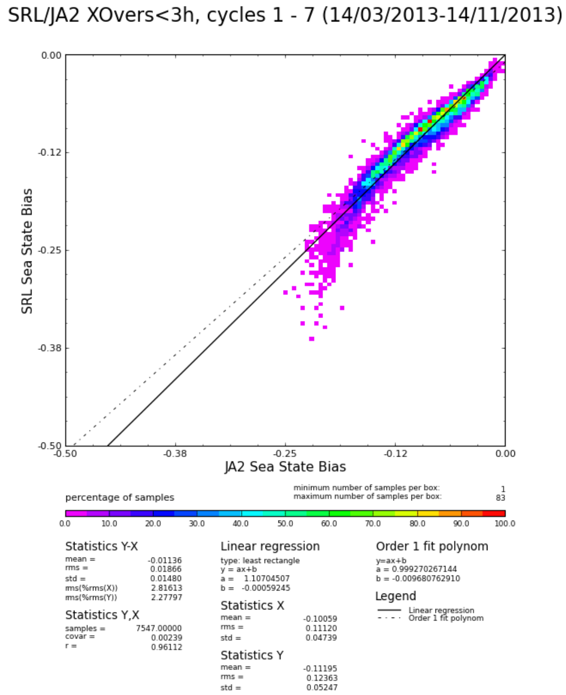

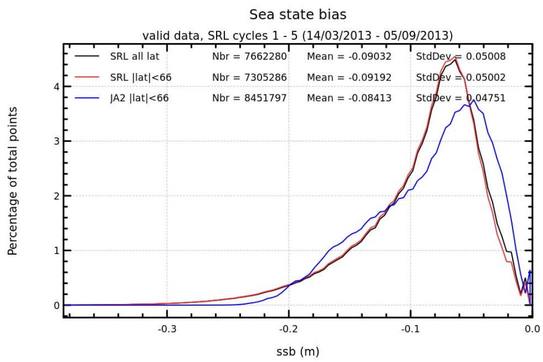

Figure 47: *Dispersion diagram of sea state bias between Saral/AltiKa and Jason-2 at 3h crossover points (computed for cycles 1 to 7) on the left and histogram (of along-track data) on the right.*

5. SSH crossover analysis

5.1. Overview

SSH crossover differences are the main tool to analyze the whole altimetry system performances. They allow us to analyze the SSH consistency between ascending and descending passes. However in order to reduce the impact of oceanic variability, we select crossovers with a maximum time lag of 10 days. This gives a measure of the performance on mesoscale time and spatial scales. Mean and standard deviation of SSH crossover differences are computed from the valid data set to perform maps or a cycle by cycle monitoring over all the altimeter period. In order to monitor the performances over stable surfaces, additional editing is applied to remove shallow waters (bathymetry above -1000m), areas of high ocean variability (variability above 20 cm rms) and high latitudes ($> |50|deg$). SSH performances are then always estimated with equivalent conditions.
The main SSH calculation for Saral/AltiKa and Jason-2 are defined below.

$$SSH = Orbit - Altimeter\ Range - \sum_{i=1}^{n} Correction_i$$

with $AltiKa$ / $Jason$-2 $Orbit = CNES\ orbit$ (standard D) for GDR products, and

$$\begin{aligned} \sum_{i=1}^{n} Correction_i &= Dry\ troposphere\ correction \\ &+ Dynamical\ atmospheric\ correction \\ &+ Radiometer\ wet\ troposphere\ correction \\ &+ Ionospheric\ correction \\ &+ Sea\ state\ bias\ correction \\ &+ Ocean\ tide\ correction\ (including\ loading\ tide) \\ &+ Earth\ tide\ height \\ &+ Pole\ tide\ height \end{aligned}$$

Hereafter a reminder of the standards used (from GDR products: GDR-T Patch1 for Saral/AltiKa and GDR-D for Jason-2):

Parameter	Saral/AltiKa	Jason-2
Orbit	CNES POE-D (Doris/Laser)	CNES POE-D (Doris/Laser/GPS)
Dynamic atmospheric correction (Inverse barometer correction + Non-tidal High-frequency Dealiasing Correction)	Computed from ECMWF atmospheric pressures after removing S1 and S2 atmospheric tides (for inverse barometer) + Mog2D High Resolution ocean model	
		.../...

Parameter	Saral/AltiKa	Jason-2
Radiometer wet troposphere correction	MWR using P1 (dual-frequency radiometer)	AMR (tri-frequency radiometer)
Ionospheric correction	Based on Global Ionosphere TEC Maps from JPL	dual-frequency altimeter ionosphere correction
Sea State Bias	3.5% of SWH values	MLE4 version derived from 1 year of MLE4 Jason-2 altimeter data with version 'd' geophysical models
Global ocean tide (load tide included)	GOT 4.8 ocean tide	
Earth tide	From Cartwright and Taylor tidal potential	
Pole tide	Wahr [1985]	
Mean Sea Surface	CNES_CLS_2011	

Table 7: *S*tandards used for Saral and Jason-2

When not otherwise stated, the standards from table 7 are used.

5.2. Mean of SSH crossover differences

Hereafter, analysis are done over the first 7 cycles of Saral/AltiKa using GDR-T Patch1 products. For comparison, Jason-2 GDR data are shown over the same period. The map of SSH mean ascending/descending differences at crossovers should ideally by close to zero. Geographically correlated patterns on such maps indicate systematic differences between ascending and descending passes. This can indicate either problems in the orbit computation or with geophysical corrections. Comparing the maps of mean SSH differences over roughly 8 months of data for Saral/AltiKa and Jason-2 (figure 48) shows that there are no very strong differences, though Saral/AltiKa is still in the verification phase and several algorithms are not yet fully tuned or not tuned at all (radiometer wet troposphere correction, sea state bias, ...). Nevertheless it is clear that the amplitude of the SSH differences is smaller for Jason-2 than for Saral/AltiKa. The Jason-2 map shows geographically large correlated patterns (positive signal in North Pacific and Indian Ocean, negative signal in South Pacific and most of Atlantic Ocean), which have small amplitudes (generally less than 1 cm). This large scale pattern is very likely related to orbit computation. The map of Saral/AltiKa SSH differences at crossovers is generally negative, except for :

- very high latitudes, especially east of Greenland
- a patch in southern Pacific and in the Gulf of Alaska

Using other standards, such as FES 2004 ocean tide instead of GOT 4.8 solution, changes some of the patterns (figure 49). For Saral/AltiKa, several regions, especially in high latitudes with shallow bathymetry, are concerned. The positive patch east of Greenland visible on the maps when using GOT 4.8, disappears when using FES 2004, but other strong patches appear instead (positive for

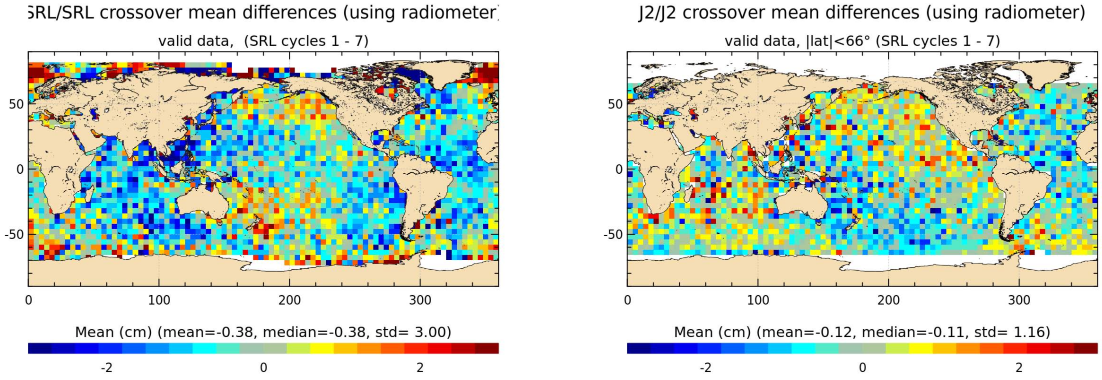

Figure 48: *Map of mean of SSH crossovers differences for Saral/AltiKa (left) and Jason-2 for Saral cycles 1 to 7. Color scales are between ± 3 cm.*

Barents Sea, Hudson Bay, Sea of Okhotsk, negative in the Arabian Sea).

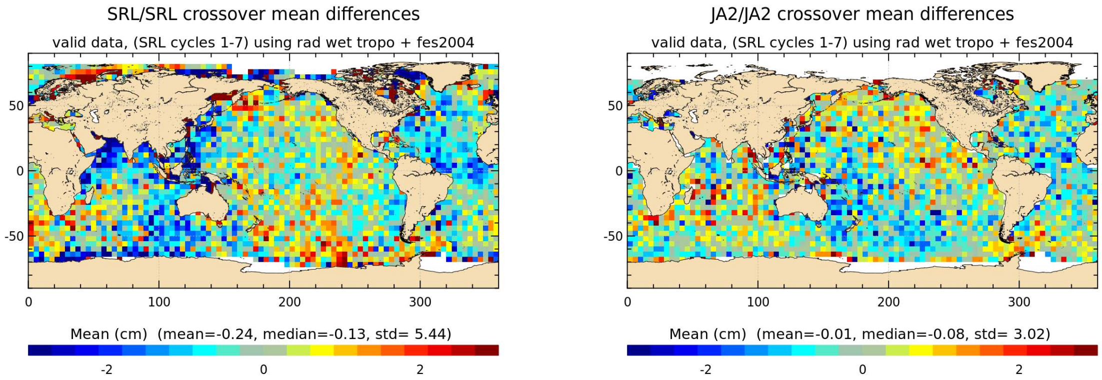

Figure 49: *Map of mean of SSH crossovers differences for Saral/AltiKa (left) and Jason-2 for Saral cycles 1 to 7. Color scales are between ± 3 cm. Using FES 2004 ocean tide instead of GOT 4.8.*

Generally the ascending/descending SSH differences are slightly negative (see bottom of figure 50). But this can vary in function of the selection used: for Saral/AltiKa it is around -5 mm when using a selection of crossover points with $|latitude| < 50^{\circ}$. Plotting the mean SSH differences in function of longitude or latitude (top of figure 50) shows that whereas for Jason-2 this is almost constant over all latitudes, for Saral/AltiKa the ascending/descending SSH difference has a stronger dependency on latitude and longitude. It is generally negative for low and moderate latitudes, but becomes positive for very high latitudes.

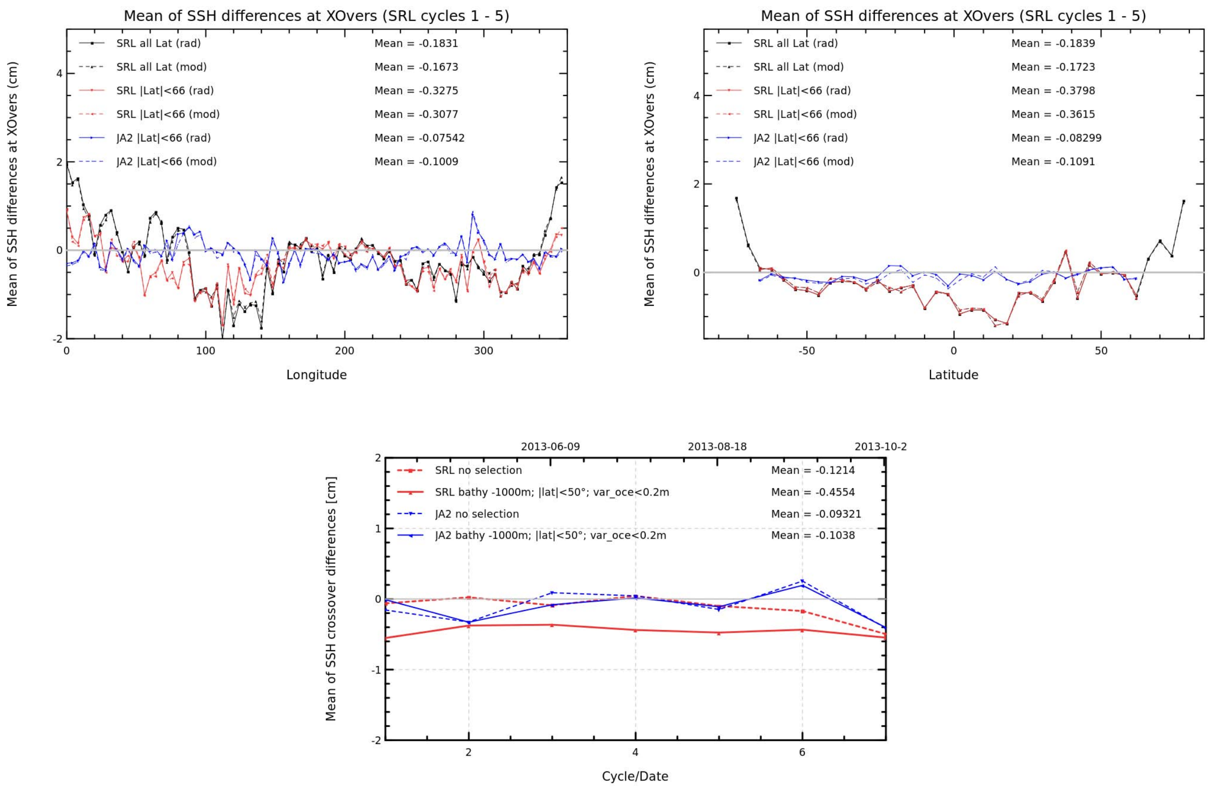

Figure 50: *Top: Mean of SSH crossover differences for Saral/AltiKa and Jason-2 GDR per 4° longitude (left) and latitude (right) bands. Bottom: Cycle per cycle monitoring of ascending/descending SSH differences at mono-mission crossovers for Saral/AltiKa and Jason-2 for Saral cycles 1 to 7. Two selections are used: all valid crossover points are used (dotted lines), only crossover points with |latitude| < 50°, bathymetry < -1000 m and ocean variability < 20 cm rms are used (plain lines).*

5.3. Mean of SSH crossover differences between Saral and other missions

Dual-mission crossover performances are computed between Saral/AltiKa and Jason-2, as well as Jason-1. Mean SSH differences at Saral/Jason-2 crossovers (figure 51) have a bias of about -6.5 cm (SRL-JA2), when using model wet troposphere correction. This bias is not yet explained. When using radiometer wet troposphere correction, the bias is approximately 4 mm smaller (related to a bias of roughly 5 mm between radiometer and ECMWF wet troposphere corrections for Jason-2). The map shows regional structures of about ±2 cm. There is a strip of positive difference of about 2 cm around 50° S, a region with generally high significant wave height. This difference is likely due to differences in sea state bias, as Saral/AltiKa sea state bias is not tuned in Patch1, but only 3.5% of SWH value. See also chapter 7.3.2. for Saral/Jason-2 crossover maps using different solutions of sea state bias. Otherwise large scale differences are observable (positive difference in the Atlantic ocean and negative difference in the Pacific ocean), this might be related to differences in the orbit computation. The algorithm to compute radiometer wet troposphere correction for Saral/AltiKa is not tuned for Patch1 data. Indeed differences in the tropical region (eastern Pacific, around Indonesia, ...) on the left map of figure 51 (using radiometer wet troposphere correction for both missions) are related to the difference between the two radiometer wet troposphere corrections.
Till 20th June of 2013, Jason-1 data are also available, which covers almost the first 3 cycles from

Saral/AltiKa. After updating the ocean tide to GOT 4.8 (instead of GOT 00V2 available in the GDR-C products of Jason-1), the standards are very close to the ones available in the GDR-D Jason-2 product (for the studied period). Crossover difference maps between Saral/AltiKa and Jason-1 (figure 52) show similar structures, as maps between Saral/AltiKa and Jason-2:

- a positive structure around $50^{\circ}S$ probably related to the sea state bias
- differences especially in tropical regions related to the radiometer wet troposphere corrections
- large scale differences (positive in Atlantic ocean, negative in Pacific ocean) appear clearly when using model wet troposphere correction. These structures are probably related to the orbit computation.

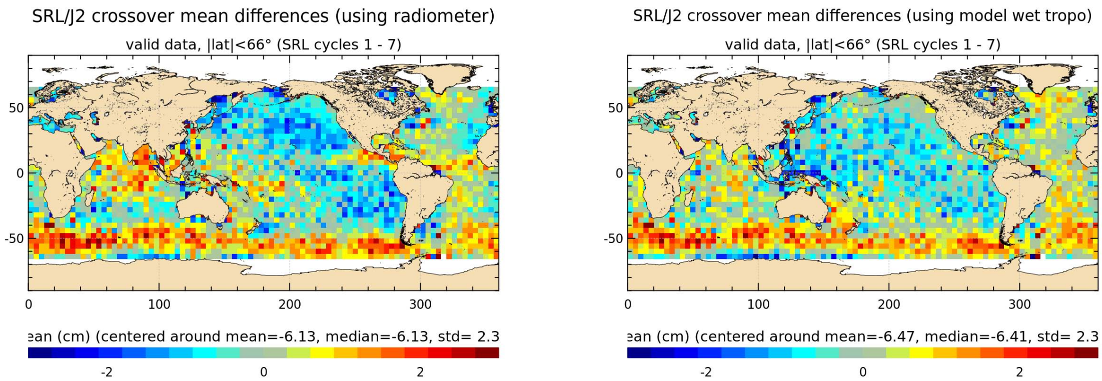

Figure 51: *Map of mean of SSH crossovers differences between Saral/AltiKa and Jason-2 using either radiometer wet troposphere correction (left) or ECMWF model wet troposphere correction (right) for both missions. The maps are centered around the mean.*

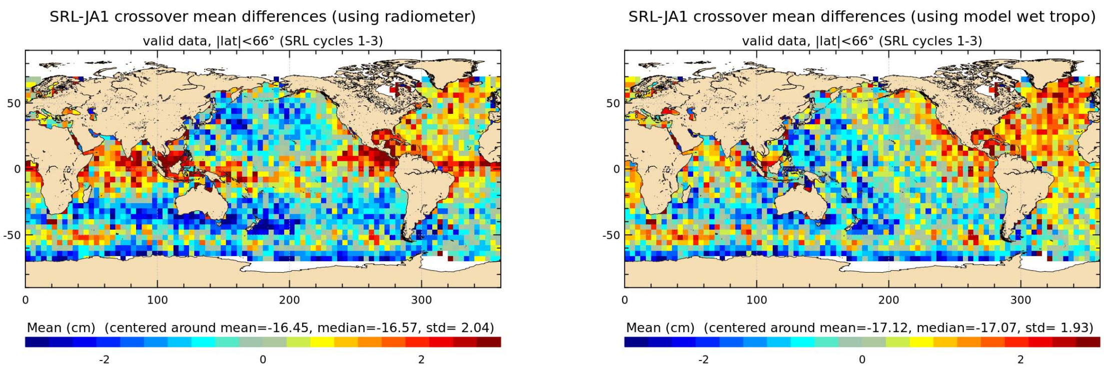

Figure 52: *Map of mean of SSH crossovers differences between Saral/AltiKa and Jason-1 using either radiometer wet troposphere correction (left) or ECMWF model wet troposphere correction (right) for both missions. The maps are centered around the mean.*

The temporal evolution of this difference is monitored in order to detect if there are drifts or jumps indicating a problem in one of the missions. This monitoring is hereafter done on the base of Jason-2 cycles and using geographical selections. It is shown on figure 53. Whereas using model wet troposphere correction for both missions shows a quite stable curve (except for some cycle to cycle variations), using radiometer wet troposphere corrections reveals a drift at least during fall. This is related to the Saral/AltiKa radiometer wet troposphere correction, see chapter 7.1. for further explanations. The last part of the curves (IGDR part) seems to show an increased bias between Saral/AltiKa and Jason-2 (independently from using radiometer or model wet troposphere correction). Note that this is no longer the case when using Patch2 data (see [17]).

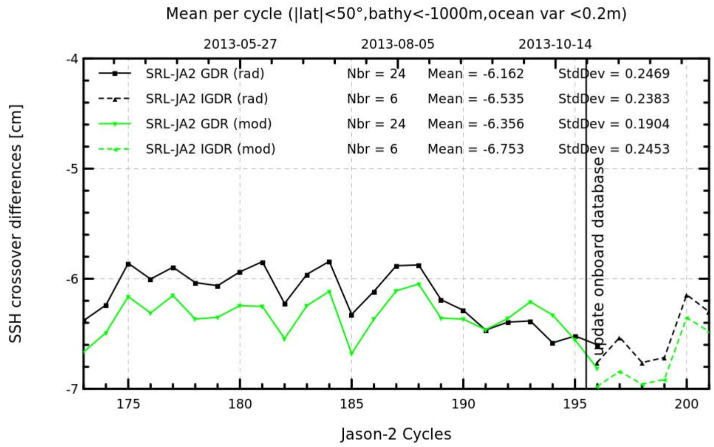

Figure 53: *Monitoring of mean of Saral - Jason-2 differences at crossovers using radiometer wet troposphere correction (black line) or ECMWF model wet troposphere correction (green line) for GDR data (plain lines) and IGDR (dotted lines). Statistics are computed on base of Jason-2 cycles.*

5.4. Standard deviation of SSH crossover differences

As the altimeter specifications are better for Saral/AltiKa than for Jason-2 (smaller footprint, 40 Hz elementary data instead of 20 Hz, higher vertical resolution) the altimeter noise is lower for Saral/AltiKa than for Jason-2, see also the power spectrum in chapter 7.2.. It could be expected that Saral/AltiKa also performs better at crossover points than Jason-2. This is the case when interpolating the data on the positions of the crossover points by spline without taking into account the noise of the range and using model wet troposphere correction for both missions (see dotted lines on figure 54). Nevertheless the range noise is generally (when not otherwise indicated) taken into account when computing crossover points, it is derived from the power spectrum of 1 Hz data (3 cm for Jason-2, 2.5 cm for Saral/AltiKa). In this case, the performance of Jason-2 is better (plain lines). But keep in mind, that sea state bias for Saral/AltiKa is currently 3.5% of the SWH value. Using dedicated sea state bias models (non-parametric or hybrid model) reduce significantly the standard deviation of SSH differences at crossover points (see also chapter 7.3.2.).

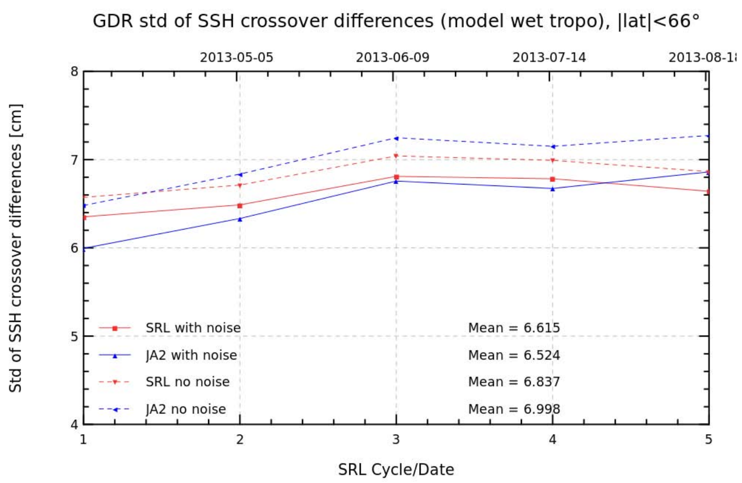

Figure 54: *Cycle by cycle standard deviation of SSH crossover differences for Saral/AltiKa (red) and Jason-2 (blue) when either taking into account (plain lines) or not (dotted lines) the noise of the range during interpolation by spline of data on crossover point locations. Model wet troposphere correction is used for both missions and data are limited to* $|latitude| < 66^\circ$.

The cycle per cycle standard deviation of crossover differences are plotted on the left of figure 55 according to different crossover selections. 3 selections are applied:

- Black curve: no selection is applied. The mean value is 7.0 cm. It shows a beginning of an annual signal linked to the sea ice extension variations.
- Red curve: shallow waters have been removed (bathymetry < -1000m). The previous signal has been removed by this selection.
- Green curve: the last selection allows monitoring the Saral/AltiKa system performance. Indeed, areas with shallow waters (> -1000 m), of high ocean variability (>20 cm) and of high latitudes ($|lat| > 50^\circ$) have been removed. The standard deviation then provides reliable estimates of the altimeter system performances. Though not all algorithms are tuned for Patch1

data (sea state bias, radiometer wet troposphere correction) the performance of Saral/AltiKa is quite good with a standard deviation value of about 5.6 cm.

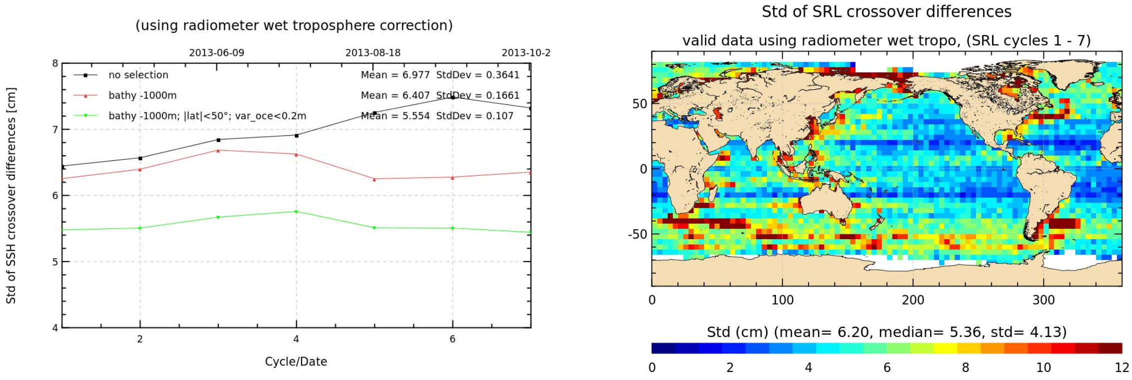

Figure 55: *Cycle by cycle standard deviation of SSH crossover differences for Saral/AltiKa using several selections (left), map of standard deviation at crossover points (right). Radiometer wet troposphere correction is used.*

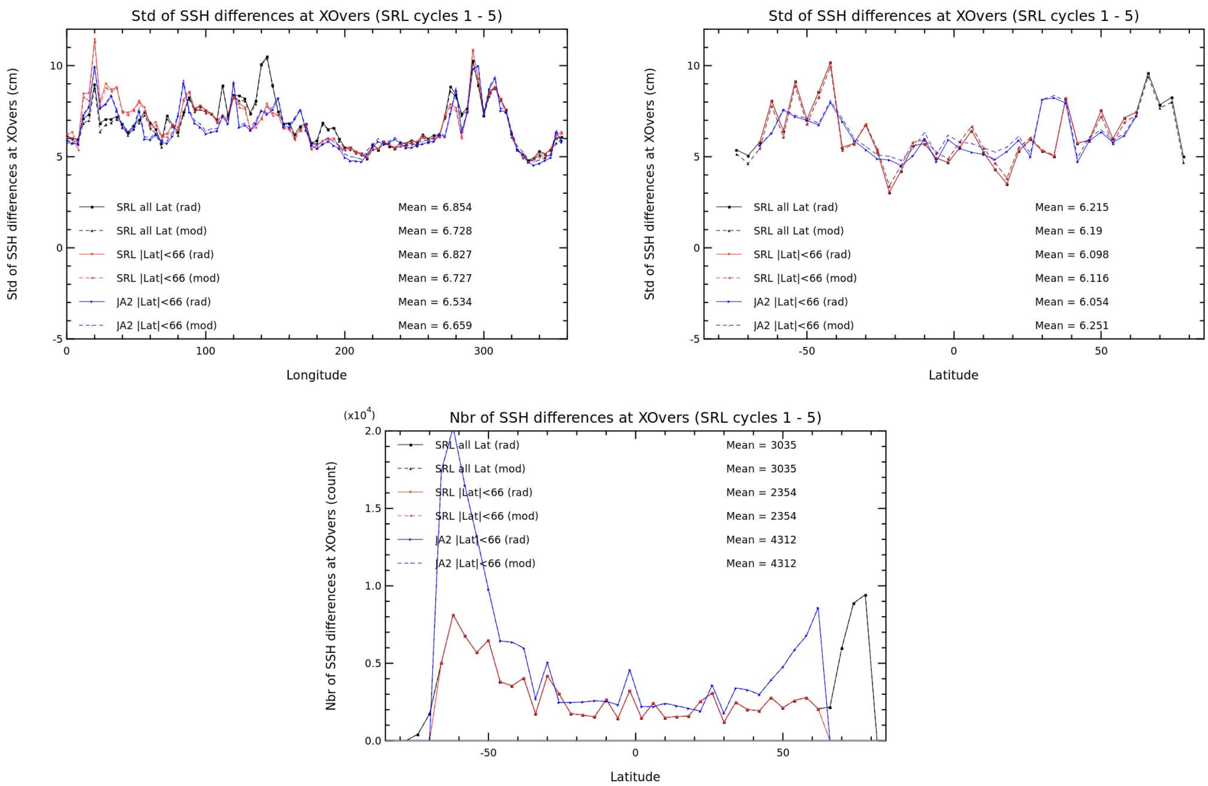

Figure 56: *Std of SSH crossover differences for Saral/AltiKa and Jason-2 GDR per 4° longitude (left) and latitude (right) bands for Saral cycles 1 to 5. Bottom: Number of SSH crossover differences for Saral/AltiKa and Jason-2 GDR per 4° latitude bands.*

The map of standard deviation of crossover differences overall the Saral/AltiKa period on the right of figure 55 shows usual results with high variability areas linked to ocean variability.

Displaying the standard deviation at crossover points in function of longitude or latitude bands (figure 56) for Saral/AltiKa and Jason-2 shows curves in-line with the previous map (increased values for latitudes and longitudes with increased ocean variability). Furthermore, the impact on meso time-scale of using radiometer or ECMWF model wet troposphere correction is visible. Whereas for Jason-2 using radiometer wet troposphere correction reduces for all latitude bandes the standard deviation, for Saral/AltiKa this is only the case for low latitudes. For latitudes higher than 40°, using ECMWF model wet troposphere correction yields better results.

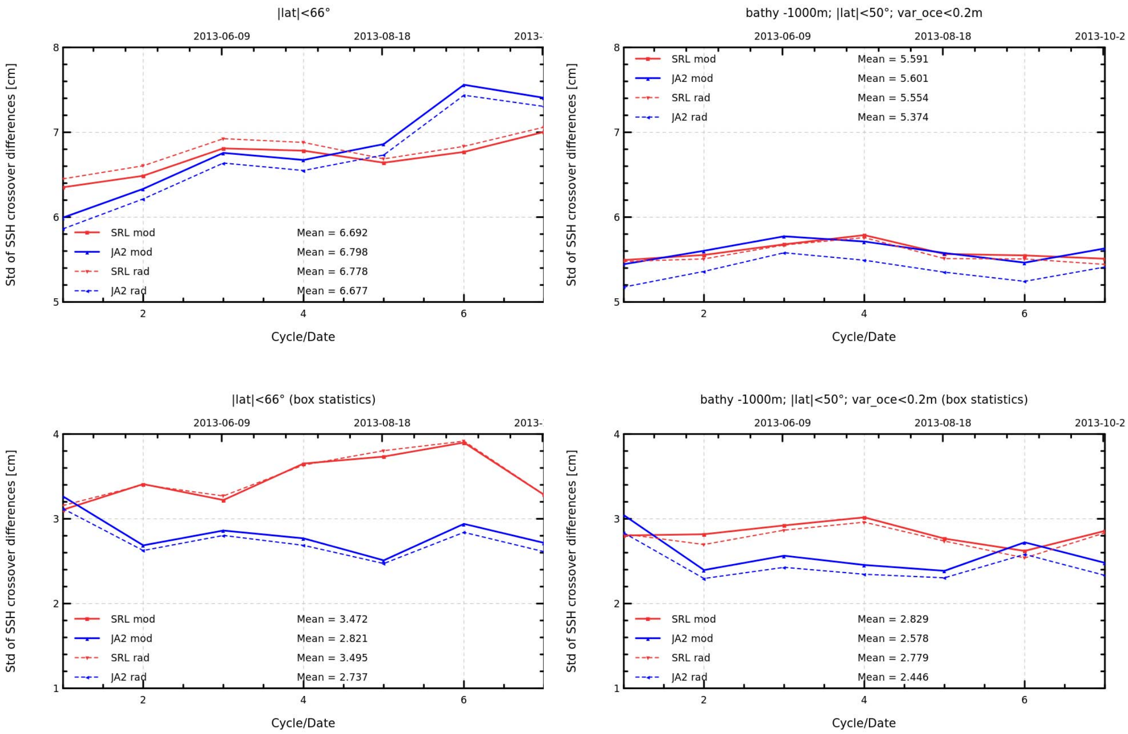

Figure 57: *Cycle per cycle monitoring of standard deviation of SSH crossover differences for Saral/AltiKa and Jason-2 GDR for Saral cycles 1 to 7 using radiometer (dotted lines) or model (plain lines) wet troposphere correction and different geographical selections: statistics over all crossover points with* $|latitude| < 66^{\circ}$ *(top left), over all crossover points with bathymetry < -1000m,* $|latitude| < 50^{\circ}$*, and oceanic variability < 0.2 m (top right). Bottom: statistics computed for crossover points binned in* $4^{\circ}x4^{\circ}$ *boxes (left: selection of* $|latitude| < 66^{\circ}$*, right: selection of bathymetry < -1000m,* $|latitude| < 50^{\circ}$*, and oceanic variability < 0.2 m).*

Comparing the evolution of the standard deviation of crossover differences for Saral/AltiKa and Jason-2 (top of figure 57), confirms higher values for Saral (till cycle 4) when taking into account crossover points up to $\pm$ 66° latitude, especially when using radiometer wet troposphere correction. Using stricter geographical selections (top right of figure 57), yields similar results for Jason-2 and Saral/AltiKa when using ECMWF model wet troposphere correction (5.6 cm). The values are similar using radiometer or ECMWF model wet troposphere correction for Saral/AltiKa, whereas for Jason-2 a clear improvement is visible when using radiometer wet troposphere correction (5.4

cm). These results confirm the previous analyses, and show that there is improvement possible concerning radiometer wet troposphere correction retrieval algorithms (which are currently not yet fully tuned). **See also chapter 7.3.3. for results using the radiometer wet troposphere correction which will be used in Patch2**.

The previous statistics were computed over the crossover points available each cycle. Nevertheless the distribution of available crossover points varies strongly with latitude and is also quite different for Saral/AltiKa and Jason-2, related to the orbit configuration. When limiting to $|latitude| < 66^{\circ}$, Jason-2 has especially numerous crossovers (several times more than Saral/AltiKa) in high latitudes (around 60°) as shown on bottom of figure 56. Note that in these regions problems related to sea ice not entirely edited may occur and have an impact on the quality of SSH differences at crossovers. Computing statistic per boxes, allows to level this difference (bottom of figure 57). The statistics yield with this method 2.8 cm for Saral/AltiKa and 2.6 cm for Jason-2 when using model wet troposphere correction and a selection of bathymetry < -1000m, $|latitude| < 50^{\circ}$, and oceanic variability < 0.2 m. When selecting crossovers till 66° latitude, using the box statistics shows also clearly a reduction of Jason-2 standard deviation compared to Saral/AltiKa.

5.5. Performances at crossover points of the different product types (Ogdr/Igdr/Gdr)

Saral/AltiKa data are also available as Ogdr and Igdr products, which are more rapidly available than Gdr products. The main difference between the different data products are listed in table 8.

Auxiliary Data	Impacted Parameter	Ogdr	Igdr	Gdr
Orbit	Satellite altitude, Doppler correction, ...	DORIS Navigator	Preliminary (Doris MOE)	Precise (Doris + Laser POE)
Meteo Fields	Dry/wet tropospheric corrections, U/V wind vector, Surface pressure, Inverted barometer correction,...	Predicted	Restituted	Restituted
Pole Location	Pole tide height	Predicted	Predicted	Restituted
Mog2D	HF ocean dealiasing correction	Not available	Preliminary	Precise
GIM	Ionosphere correction	Predicted	Restituted	Restituted

Table 8: Differences between the auxiliary data for the O/I/Gdr products (from [4])

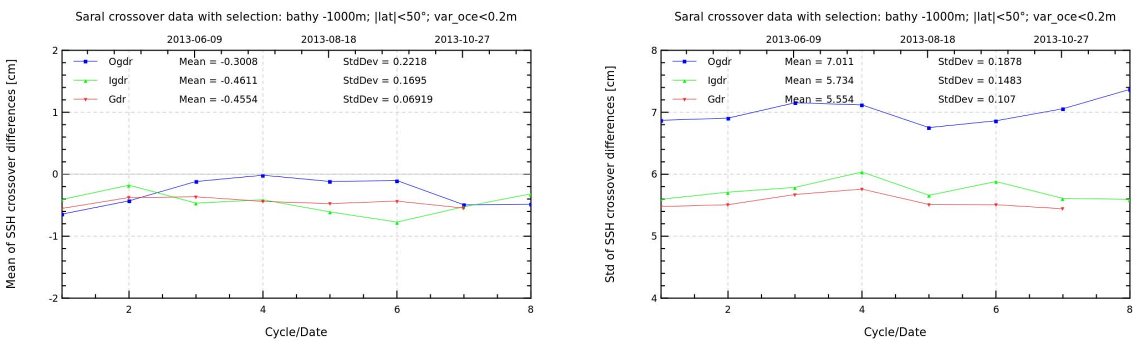

Figure 58: *Cycle per cycle monitoring of mean and standard deviation of SSH crossover differences for Saral/AltiKa using radiometer wet troposphere correction and geographical selection (|latitude| < 50°, bathymetry < -1000 m and ocean variability < 20 cm rms).*

Using geographical selections, the mean and standard deviation of ascending/descending SSH differences at crossover points are shown for the different data products on figure 58. Whereas Igdr and Gdr products show a quite stable value of the mean, the Ogdr product shows likely a periodical signal, which is probably related to the Doris/Navigator orbit solution. Standard deviation yields 7.0 cm for Ogdr (which is already quite good for Ogdr data thanks to Doris/Navigator orbit of the same generation as the one of Jason-2), 5.7 cm for Igdr and 5.6 cm for Gdr. Note that during the first year of Envisat (before the reprocessing), the standard deviation of Envisat Gdr data was 5.8 cm (of the same performance as the Igdr data from Saral/AltiKa).

5.6. Estimation of pseudo time-tag bias

The pseudo time tag bias is found by computing at SSH crossovers a regression between SSH and orbital altitude rate ($\dot{H}$), also called satellite radial speed :

$$SSH = \alpha \dot{H}$$

This method allows us to estimate the time tag bias but it absorbs also other errors correlated with $\dot{H}$ as for instance orbit errors. Therefore it is called "pseudo" time tag bias.

The Jason satellites had a pseudo datation bias close to -0.28 milliseconds with an approximately 60-days signal. The origin of this pseudo time tag bias of the Jason satellites was found by CNES in 2010 [5]. It has a mean of about -0.25 milliseconds and is dependent on the altitude of the satellite. For Jason-2 GDR-D data, the datation was directly modified in order to correct it properly, whereas for Jason-1 GDR-C product it is taken into account thanks to a correction (pseudo_datation_bias_corr_ku). Therefore the average of the pseudo datation bias is now close to zero for the Jason satellites, nevertheless the periodic signal remains and is not yet explained.
Figure 59 shows the monitoring of the pseudo datation bias for SARAL/AltiKa and Jason-2 on a cyclic basis (respectively 35 and almost 10 days).

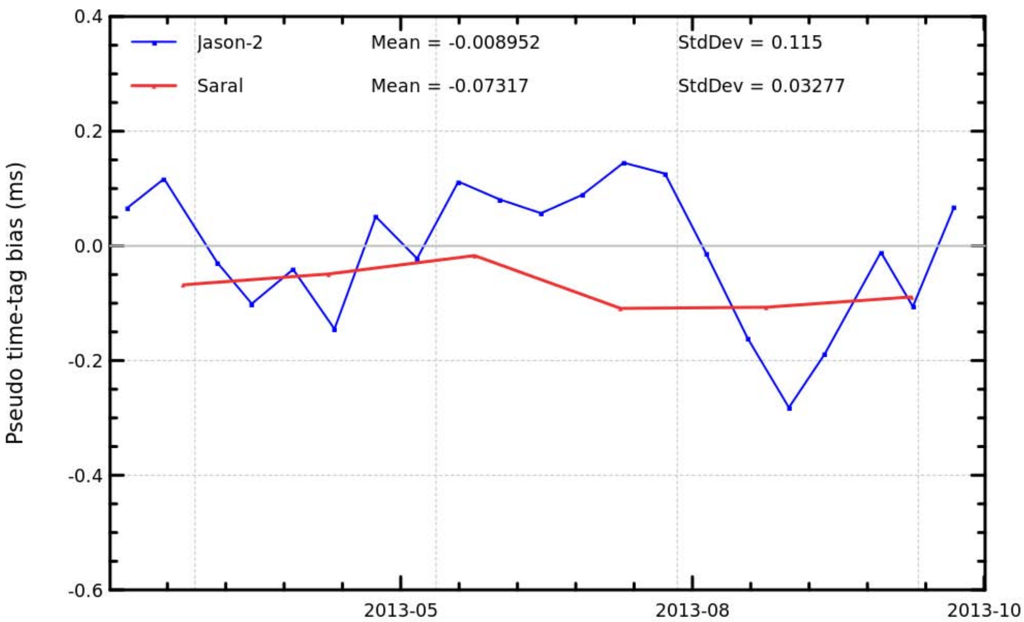

Figure 59: *Cyclic monitoring of pseudo time tag bias for Saral/AltiKa.*

6. Sea Level Anomalies (SLA) Along-track analysis

6.1. Overview

The Sea Level Anomalies (SLA) are computed along track from the SSH minus the mean sea surface with the SSH calculated as defined in previous section 5.1. :

$$SLA = SSH - MSS(CNES/CLS2011)$$

The maps of SLA (see figure 61) shown over the period of Saral/AltiKa cycle 2 are very similar between Saral/AltiKa, Jason-2 and Jason-1. Even small structures are recognizable on all three maps. This shows the already very good data quality of the Saral/AltiKa data. Note that multi-mission analysis systems, such as DUACS (see [10]) or the Australian multi-mission analysis system (see [11]) included Saral/AltiKa Ogdr and Igdr data operationally in their systems (in order to compensate for the loss of Jason-1) as soon as they were available to users (early July 2013, see [16]).

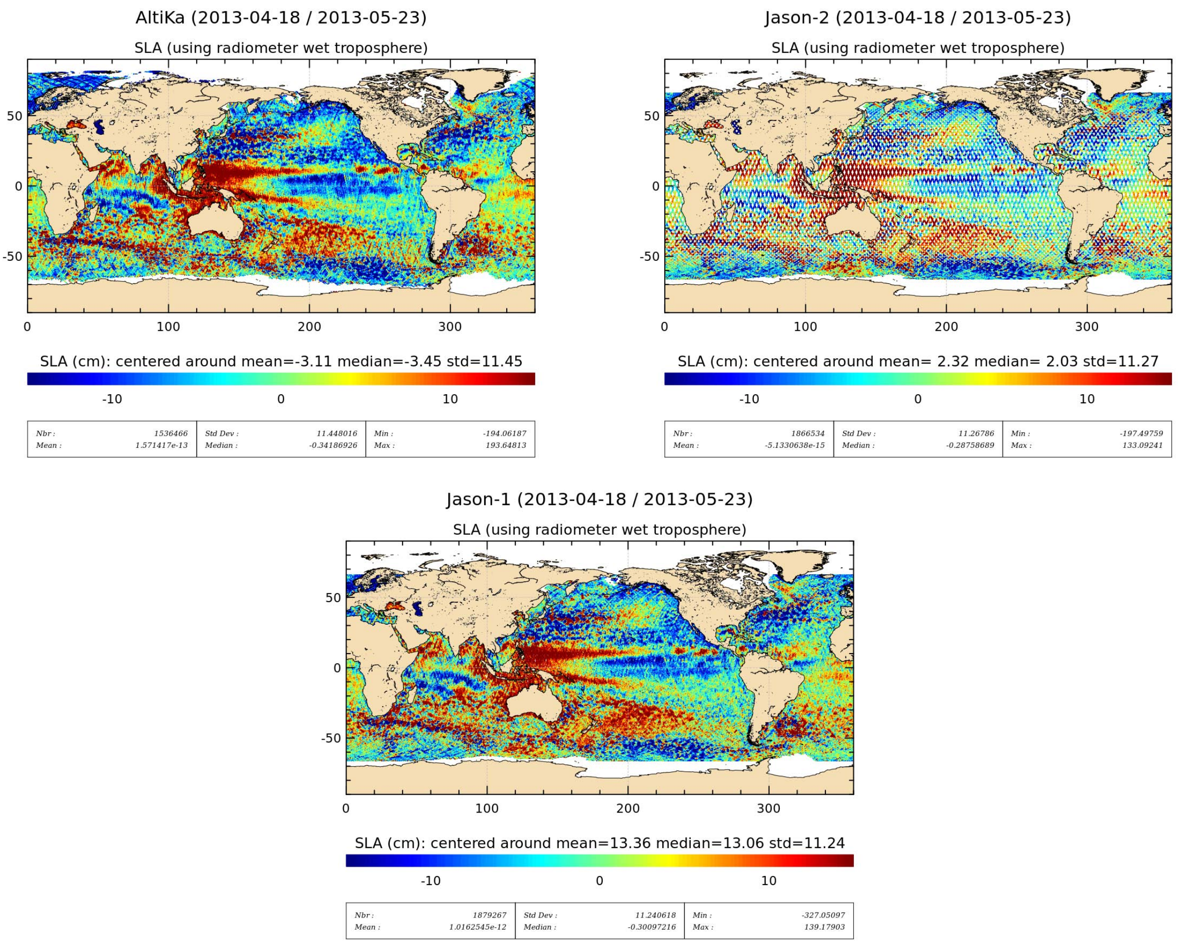

Figure 60: *Map of (centered) SLA for Saral/AltiKa (top left), Jason-2 (top right) and Jason-1 (bottom) GDR data for Saral/AltiKa cycle 2.*

6.2. Along-track performances for Saral/AltiKa (GDR-T Patch1) and Jason-2

SLA analysis is a complementary indicator to estimate the altimetry system performances. It allows us to study the evolution of SLA mean (detection of jump, abnormal trend or geographical correlated biases), and also the evolution of the SLA variance highlighting the long-term stability of the altimetry system performances. Hereafter daily monitoring of mean (top left of figure 61) and standard deviation (top right of figure 61) of Saral/AltiKa and Jason-2 SLA are shown.

Saral/AltiKa and Jason-2 daily mean of SLA show similar signals and evolution. There is an offset between Saral/AltiKa and Jason-2 SLA of around 6.5 cm when using model wet troposphere correction and around 6.1 cm when using model wet troposphere correction (see bottom of figure 61). The difference of several mm in the bias depending on the type of wet troposphere correction used is due to radiometer and ECMWF wet troposphere correction difference for Jason-2, which is around 5 mm (indeed the Jason-2 SLA curves using either radiometer or model wet troposphere correction are separated by a small offset, see top left of figure 61). Saral/AltiKa radiometer and model wet troposphere correction have generally no offset (for Patch1 data), therefore the curves are superposed, except for a period in summer/fall 2013, when a hot calibration count saturation

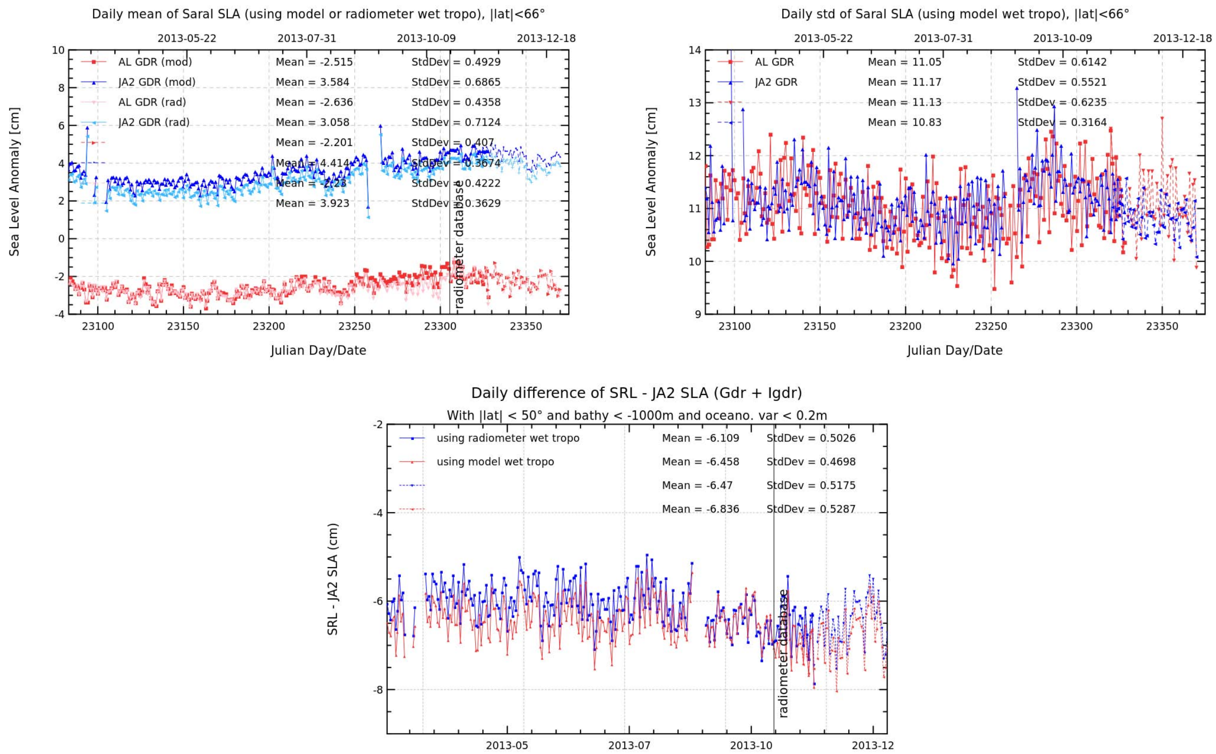

Figure 61: *Daily monitoring of mean (top left) and standard deviation (top right) of SLA (using either radiometer or model wet troposphere correction) of GDR data (plain lines) and IGDR data (dotted lines). The statistics are done for valid data with |latitudes| < 66°. Bottom: Difference of daily Saral/AltiKa minus Jason-2 SLA using either radiometer or model wet troposphere correction. The statistics are done for valid data with |latitudes| < 50°, bathymetry < -1000 m and low ocean variability.*

occurred (for more details see chapter 7.1.) and the radiometer wet troposphere correction started to drift. This was corrected on 2013-10-22 with a modification of the radiometer on-board database.

Monitoring the stability of the SLA bias between two missions which are not on the some ground-track is less precise than it was the case of Jason-1/Jason-2 or Topex/Poseidon and Jason-1 during the flight formation phase. Nevertheless the problem of hot calibration count saturation is also visible on the Saral minus Jason-2 SLA differences (see bottom of figure 61). During the first few months, there was an offset between SLA differences using either radiometer or model wet troposphere correction. During summer and fall this offset reduced (SLA bias using radiometer wet troposphere correction became even greater than SLA bias using model wet troposphere correction). After the radiometer on-board database modification the offset is restored. Nevertheless end of 2013, even the SLA bias using model wet troposphere correction seems increased, this is under investigation.
Daily standard deviation of Saral/AltiKa and Jason-2 SLA are very similar (top right of figure 61).

6.3. Along-track performances of the different product types (Ogdr/Igdr/Gdr)

Saral/AltiKa products are available for three data types (with different latency and precision): Ogdr, Igdr and Gdr. There are also some differences in the product content (see table 8). Hereafter the daily mean and standard deviation of SLA of the different data types are monitored (see figure 62). Note that only the Gdr data are an homogeneous data set (using Patch1 version for cycles 1 to 7). For Ogdr and Igdr data Patch1 version was only used from July onwards (for precise dates see table 1). This explains the jumps visible in the Ogdr and Igdr SLA series. Ogdr SLA exhibits furthermore some additional short-term (about 14 days period) and long-term (probably one-year period) signals. These are explained in chapter 7.4.. Mean of Igdr and Gdr SLA are already very close (when using Patch1 version). Standard deviation of SLA shows very good values (between 11 and 12 cm): standard deviation of Gdr product is the lowest and the one of Ogdr products is the highest. But even the performance of Ogdr products is already very good (thanks to the good quality of the Doris/Diode navigator orbit).

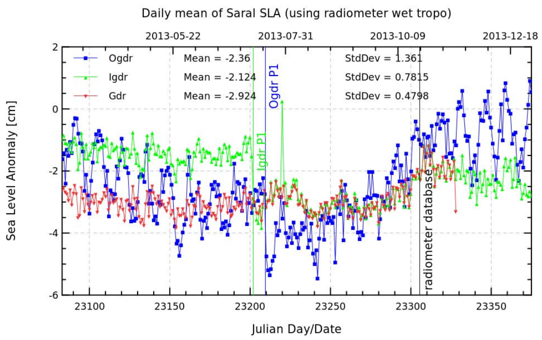

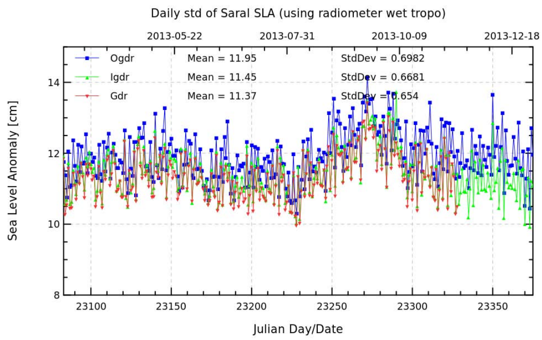

Figure 62: *Daily monitoring of mean and standard deviation of valid Saral/AltiKa SLA (with radiometer wet troposphere correction) for Ogdr, Igdr and Gdr products. No particular selection is used (latitude is not limited).*

7. Particular Investigations

7.1. Saturation of 37 GHz brightness temperature

A couple of months after the launch of Saral/AltiKa, the 37 GHz brightness temperature started to drift (top left of figure 63). This was not due to a problem of the radiometer instrument itself, but rather due to a problem in the parameterization. Indeed the hot calibration counts started to saturate. This had an impact on radiometer related variables, such as radiometer wet troposphere correction (top right of figure 63), atmospheric attenuation (bottom right of figure 63) and liquid water content (bottom left of figure 63), which all show a drift.
The saturation of the hot calibration was corrected on 22th of October 2013 by modifying the on-board radiometer database values. This had an impact on the radiometer wet troposphere correction of around 6 mm.

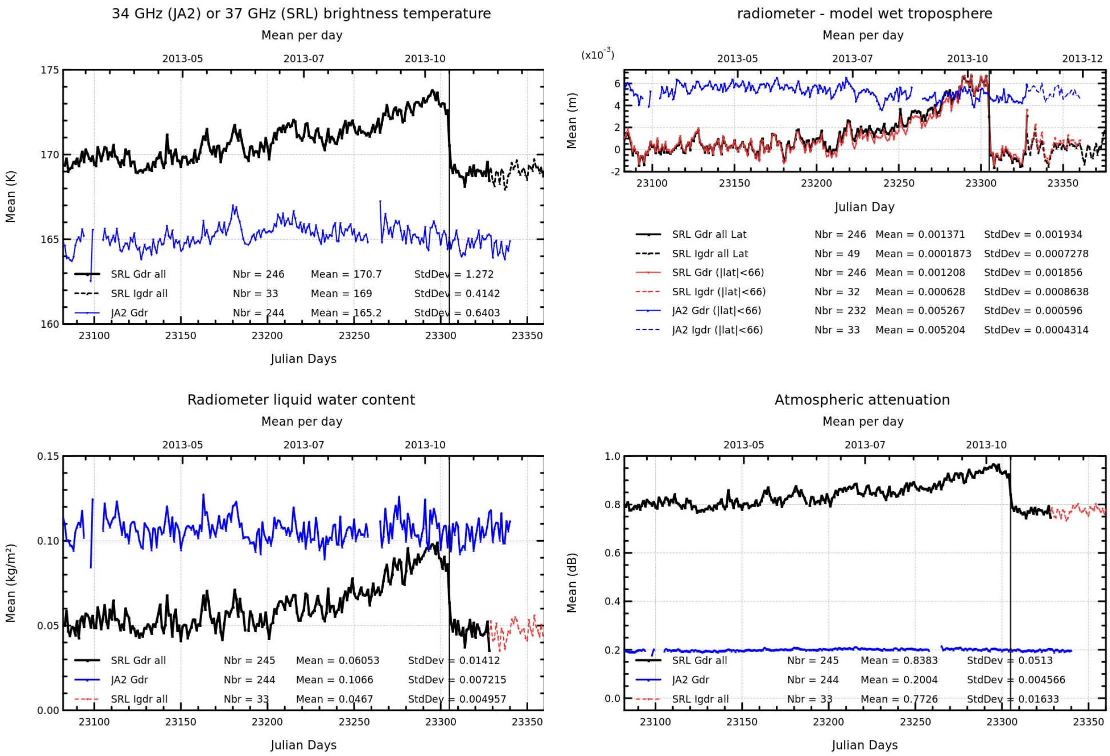

Figure 63: *Daily monitoring of mean (valid) values of (34/37 GHz) brightness temperature (top left), radiometer minus ECMWF wet troposphere correction difference (top right), radiometer liquid water content (bottom left) and atmospheric attenuation (bottom right). The vertical black line indicates when the saturation problem was corrected.*

The radiometer experts are currently investigating, if the impact of the hot calibration saturation on the radiometer wet troposphere correction might be corrected in a future reprocessing of the Saral/AltiKa GDRs. Nevertheless this is not just a global constant drift, but also dependent on the wet troposphere content itself. Indeed relatively dry troposphere regions (0 to 10 cm wet troposphere correction content) and wet troposphere regions (30 to 50 cm wet troposphere correction content) are stronger impacted by the drift, than regions with moderate wet troposphere (10 to 20 cm or 20 to 30 cm wet troposphere correction content), see left of figure 64. Separating the wet troposphere content of Jason-2 in several ranges, shows quite stable curves (right of figure 64).

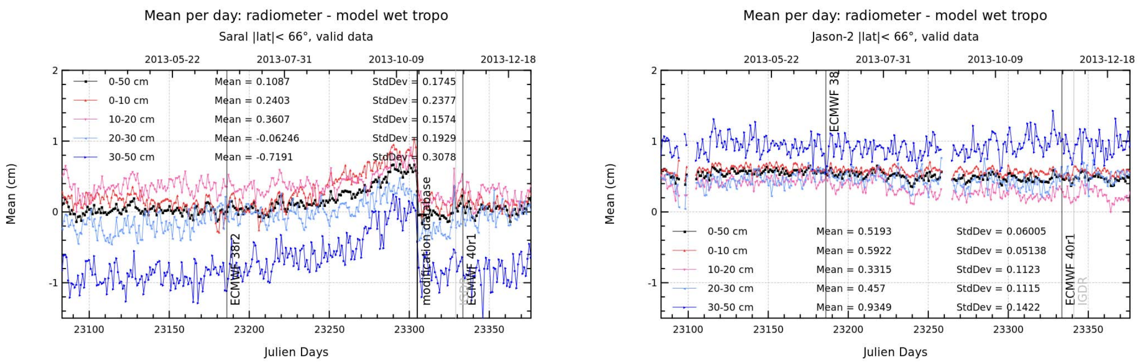

Figure 64: *Daily monitoring of mean (valid) values of radiometer minus ECMWF model wet troposphere correction differences for different ranges of wet troposphere correction values.*

7.2. Power spectrum

Computing power spectra from uncorrected SLA (orbit - range - MSS) or significant wave height, is a possibility to assess the altimeter noise (and therefore the performance of the altimeter instrument). Comparison of Saral/AltiKa and Jason-2 uncorrected SLA spectra (on the left of figure 65) shows that the noise of 40 Hz AltiKa data is 5.5 cm, whereas for 20 Hz Jason-2 data the noise is 7.7 cm. The SLA spectrum of AltiKa is closer to the theoretical SLA ocean spectrum than it is the case for Jason-2 for spatial scales between 90 and 50 km. The spectral bump is also present on the AltiKa SLA spectrum, but it only impacts spatial scales smaller than 50 km (90 km for Jason-2). This spectrum is the result of two opposed effects. On the one hand, the Saral/AltiKa foot print is reduced (compared to Jason-2), which reduces the spectral bump. On the other hand, measurements in Ka-band are more sensitive to perturbations within the footprint. These perturbations are related to rain and humidity of the atmosphere. This should increase the energy level of the spectral bump.

Concerning the SWH spectrum (on the right of figure 65), the noise of AltiKa 40 Hz SWH is 32.4 cm, whereas it is 50.9 cm for Jason-2 20 Hz SWH. Again, the spectral bump in AltiKa SWH spectrum, impacts smaller spatial scales than for Jason-2.

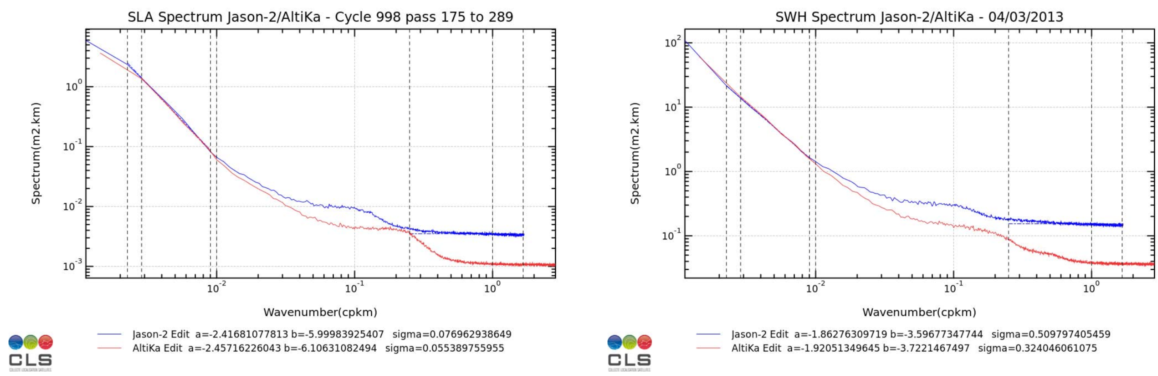

Figure 65: *Power spectrum of SLA (orbit - range - mss) on the left and SWH on the right of high resolution data of Saral/AltiKa (40 Hz data) and Jason-2 (20 Hz data). Figures from Poisson et al. [18].*

7.3. Future evolutions of the GDR product (GDR-T Patch2)

During 2013 the GDRs were produced with the so-called Patch1 (the global attribute "references" in the netcdf files is set to: L1 library=V3.1p1p2, L2 library=V4.2p1p6p9p10, Processing Pilot=V3-4-1p2p5p6p7p8p9). But work is ongoing concerning the improvement of the standards and dealing with the particularities of the Ka-band. The next version of standards (still called GDR-T, but the global attribute "references" in the netcdf files will have different values (L1 library=V4.1, L2 library=V5.2, L3 library=V4-2)), the Patch2 will be used in the beginning of 2014 (from GDR cycle 8), and GDR cycles 1 to 7 will be reprocessed with the same version. All the modifications of Patch2 are recalled in **Content of Patch2**. They were endorsed by the Preliminary Verification Workshop AltiKa held end of August 2013 in Toulouse, France (see `http://www.aviso.oceanobs.com/en/courses/sci-teams/altika-science-team/2013-saral-nrt-verification-workshop.html`). Hereafter the impact of some of the modifications in the Patch2 are already shown.

7.3.1. Altimeter wind speed algorithms

The altimeter wind speed present in the current GDR-T (Patch1) is not usable, since the look-up table from Jason-1 is used, but the Ka-band backscattering coefficient is very different from the Ku-band one. Lillibridge et al. ([13]) have developed a wind speed model for Ka-band altimetry. For Patch2 the one-dimensional model was chosen (which is based on the one used for Envisat ([1])). Results using this new wind speed model for Saral/AltiKa were also shown during OSTST 2013 meeting by Scharroo et al. ([22]).

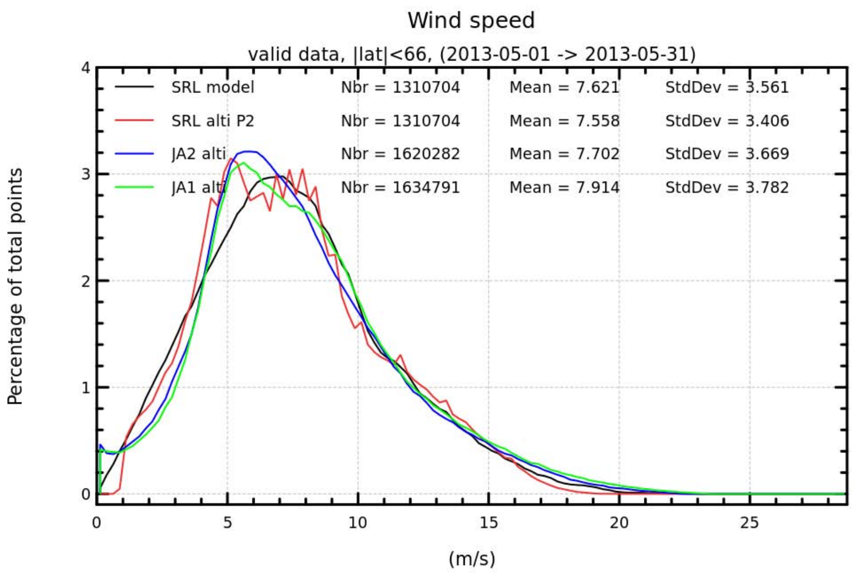

Figure 66: *Histogram of model (black) and altimeter (Saral P2: red, JA2 GDR-D: blue, JA1 GDR-C: green) for May 2013.*

Hereafter (figure 66), only a histogram of the wind speed for a one-month period is shown. The

Saral/AltiKa altimeter wind speed which will be in Patch2, has similar values as the ECMWF model wind speed and altimeter wind speeds from Jason-1 or Jason-2. Nevertheless the shape shows a kind of bi-modal behavior and wind speed only starts around 1 m/s (as it is also the case for the Envisat altimeter wind speed).

Note that the Lillibridge et al. wind speed model was developed using backscattering coefficients corrected with a model atmospheric attenuation, whereas in the GDR-T Patch2 the wind speed algorithm will be applied to the backscattering coefficient corrected for a atmospheric attenuation based on the radiometer data and a neural network solution (Patch2). It is possible to do so, as the Patch2 atmospheric attenuation and the model atmospheric attenuation used by Lillibridge et al. are not biased one with respect to the other. Once that one year of Saral/AltiKa data are available, another wind speed algorithm will be developed in the frame of the PEACHI project ([27]). It will likely be used for the Patch3 version (end of 2014) of the Saral/AltiKa data.

7.3.2. Sea state bias solutions

The Sea State Bias solution used in the Patch1 GDR-T is a simple linear relation of the significant wave height: SSB = 3.5% * SWH. Nevertheless this is overestimated and furthermore the relation between SSB and SWH is not entirely linear. Patch2 GDR-T will contain a hybrid SSB solution developed by R. Scharro (based on 5 cycles of Saral/AltiKa GDR data). This solution was developed as follows (personnel communication by R. Scharroo):

1. Use "direct method" to grid sea level anomaly as function of SWH and sigma0
2. Fit BM4 model
3. Compute residuals
4. Blend residuals into parametric solution

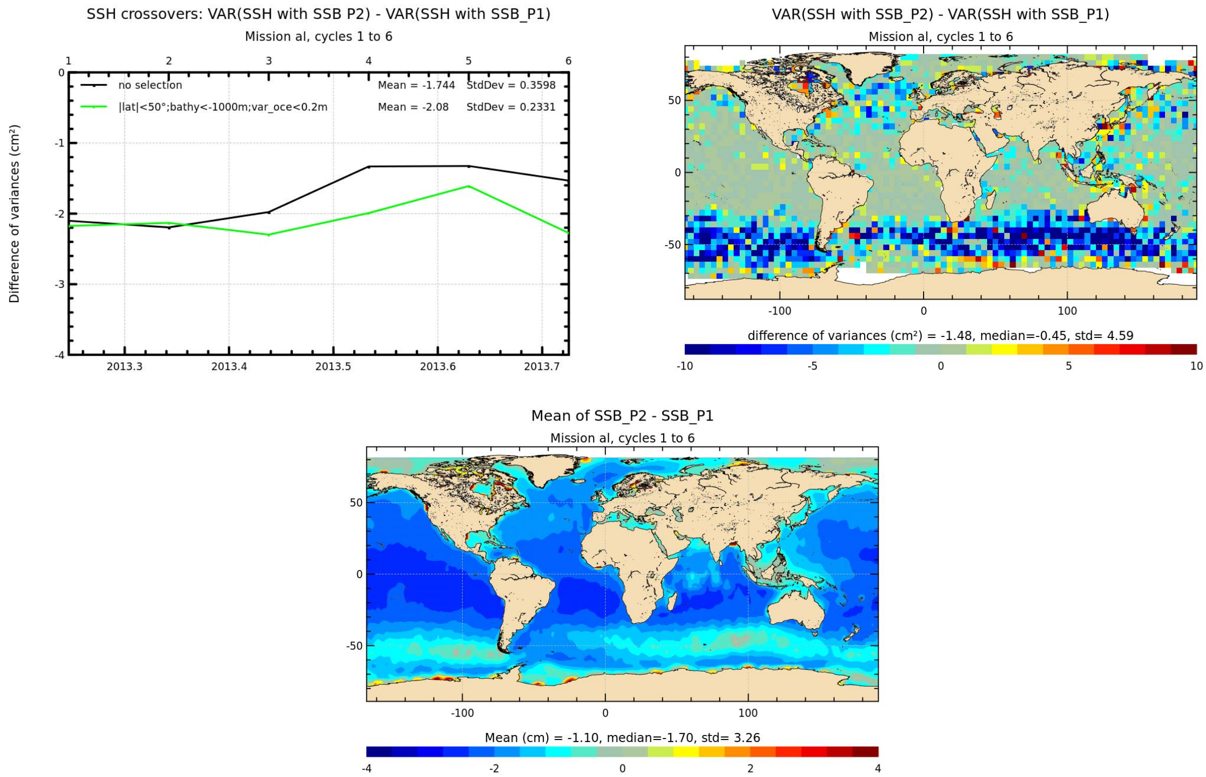

Figure 67: *Difference of variances of SSH differences at crossover points, using different sea state bias solutions (variance of SSH with SSB from Patch2 minus variance of SSH with SSB from GDR-T Patch1). Top left: cyclic monitoring for two different selections of crossover points: no special selection (black line) and only crossover points with $|latitude| < 50°$, $bathymetry < -1000m$ and low oceanic variability are selected (green line). Top right: Map of differences of variances. Bottom: Map of sea state bias differences (sea state bias solution from Patch2 − sea state bias used in GDR-T Patch1 (3.5%*SWH)). Note that for the model wet troposphere correction was used here.*

For more information on this method see Scharro et al. [21]. As it is a direct method, the current bias of Saral/AltiKa SLA (versus the Mean Sea Surface), currently around −3 cm for GDR-T

Patch1, will be reduced in Patch2. However, for the Patch2 the two-dimensional SSB solution (SSB dependent on SWH and backscattering coefficient) was converted in a one-dimensional solution (SSB only dependent on SWH).

The difference map of the two sea state bias solutions (SSB solution from Patch2 minus 3.5%*SWH), shown on bottom of figure 67, reveals a mean difference of -1.1 cm. Note that for this map all data were used (except over land), regardless if valid or not. The positive differences near the coasts (Antarctic, Bay of Bengal, ...) are probably related to not valid data, therefore the difference between the two sea state bias solution is likely higher (in absolute values), as also suggested by the median value of -1.70 cm. The solutions are less different for high significant wave heights. The mean value of the sea state bias of Patch2 is in absolute values larger than the SSB in Patch1. This impacts the SLA value and so the SLA in Patch2 is above the one in Patch1.

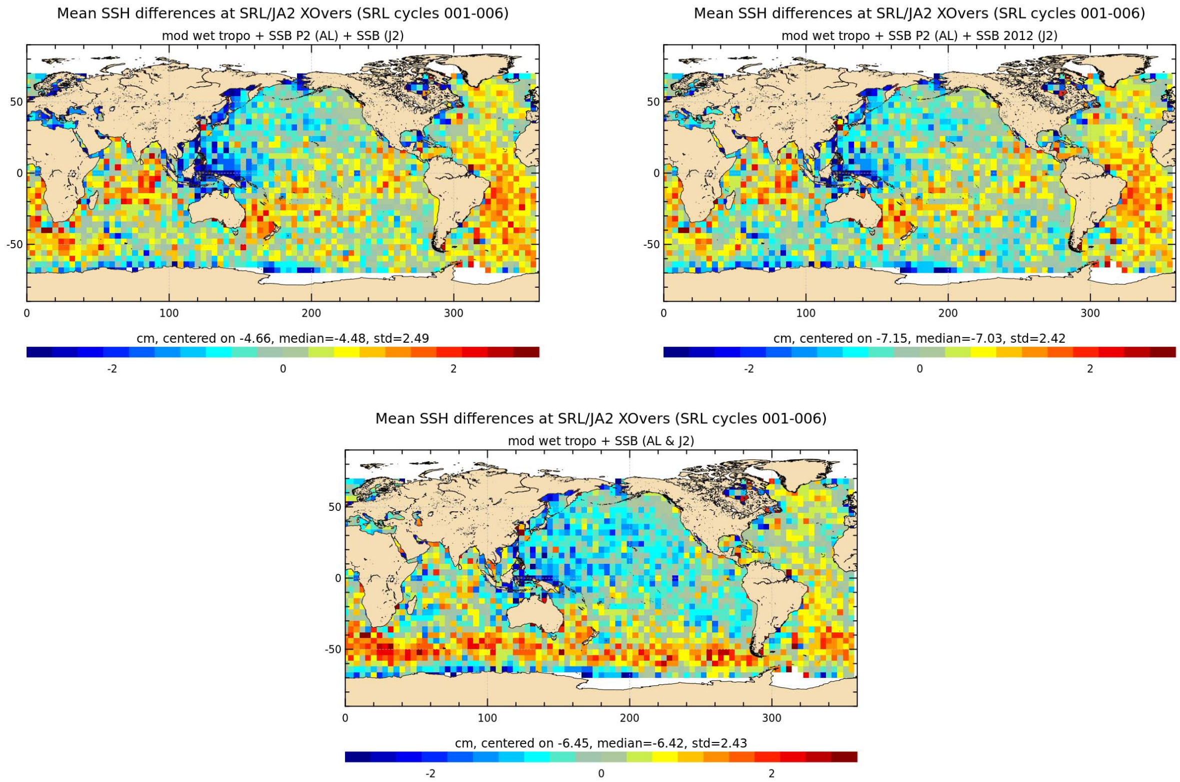

Figure 68: *SSH difference maps at multi-mission crossover points (Saral/AltiKa minus Jason-2) using model wet troposphere correction. Using sea state bias solutions from the GDR products (Saral/AltiKa: GDR-T Patch1, Jason-2: GDR-D) on bottom, using updated sea state bias (the one which will be available in Patch2) for Saral/AltiKa (top left) and updated sea state bias solution for both Saral/AltiKa (SSB Patch2) and Jason-2 (2012 solution, see [26]) on top right.*

The difference of variances of SSH differences at crossover points shows a reduction close to 2 cm2 over the 6 cycles analyzed (top left of figure 67). The top right figure 67 shows the geographical distribution of this difference. The Patch2 sea state bias solution reduces the SSH variance strongly (up to -10cm) in the region of high significant wave heights (around 50˚S). The sea state bias solution of Patch2 will therefore have a strong positive impact on the performance at meso-scales of

Saral/AltiKa data.

Concerning the geographical biases between Saral/AltiKa and Jason-2, the bottom of figure 68 shows the SRL/JA2 crossover difference map when using the following GDR products: Saral/AltiKa GDR-T Patch1 and Jason-2 GDR-D, similar to the figure 51. Differences up to 2 cm amplitude occur in the high significant wave height region. Slightly positive values are found in the Atlantic ocean and slightly negative values are found in the Pacific ocean.
The maps using updated sea state bias solutions in SSH difference computation are shown on top of figure 68. The structures of the regional biases are very similar. Notably the positive difference for high significant wave height has disappeared (thanks to the Patch2 SSB solution). Nevertheless other structures are evidenced, such as negative difference for regions of low significant wave height.
Concerning the global bias between Saral/AltiKa and Jason-2, it is close to -6.5cm with the official products. Using the Patch2 SSB solution, will reduce this bias to around -4.7cm. But using in addition the Jason-2 2012 sea state bias solution, increases again the bias between the two missions (-7.2cm).

7.3.2.1. Sea state bias solution from PEACHI project

The PEACHI (Prototype for Expertise on AltiKa for Coastal Hydrology and Ice) project is a CNES initiative to provide experimental improvements of Ka altimeter measurements in open ocean, coastal areas, but also in continental and sea ice domains. It aims at improving the reliability, the accuracy and the precision of the geophysical parameters with new or better algorithms [27].

Thanks to the PEACHI prototype a new sea state bias correction (SSB_CNES_CLS_PEACHI_2013) was computed, see [19]. This solution was computed with GDR data from cycles 1 to 4 using SSH differences at crossover points. For this sea state bias solution, ECMWF model data for wind speed and wet troposphere correction were used. This model will not be present in Patch2, but an updated version (using Saral/AltiKa data over a year period) might be present in Patch 3 (expected for end of 2014).

The PEACHI SSB solution shows significant improvement versus the Patch1 SSB solution in the same regions as the Patch2 SSB solution: around 50°S, but also in North Atlantic (right side of figure 69). In addition this improvement is generally stronger than the improvement provided by the Patch2 SSB solution. The variance reduction (compared to Patch1 SSB) is systematically stronger (left of figure 69) when using PEACHI SSB solution than when using Patch2 SSB solution.

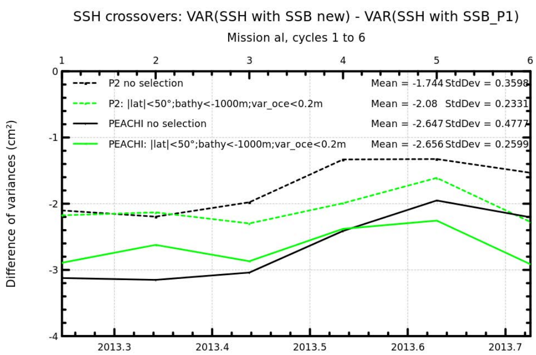

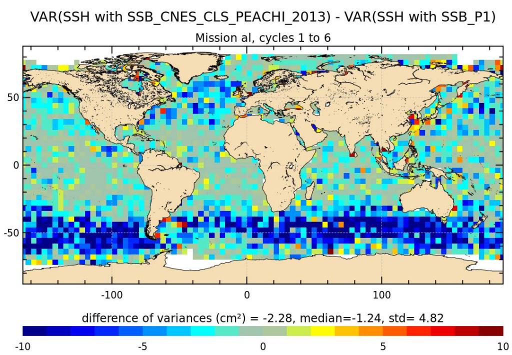

Figure 69: *Differences of variances of SSH at crossover points, using different sea state bias solutions (Variance of SSH with SSB from PEACHI (or Patch2) minus variance of SSH with SSB from GDR-T Patch1). Left: Cyclic monitoring for two different selection of crossover points: no special selection (black line) and only crossover points with* $|latitude| < 50\,^{\circ}$*,bathymetry* < -1000*m and low oceanic variability are selected (green line). Patch2 SSB solution (dotted lines) and PEACHI SSB solution (plain lines) are compared to Patch1 SSB solution. Right: Map of difference of variances. Note that model wet troposphere correction was used here.*

7.3.3. Improved radiometer wet troposphere correction

For Patch2, the neural network coefficients have been updated. This has an impact on the radiometer related parameter, such as the radiometer wet troposphere correction. Hereafter, this impact is studied using either Patch1 or Patch2 (algorithm) radiometer wet troposphere correction, all other parameters are from Patch1 GDR-T data.
The difference of the two radiometer wet troposphere corrections is shown on top right of figure 70. Differences of around 2 cm amplitude are present in equatorial regions, especially in the Indonesian region, showing that the Patch2 radiometer wet troposphere correction is in these regions dryer than the Patch1 one. The SLA of Patch 2 will in these regions decrease compared to Patch 1 SLA. The global impact is around 5 mm.

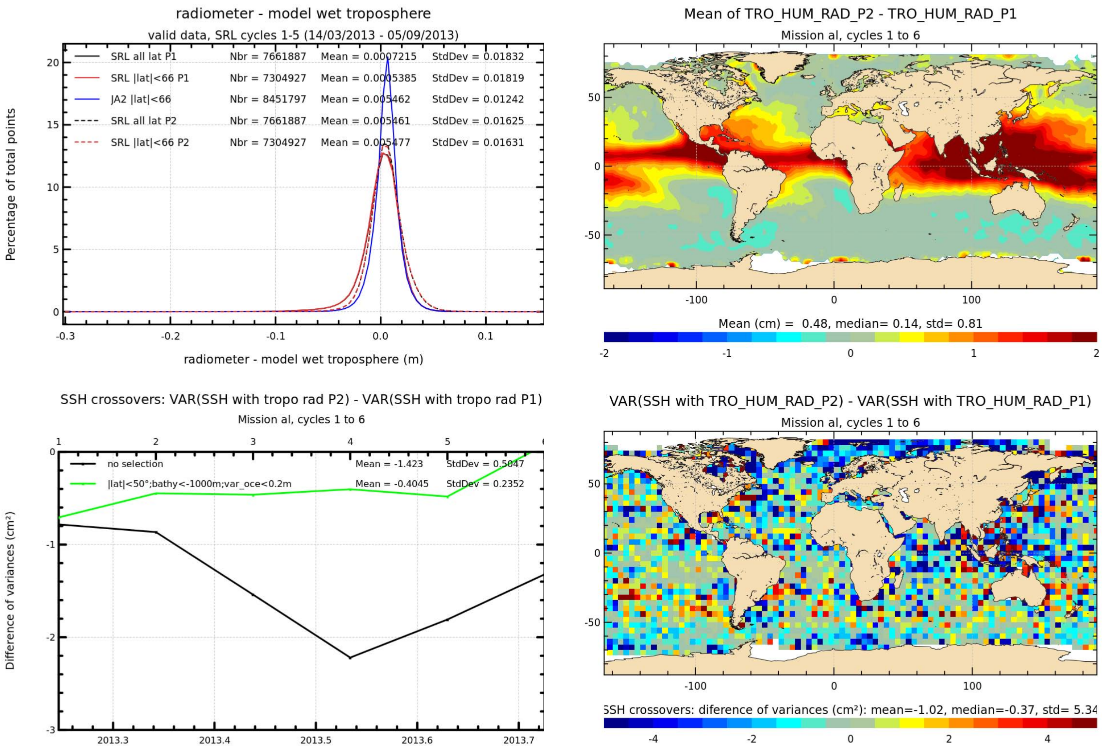

Figure 70: *Top left: Histogram of radiometer (from Patch1 data or updated with Patch2 algorithm) - ECMWF model wet troposphere for Saral/AltiKa cycles 1 to 5. Top right: difference map of radiometer wet troposphere correction Patch2 minus Patch1. Bottom: Differences of variances of SSH at crossover points, using different radiometer wet troposphere corrections (Variance of SSH with radiometer wet troposphere correction from Patch2 algorithm minus variance of SSH with radiometer wet troposphere correction from GDR-T Patch1). Bottom left: Cyclic monitoring for two different selection of crossover points: no special selection (black line) and only crossover points with* $|latitude| < 50^{\circ}$*,bathymetry* $< -1000m$ *and low oceanic variability are selected (green line). Bottom right: Difference map of SSH variances at crossover points.*

Histograms of the radiometer minus ECMWF model wet troposphere correction shows that it will be slightly biased with Patch2 (5 mm, as it is also also for Jason-2), but the standard deviation will be reduced from 1.8 cm (Patch1 data) to 1.6 cm for Patch2 data (see top left of figure 70). Note that standard deviation for Jason-2 wet troposphere difference is 1.2 cm (but this is partly related to the fact that Jason-2 has a tri-frequency radiometer, whereas the one of Saral/AltiKa is a dual-frequency radiometer, which makes the wet troposphere correction retrieval more difficult).

Using the Patch2 radiometer wet troposphere correction for SSH computation, has a small impact on the performance of Saral/AltiKa at crossover points when considering only crossover points with the following selection: $|latitude| < 50^{\circ}$,bathymetry < -1000m and low oceanic variability. In this case the Patch2 radiometer wet troposphere correction leads to a small variance reduction of around 0.4 cm2 (green line on bottom left of figure 70). When considering crossover points without special selection (black line), the SSH variance reduction due to Patch2 radiometer wet troposphere correction increases to 1.4 cm2. This behavior becomes clear on the difference map of SSH variances (bottom right of figure 70): the region of highest variance reduction is in high northern latitudes, whereas it is lowest for the latitude band of 20 to 50°S.
To conclude, the Patch2 radiometer wet troposphere correction has globally a positive impact on the Saral/AltiKa performance at crossover points.

7.3.4. Comparison between GDR-T patch1 data and data updated with patch2 algorithms

Hereafter GDR-T Saral/AltiKa data were updated as much as possible with the algorithms which will be used for Patch2. This concerns the sea state bias correction and the radiometer wet troposphere correction. In the following data from current GDR-T (Patch1 version) are compared with updated GDR-T (Patch2 like).

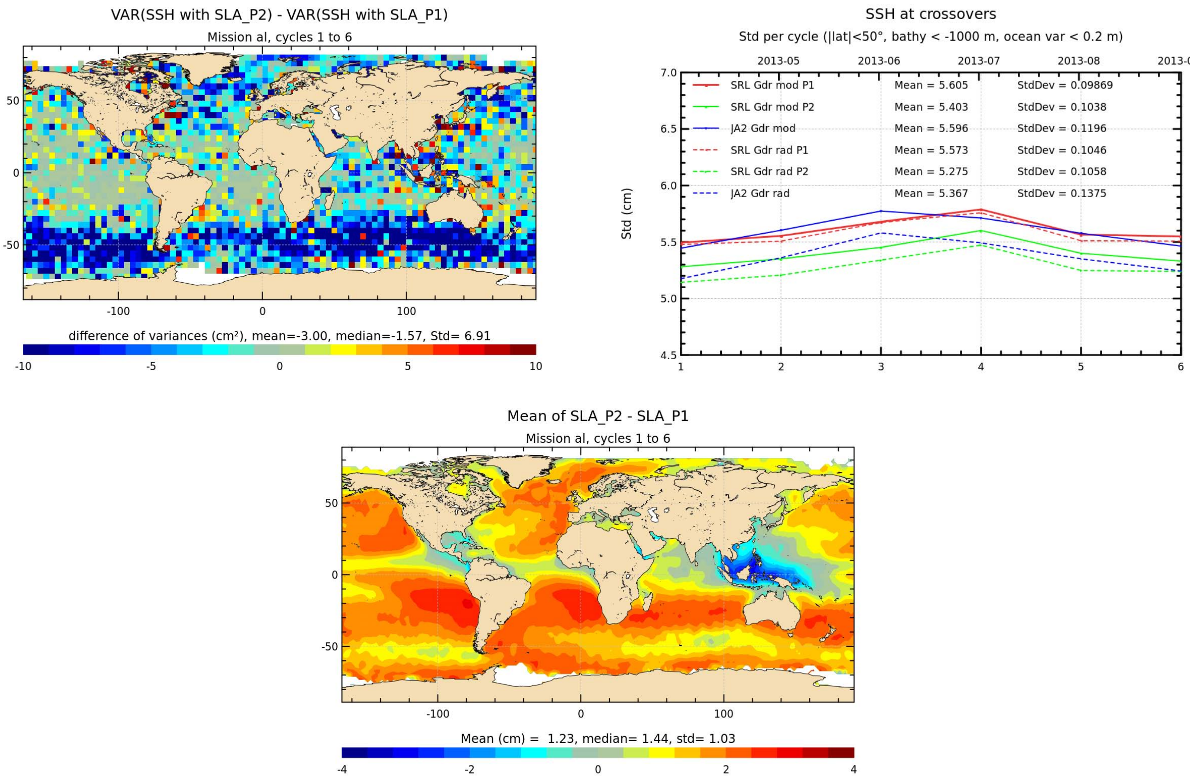

Figure 71: *Difference of variances of SSH differences at crossover points using data from Patch1 or data close to Patch2. Top left: Difference map of SSH variances (variance (SSH Patch2 like) - variance (SSH with Patch1 data). Note that radiometer wet troposphere correction is used. Top right: cyclic monitoring of standard deviation of SSH differences at mono-mission crossover points (using the following selection:*$|latitude| < 50^{\circ}$*,bathymetry* $< -1000m$ *and low oceanic variability). Statistics are shown using either radiometer (dotted lines) or model (plain lines) wet troposphere correction. Bottom: Difference map of SLA using either Patch2 like data or Patch1 data (over Saral/AltiKa cycles 1 to 6). Note that radiometer wet troposphere corrections are used.*

Comparing SLA of Patch2 like data and Patch1 data, shows that Patch2 like SLA is in average 1.2 cm higher than Patch1 SLA (see bottom of figure 71). This is due to the Patch2 SSB solution which has stronger values than Patch1 SSB solution (as SSB is a negative correction, SLA values increase), see also chapter 7.3.2.. Nevertheless this increase is not geographically homogeneous. In addition to the geographical differences due to the differences between the two SSB solutions, the new radiometer wet troposphere correction decreases locally the SLA values. This is especially the case for the region around Indonesia.

Concerning the difference map of SSH variances (using Patch2 like data or Patch1 data), it is very similar to the map shown on top right of figure 67, showing the large contribution of the SSB Patch 2 solution to the improvement. But there is also a variance reduction in high northern latitudes (thanks to the Patch2 radiometer wet troposphere correction). The global variance reduction (approximatively 3.2 cm2) for a selection of $|latitude| < 50^{\circ}$,bathymetry < -1000m and low oceanic variability (using Patch2 like data instead of Patch1 GDR-T data), is greater than the sum of the individual reductions of either the Patch2 SSB (around 2 cm2, see chapter 7.3.2.) or the Patch2 radiometer wet troposphere correction (around 0.4 cm2, see chapter 7.3.3.). For Patch2 like data, the use of the radiometer wet troposphere correction helps to reduce the variance of ascending/descending SSH differences: the figure decreases from 5.4 cm (with model wet troposphere correction) to 5.28 cm (with radiometer wet troposphere correction) which corresponds to a variance reduction of 1.36 cm2 (see top right of figure 71). The Patch2 standard deviation of SSH differences at crossovers using radiometer data (5.28 cm) is even smaller than the figure for Jason-2: 5.37 cm (though this is probably favored by a more advantageous spatial distribution of Saral/AltiKa crossover points compared to Jason-2).
In conclusion the improved algorithms for Patch2 will have a significant positive impact on Saral/AltiKa performance at crossover points.

7.4. Temporal signal in the OGDR SLA for Jason-2 and Saral/AltiKa

Monitoring of OGDR SLA showed temporal signals (see left of figure 72) for Saral/AltiKa as well as Jason-2 data. These signals are strongly reduced when replacing OGDR orbit solution by MOE (Medium Orbit Ephemeris) orbits. Note that the orbit solution furnished with the OGDR products are based on Doris/Diode measurements, but they are computed by TRIODE software. Monitoring of the difference between the TRIODE orbit (from OGDR products) and POE/MOE (see on right side of figure 72), shows that the temporal signals come from the OGDR orbit solution (and not from other corrections which are different between OGDR and I/GDR).

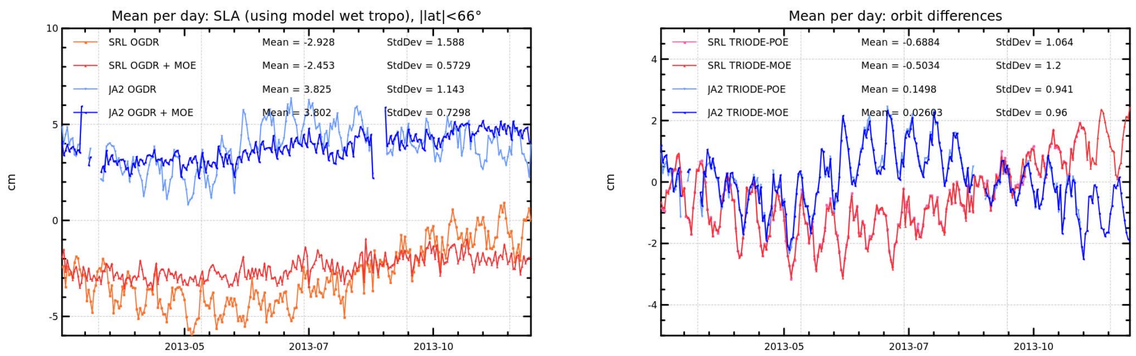

Figure 72: *Daily mean of OGDR SLA for Saral/AltiKa (orange) and Jason-2 (light blue), as well as OGDR SLA, where the product orbit solution (TRIODE) is replaced with MOE orbit on the left. Daily mean differences between TRIODE and POE orbits on the right*

When adjusting sinusoidal signal to the difference between TRIODE and MOE/POE orbits (see figure 73), the temporal signals are composed of a short-term signal around 14 days (though Jason-2 signal is slightly shorter) and a longer-term signal: around one year for Saral/AltiKa and less than 6 months for Jason-2.

Investigations by Doris/Diode experts found an explanation for the short-term signal (see [12]). When comparing Diode orbits (coming from board bulletins) with POE, this short-term signal is not observable (see figure 74). Indeed, in the TRIODE software some approximations are done in the TRIODE reference system (position of the moon), in order to speed-up computation. A new version of TRIODE was developed, which corrects the approximation. This will be active for Saral/AltiKa OGDR, when they switch to Patch2. The longer-term signal is under investigation, but might also vanish when the new version of TRIODE is used.

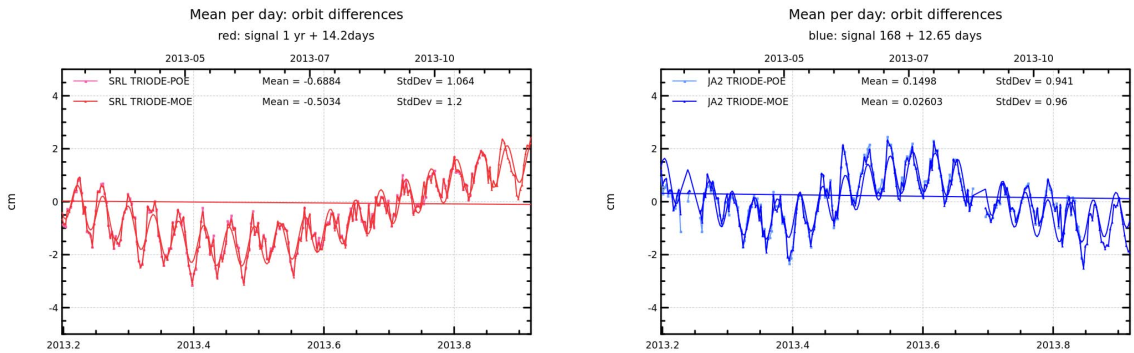

Figure 73: *Daily mean of differences between TRIODE and POE/MOE orbits for Saral/AltiKa (left) and Jason-2 (right).*

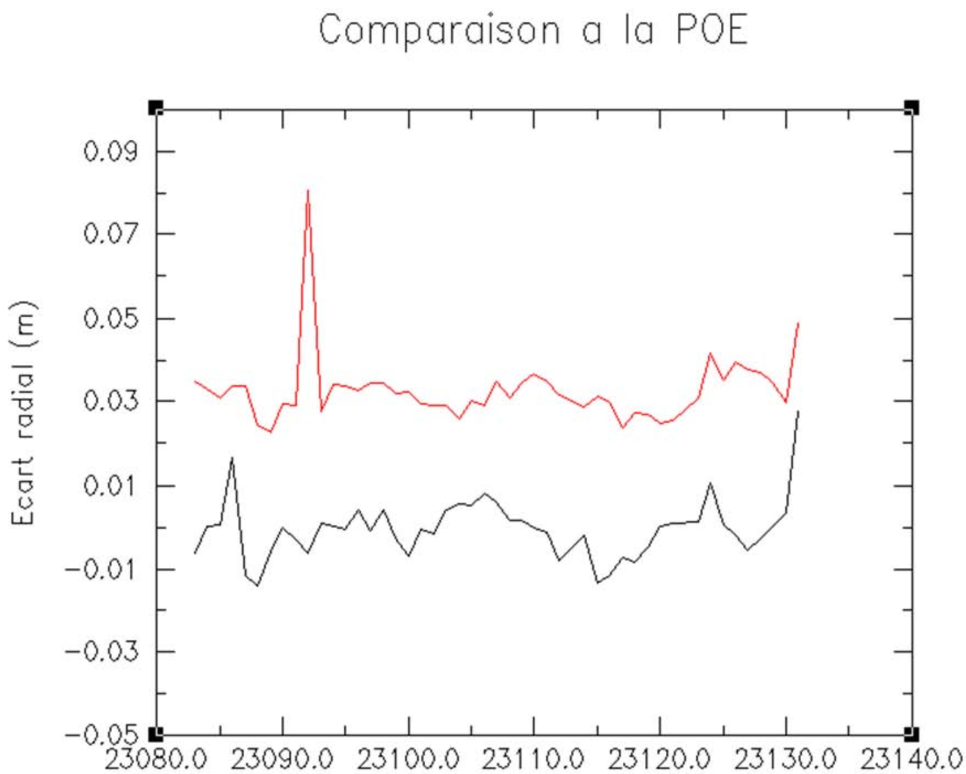

Figure 74: *Rms (red) and mean (black) of differences between Diode (from board bulletins) and POE. Figure from C. Jayles.*

7.5. Behaviour near coasts

As Saral/AltiKa uses Ka-band frequency it has a reduced footprint compared to Ku-band altimeters and therefore its spatial resolution is higher. This is especially the case for the 40 Hz data, which have a data point every around 175 m (along-track). Concerning 1 Hz data, they have a data point every around 7 km, this is a longer distance than for Jason-2 (around 5.8 km), but as Saral/AltiKa has a smaller footprint, it should be less impacted when approaching coasts.

On figure 75, several parameters (range_rms, range_numval, sig0, and tb_ka) for different altimeter missions are binned in 1 km sections in function of coast distance. For each bin the mean value is plotted. Generally, Saral/AltiKa data are less (or later) impacted by the approaching coast than the other missions.

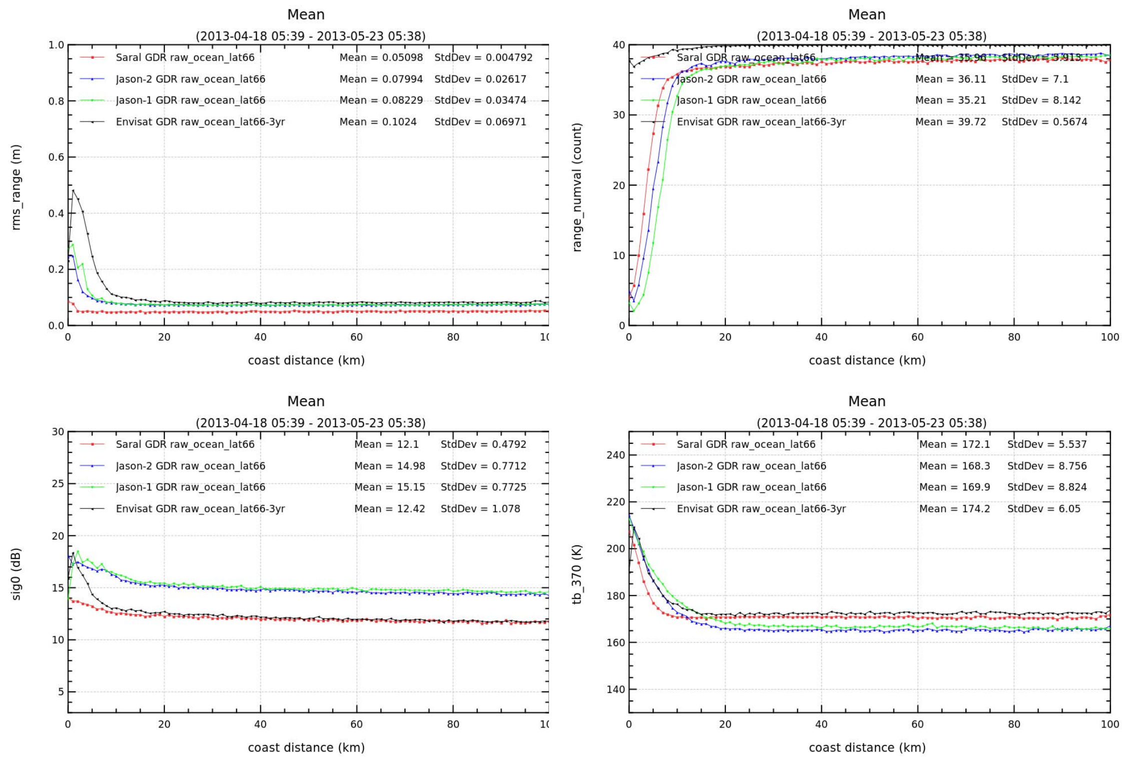

Figure 75: *Mean of rms of elementary range (top left), number of elementary range (top right), backscattering coefficient (bottom left) and 37/34 GHz brightness temperature (bottom right) in function of coast distance (1km bins) for Saral/AltiKa, Jason-1, Jason-2, and Envisat over a 35 day period. Envisat data are from 3 years earlier. Ku-band number of elementary range (JA1, JA2, EN) is multiplied by 2.*

7.6. Impact of test orbit solution using EIGEN6S2 gravity field

CNES POD (precise orbit determination) department released before OSTST 2013 a new set of test orbits (for Jason-1, Jason-2, Envisat, Cryosat-2 and Saral/AltiKa) using a new gravity field : EIGEN6S2 instead of EIGEN-GRGS_RL02bis_MEAN-FIELD (currently used in POE-D standard and used in Jason-2 GDR-D and Saral/AltiKa GDR-T). The EIGEN6S2 gravity field is based on GRACE data till 2012 and besides the periodic annual and seasonal components, this new field accounts for non-linear inter-annual variability with a piecewise linear model (bias and drift per year). Data beyond 2012 are extrapolated with zero-drift (see L. Cerri presentation [7]).
Though for the other missions, the orbit solution using EIGEN6S2 gravity fields has an impact (see [15]), for Saral/AltiKa no real impact is noticeable. The difference map of the two orbit solutions (bottom of figure 76) shows some regional differences, but with a small amplitude (± 3 mm). The maps of SSH differences at crossovers points (top of figure 76) are very similar using either POE-D or EIGEN6S2 orbit. For Saral/AltiKa both orbit solutions are equivalent (though this might change with a longer time series).

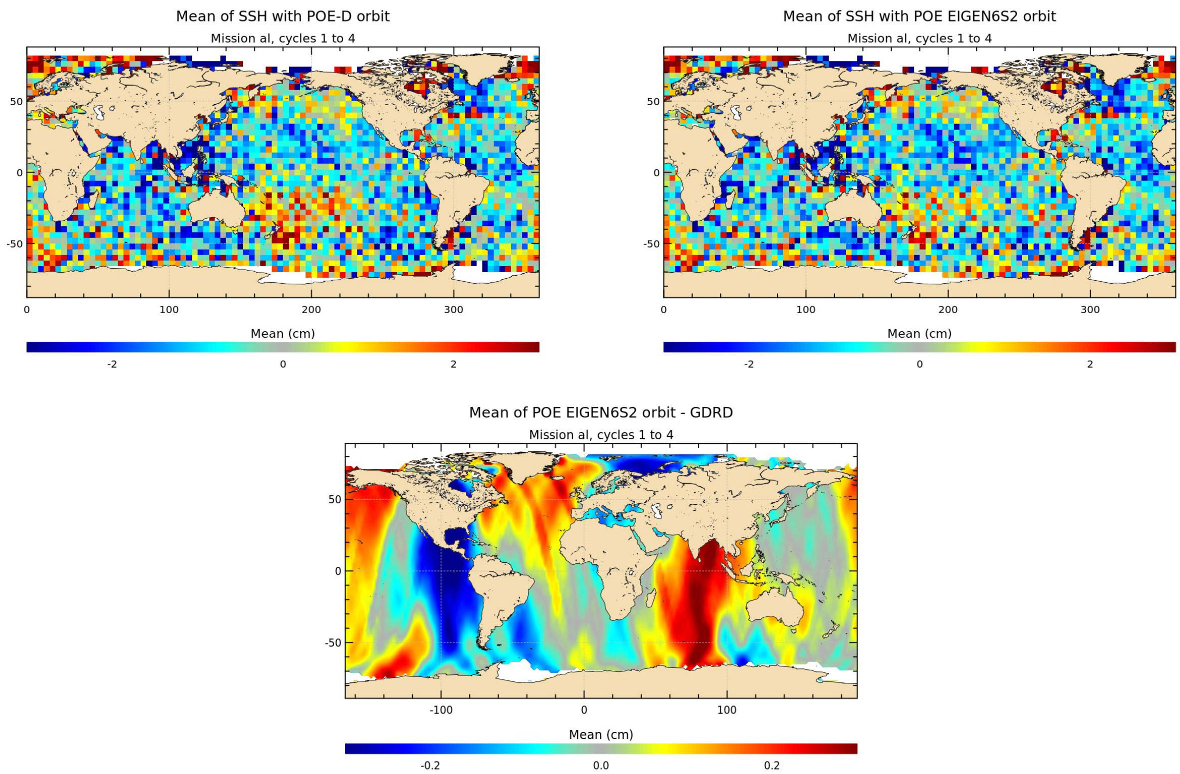

Figure 76: *Maps of mean of SSH differences at crossovers using POE-D (from GDR products) standard (top left) or EIGEN6S2 POE (top right) for Saral/AltiKa cycles 1 to 4. Map of orbit differences (POE EIGEN6S2 - POE-D) for Saral/AltiKa cycles 1 to 4.*

7.7. Ground track of Saral/AltiKa

Saral/AltiKa was meant to fly on the same historical ground-track as Envisat. After the launch, Saral/AltiKa reached its operational orbit on 2013-03-13, just one day before cycle 1 started. But it became evident, that this ground-track was very close to, but not exactly like the Envisat ground-track: at high latitudes the Saral/AltiKa ground track was 2.2 km further north or south than the Envisat ground-track. An inclination maneuver was performed on 2013-07-29 with a commanded inclination correction of 0.023 deg, but the realized maneuver was stronger than expected. The resulting Saral/AltiKa inclination was a bit lower than the Envisat one's. On 3rd and 7th of October 2013, two more inclination maneuvers were performed. As a result, Saral/AltiKa has reached the Envisat ground-track. This is illustrated on left side of figure 77, showing the maximum latitude for each pass of Saral/AltiKa (red curve) and for comparison for two years of Envisat (during it was on its repeat track). Since 2013-10-07, Saral/AltiKa has a maximum latitude of 81.5°, as it was also the case for Envisat. This maximum latitude shows a small drift, as for Envisat, where several times per year an inclination maneuver was performed, in order to keep the maximum latitude constant.
As for Envisat (in addition to the inclination maneuvers), station keeping maneuvers are performed for Saral/AltiKa in order to keep the ground-track in a ± 1km window (considering across-track direction) versus the theoretical ground-track (see right side of figure 77).

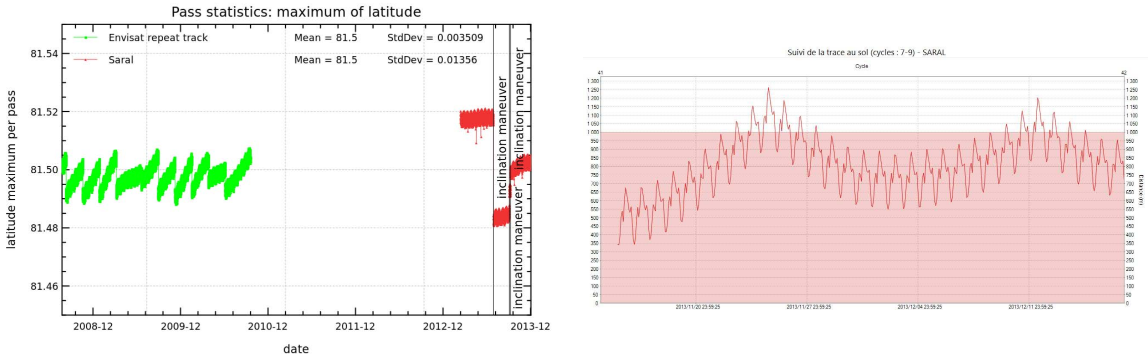

Figure 77: *Left: pass statistics showing maximum of latitude for (approximatively 2 years of) Envisat repeat track and Saral/AltiKa. Right: Monitoring of the Saral/AltiKa versus the theoretical ground-track over a period of 2 months (figure from [8]).*

7.8. Exploring the behavior of a Ka-band altimeter over the Arctic Ocean

A poster concerning the behavior of the Saral/AltiKa altimeter over the Arctic Ocean was presented at OSTST 2013 (Boulder, USA). It is shown in figure 78 and also available on Aviso website [20].

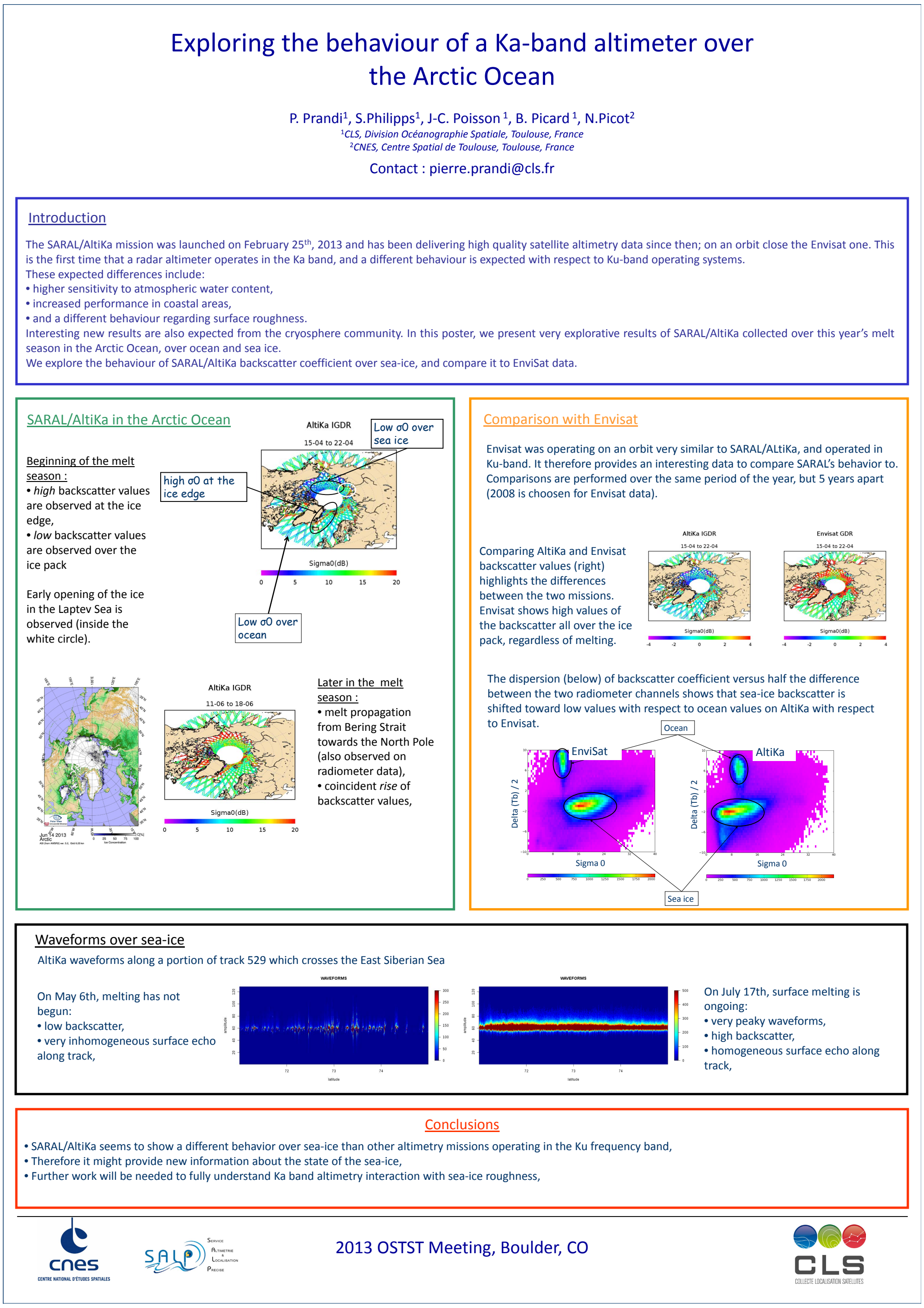

Figure 78: *Poster presented at OSTST 2013 [20].*

8. Conclusion

Saral/AltiKa was launched on February, 25th 2013. Since March, 13th, Saral / AltiKa is on its operational orbit. Its the first altimeter satellite using the Ka-band frequency, instead of Ku-band. Despite this new frequency, the OGDR/IGDR products were opened to users end of June/ beginning of July 2013. The GDR products (GDR-T version Patch1) were available to the PI from 2nd of August 2013 onwards. Following the Saral/AltiKa NRT Verification workshop held end of August 2013 in Toulouse, the GDRs were released to all users from 12th September 2013.

Though direct point to point comparison to other satellites are not possible (due to different ground tracks), many comparison with Jason-2 (and also during a couple of months with Jason-1) were possible. This gives valuable insight in the Saral/AltiKa data quality.

The main fear, of up to an additional 5% of lost or edited data due to sensitivity of Ka-band to rain, became not reality. Indeed, when considering periods without data gaps due to scheduled calibrations or occasional acquisition station problems, Saral/AltiKa has only 0.1% of additional data lost (probably due to sensitivity to rain) over ocean compared to Jason-2. Concerning data editing over ocean (after removing land and sea ice), Saral/AltiKa edits also less data (2.4%) than Jason-2 (3.8%).
Saral/AltiKa is still in the verification phase and several algorithms are not yet tuned or fully tuned (sea state bias, altimeter wind speed (not usable in Patch1), radiometer wet troposphere correction, sea ice flag, rain flag, ...). Despite this, the along-track performance and the performance at crossover points (representative for meso-scale) are already very good: at the same order as Jason-2.
Beginning of 2014, data standard switched to Patch2 (with a reprocessing of all already released GDR data), which brings many improvements (see [17]). A great deal of work is still to be done (computing a sea state model and wind speed algorithm with one year of data, explore the particularities of the Ka-band, ...), which will partly be done in the frame of the PEACHI project (Prototype for Expertise on AltiKa for Coastal Hydrology and Ice, [27]).

Saral/AltiKa is a key mission side by side with Jason-2 and Cryosat in multi-mission analysis systems such as Duacs.

9. Glossary

AMR Advanced Microwave Radiometer

CLS Collecte Localisation Satellites

CNES Centre National d'Etudes Spatiales

CNG Consigne Numerique de Gain (= Automatic Gain Control)

DEM Digital Elevation Model

DIODE Détermination Immédiate d'Orbite par Doris Embarqué

ECMWF European Centre for Medium-range Weather Forecasting

EDP Earliest Detection Part

GDR Geophysical Data Record

GDR-T Geophysical Data Record version T (test)

GIM Global Ionosphere Maps

GOT Global Ocean Tide

IGDR Interim Geophysical Data Record

JPL Jet Propulsion Laboratory (Nasa)

MLE Maximum Likelyhood Estimator

MOE Medium Orbit Ephemeris

MQE Mean Quadratic Error

MWR MicroWave Radiometer

MSS Mean Sea Surface

NSIDC National Snow and Ice Data Center

PF/RF PlatForm / RadioFrequency

PLTM PayLoad TeleMetry

POE Precise Orbit Ephemeris

OGDR Operational Geophysical Data Record

SALP Service d'Altimétrie et de Localisation Précise

SARAL Satellite with ARgos and ALtika

SSH Sea Surface Height

SLA Sea Level Anomaly

SLR Satellite Laser Ranging

SSB Sea State Bias

SWH Significant Wave Height

TEC Total Electron Content

TM TeleMetry

10. References

References

[1] Abdallah, S., 2007. Ku-band radar altimeter surface wind speed algorithm. *Proc. of the 2007 Envisat Symposium*, Montreux, Switzerland, 23-27, April 2007, Eur. Space Agency Spec. Publ., ESA SP-636.

[2] L. Aouf and J.-M. Lefèvre: The impact of Saral/Altika wave data on the wave forecasting system of Météo-France : update. Oral presentation at SARAL/AltiKa 1st Verification Workshop, 27th to 29th August 2013, Toulouse, France. Available at http://www.aviso.oceanobs.com/fileadmin/documents/ScienceTeams/Saral2013/24_wave_lotfi.pdf

[3] Brown G.S., "The average impulse response of a rough surface and its application", *IEEE Transactions on Antenna and Propagation*, Vol. AP 25, N1, pp. 67-74, Jan. 1977.

[4] SARAL/AltiKa Products handbook, July 2013 *SALP-MU-M-OP-15984-CN* edition 2.3. Available at: http://www.aviso.oceanobs.com/fileadmin/documents/data/tools/SARAL_Altika_products_handbook.pdf

[5] Boy, François and Jean-Damien Desjonqueres. 2010. Note technique datation de l'instant de reflexion des échos altimètres pour POSEIDON2 et POSEIDON3 *Reference: TP3-JPOS3-NT-1616-CNES*

[6] Guillot, A., A.K. Shukla, Mai 2013: SARAL/Altika Joint Calval Plan. *ALK-SY1-PL-198-CNES* issue 1 rev. 3.

[7] L. Cerri, A. Couhert, S. Houry, and F. Mercier: Status of GDR orbits for ocean topography missions ans prospects for future improvements. Oral presentation at OSTST, 8th-11th October 2013, Boulder, USA. Available at http://www.aviso.oceanobs.com/fileadmin/documents/OSTST/2013/oral/Cerri_POD.pdf

[8] N. Picot: Saral compte rendu de réunion RESTO_Expertise_CalVal N°7. Reference: SALP-CR-M-OP-15195-CN.

[9] Desjonquères, J. D. , Carayon, G. , Steunou, N. and Lambin, J. (2010) Poseidon-3 Radar Altimeter: New Modes and In-Flight Performances, *Marine Geodesy*, **33:1, 53 - 79**. Available at http://pdfserve.informaworld.com/542982__925503482.pdf

[10] Y. Faugere, A. Delepoulle, F.Briol, I. Pujol and DUACS Team, N. Picot, E. Bronner. Altika in DUACS: Status after 2 months (and perspectives). Oral presentation at SARAL/AltiKa 1st Verification Workshop, 27th to 29th August 2013, Toulouse, France. Available at http://www.aviso.oceanobs.com/fileadmin/documents/ScienceTeams/Saral2013/34_Altika_in_Duacs_Faugere.pdf

[11] D. Griffin and M. Cahill: Use of AltiKa NRT sea level anomaly in the Australian multi-mission analysis. Oral presentation at SARAL/AltiKa 1st Verification Workshop, 27th to 29th August 2013, Toulouse, France. Available at http://www.aviso.oceanobs.com/fileadmin/documents/ScienceTeams/Saral2013/33_multi_mission_gridding_GRIFFIN.pdf

[12] C. Jayles and J.-P. Chauveau: DORIS-DIODE (and TRIODE) Results. Oral presentation at SARAL/AltiKa 1st Verification Workshop, 27th to 29th August 2013, Toulouse, France. Available at http://www.aviso.oceanobs.com/fileadmin/documents/ScienceTeams/Saral2013/07_DIODE_perfomances_Jayles.pdf

[13] Lillibridge, J., Scharroo, R., Abdalla, S., and Vandemark, D. (2013) One-and Two-Dimensional Wind Speed Models for Ka-band Altimetry. *Journal of Atmospheric and Oceanic Technology.* doi: http://dx.doi.org/10.1175/JTECH-D-13-00167.1

[14] J. Noubel & SARAL team: Saral Mission status. Oral presentation at SARAL/AltiKa 1st Verification Workshop, 27th to 29th August 2013, Toulouse, France. Available at http://www.aviso.oceanobs.com/fileadmin/documents/ScienceTeams/Saral2013/02_mission_status_cnes_v02_Noubel.pdf

[15] A. Ollivier, S. Philipps, M. Ablain, A. Edwell, L. Cerri, and N. Picot: Assessment of Orbit Quality through the Sea Surface Height calculation - New insight in resolving long term and inter-annual signal for climate studies. Oral presentation at OSTST, 8th-11th October 2013, Boulder, USA. Available at http://www.aviso.oceanobs.com/fileadmin/documents/OSTST/2013/oral/Ollivier_Orbit.pdf

[16] N. Picot, A. Guillot, P. Senegenès, J. Noubel, N. Steunou, S. Philipps, P. Prandi, G. Valladeau, M. Ablain, S. Desai, B. Haines, S. Fleury. DATA QUALITY ASSESSMENT OF THE SARAL/ALTIKA KA-BAND MISSION. Oral presentation at OSTST, 8th-11th October 2013, Boulder, USA. Available at http://www.aviso.oceanobs.com/fileadmin/documents/OSTST/2013/oral/Picot_SARAL_Data_Quality_Assessment.pdf.

[17] S. Philipps, V. Pignot: Saral/AltiKa reprocessing GDR-T Patch2. 2014. SALP-RP-MA-EA-22345-CLS. CLS.DOS/NT/14-031.

[18] Poisson, JC, Peyridieu, S., Lasne, Y., and Thibaut, P. (2013) PEACHI Tâche 1.1: Reprise et adaptation des algorithmes de retracking. CLS-DOS-NT-13-098.

[19] Poisson, JC, Tran, N., and Thibaut, P. (2013) PEACHI Tâche 1.4: SSB. CLS-DOS-NT-13-239.

[20] P. Prandi, S. Philipps, J.-C. Poisson, B. Picard, and N. Picot: Exploring the behaviour of a Ka-band altimeter of the Arctic Ocean. Poster presented at OSTST, 8th-11th October 2013, Boulder, USA. Available at http://www.aviso.oceanobs.com/fileadmin/documents/OSTST/2013/posters/Prandi_Poster_OSTST13_ArcticExploration.pdf

[21] Scharroo, R., and J. L. Lillibridge. Non-parametric sea-state bias models and their relevance to sea level change studies, in *Proceedings of the 2004 Envisat & ERS Symposium*, Eur. Space Agency Spec. Publ., ESA SP-572, edited by H. Lacoste and L. Ouwehand, 2005.

[22] R. Scharroo, J. Lillibridge, S. Abdalla, and D. Vandemark. Early look at SARAL/AltiKa data. Oral presentation at OSTST 2013, Boulder, USA. Available at http://www.aviso.oceanobs.com/fileadmin/documents/OSTST/2013/oral/Scharroo_Early_look_at_SARAL.pdf

[23] N. Stenou, P. Sengenes, J. Noubel, N. Picot, J.D. Desjonquères, J.C. Poisson, P. Thibaut, F. Robert and N. Tavenea. ALTIKA INSTRUMENT : IN-FLIGHT STABILITY AND PERFORMANCES. Oral presentation at OSTST 2013, Boulder, USA. Available at http://www.aviso.oceanobs.com/fileadmin/documents/OSTST/2013/oral/Steunou_OSTST2013_AltiKa_Instrument.pdf

[24] SARAL System Requirements *SRL-SYS-SP-010-CNES*

[25] Thibaut, P. O.Z. Zanifé, J.P. Dumont, J. Dorandeu, N. Picot, and P. Vincent, 2002. Data editing: The MQE criterion. *Paper presented at the Jason-1 and TOPEX/Poseidon Science Working Team Meeting, New-Orleans (USA), 21-23 October*.

[26] N. Tran, S. Philipps, J.-C. Poisson, S. Urien, E. Bronner, and N. Picot. Impact of GDR_D standards on SSB corrections. *Oral presentation at OSTST meeting, Venice, Italy, 27-28 September 2012*. Available at http://www.aviso.oceanobs.com/fileadmin/documents/OSTST/2012/oral/02_friday_28/01_instr_processing_I/01_IP1_Tran.pdf.

[27] G. Valladeau, P. Thibaut, J.-C. Poisson, B. Picard, M.-L. Frery, N. Picot, and A. Guillot, 2013. SARAL/AltiKa altimeter data over open oean, coastal zones and inland waters: the PEACHI project. Poster presented at OSTST 2013, Boulder, USA. Available at http://www.aviso.oceanobs.com/fileadmin/documents/OSTST/2013/posters/Valladeau_Poster_PEACHI_Boulder_2013.pdf

11. Annex

11.1. Content of Patch1

Hereafter the content of Patch1 is recalled. All GDR data were produced with this patch, wereas IGDR data were only produced with this patch from cycle 4 pass 395 onwards.

Altimeter calibration file : The altimeter calibration stability has been analysed. Based on the actual data, we have implemented an averaging of the calibrations over a 7 days window for the low pass filter (identical to Jason-2) and 3 days for the internal path delay and total power (not used on Jason-2). This will slightly reduce the daily noise observed in the altimeter calibration data.

Altimeter characterization file : We have updated the altimeter characterization file using the flight calibration of the gain values (4 calibrations performed). The impact is very small (of the order of 0.01 dB).

Retracking look-up tables : We have updated the ocean retracking look-up tables using the flight calibration data (PTR). The impact is very small on the range and sigma0 values but of the order of 15 cms on SWH for low sea states.

MQE : We have analyzed the altimeter flight data and based on the observed MQE values over ocean a threshold of 2.3E-3 (Jason-2 value is 8E-3) is used for the 1Hz data computation.

Neural network : A first linear relation has been computed between the measured BT and the simulated one. This linear relation is applied on the 23.8 GHz only – the same analysis will be conducted on the 37 GHz and sigma0. This generates a bias on the radiometer wet tropospheric correction which is now much more consistent with the model one.

Atmospheric attenuation : The value outputted by the neural algorithm is now recorded in the level2 products (it was set to 0 at the beginning of the mission). Rad_water_vapor and rad_liquid_water: The values have been corrected to comply with the actual unit in the level2 products (kg/m^2). But the rad_liquid_water remains not reliable as an anomaly has been noticed in the neural network.

SSHA : The radiometer wet tropospheric correction is now used to compute this value (the model value was used at the beginning of the mission).

Controls parameters : The threshold values have been updated with the flight data. This is a first tuning – additional work is necessary.

11.2. Content of Patch2

Hereafter the content of Patch2 is recalled. It will probably be activated mid-January 2014. GDRs will be produced using Patch2 from cycle 8 onwards. Cycles 1 to 7 will be reprocessed with the Patch2.

Wind look-up table : The table provided by NOAA is used. This table is only based on the measured sigma0, taking into account the atmospheric attenuation (sigma0 at the surface). (Reference: Lillibridge et al. [13])

SSB look-up table : The table provided by R. Scharroo is used (same method as in [21]). We use only the significant wave height to compute the SSB.

Radiometer neural algorithm : Taking into account several months of AltiKa measurements, the neural network coefficients have been updated. Note that this modifies the radiometer related parameters (radiometer wet troposphere correction, atmospheric attenuation, radiometer liquid water content and radiometer water vapor content).

Ice-2 retracking algorithm : The algorithm has been updated taking into account the AltiKa Ka band specificities (ice2 algorithm was based on ENVISAT Ku band experience).

FES2012 tide model : This new tide model is included, improving the SSH accuracy in coastal zones. (Reference : http://www.aviso.oceanobs.com/en/data/products/auxiliary-products/global-tidefes2004-fes99/description-fes2012.html)

Matching pursuit algorithm : The algorithm based on J. Tournadre proposal has been tuned to comply to AltiKa Ka band specificities.

MQE parameter scale factor : The scale factor of the MQE has been modified.

Update of the altimeter characterization file : The altimeter characterization file has been modified in order to account for 63 values of altimeter gain control loop (AGC). This has impacts over sea ice and land hydrology, in some cases the AGC was set to default value in current P1 products.

Doris on ground processing (Triode) : The Doris navigator ground processing has been upgraded to reduce the periodic signal observed on the altitude differences with MOE/POE.